Microfluidic Selection and Applications of Aptamers

John P. Hilton

Submitted in partial fulfillment of the
requirements for the degree of
Doctor of Philosophy
in the Graduate School of Arts and Sciences

COLUMBIA UNIVERSITY

2013

Abstract

Microfluidic Selection and Applications of Aptamers

John P. Hilton

BioMEMS technology has the potential to increase the efficiency of conventional biological and medical protocols, by reducing their consumption of time and resources. Through more efficient surface-based chemical reactions and automation of tedious manual processes, orders of magnitude increases in efficiency across a number of metrics can be achieved by shifting conventional medical and biological protocols to the microscale domain. The SELEX process, by which aptamer sequences are selected via isolation from randomized libraries, is a time-consuming and resource-intensive protocol which is being performed with increasing frequency in both academic and private sector laboratories. Conventional approaches using macroscale technology cannot meet the current demand for selection of new aptamer sequences, as they require months of work and liters of expensive reagents.

Microscale approaches to the SELEX process have been receiving attention in recent years due to their initial successes in reducing the time and reagents necessary to find aptamers. In particular, microscale "selection" or partitioning of weakly bound sequences from aptamer candidates, and on-chip integration of the protocol have separately been explored as approaches to scaling and improving SELEX. Initial results have shown that this technology can reduce resource requirements for SELEX by at least an order of magnitude.

In this dissertation, a new approach to on-chip SELEX is developed which integrates highly efficient microfluidic selection and on-chip integration of the entire protocol. As a result, further reductions in processing time and reagent requirements can be realized. A demonstration of aptamer capabilities is first achieved via the development of a microfluidic aptasensor for cocaine, which utilizes aptamer-coated microbeads and fluorescent detection. Secondly, a technology necessary for on-chip integration of SELEX is developed: a novel bead-based polymerase chain reaction (PCR) protocol which vastly simplifies procedures for the capture and resuspension of ssDNA in solution. This protocol is then integrated on-chip with bead-based partitioning of weakly bound sequences to develop a microchip which performs temperature-specific isolation of aptamer sequences from a randomized library. Finally, this approach is further developed into a microfluidic SELEX chip which is capable of performing multiple rounds of temperature-specific SELEX. The novel bead-based protocol is shown to efficiently isolate target-binding sequences from a random library in a fraction of the time previously reported. As a result, this research provides a schematic for the development of highly efficient, integrated microfluidic SELEX devices. Such devices have the potential to impact a variety of fields including medical diagnostics, drug detection, and aptamer-based therapeutics.

Table of Contents

Abstract

Acknowledgements **v**

Dedication **vi**

List of Figures **vii**

List of Tables **xiii**

Nomenclature **xiv**

List of Abbreviations **xv**

Chapter 1: Introduction **1**

1-1 Biomedical Microelectromechanical Systems 1

1-1.1 Affinity Binding in Microfluidics 1

1-2 Aptamers 2

1-2.1 Comparison to other affinity binders 3

1-2.2 Applications of Aptamers 4

1-3 SELEX for determining aptamer sequences 6

1-3.1 Conventional SELEX technology 9

1-3.2 Microfluidic SELEX implementations 11

1-4 Significance of this work 17

1-4.1 Integration of microfluidic selection and amplification for highly efficient SELEX 18

1-4.2 Temperature-specific microfluidic selection 19

1-4.3 Summary 20

1-5 Organization of dissertation 20

Chapter 2: A Microfluidic Affinity Sensor for the Detection of Cocaine **22**

2-1 Introduction 22

2-2 Principle and Design 26

2-3 Experimental 28

2-3.1 Materials and Instrumentation 28

2-3.2 Experimental Protocol 29

2-4 Results and Discussion 31

2-4.1 Device Calibration 31

2-4.2 Transient Response 33

2-4.3 Detection of Cocaine 35

2-4.4 Improving Detection Limits by Continuous-Flow Concentration 37

2-4.5 Thermally Based Device Regeneration 38

2-5 Conclusions 41

Chapter 3: Bead-based Polymerase Chain Reaction on a Microfluidic Chip **43**

3-1 Introduction 43

3-2 Materials and Methods 45

3-2.1 Bead-Based PCR Method 45

3-2.2 Microchip Design and Fabrication 47

3-2.3 Application to Pathogenic DNA Detection 50

3-2.4 Materials, Reagents, and Experimental Procedures 52

3-3 Results and Discussion 55

3-3.1 Physical Characterization of the Device 55

3-3.2 Effects of Experimental Parameters on Bead-Based PCR 58

3-3.3 Investigation of Detection Sensitivity 65

3-3.4 Integrated Bead-Based PCR Operation 68

3-4 Conclusions 70

Chapter 4: Isolation of Thermally Sensitive Aptamers on a Microchip 72

4-1 Introduction 72

4-2 Materials and Methods 75

4-2.1 Integrated Temperature-Specific Bead-Based Microfluidic Selection 75

4-2.2 Integrated Bead-Based Polymerase Chain Reaction 76

4-2.3 Design and Fabrication 77

4-2.4 Materials 80

4-2.5 Experimental Protocol 81

4-3 Results and Discussion 83

4-3.1 Physical Characterization of the Device 83

4-3.2 Microfluidic Aptamer Isolation 85

4-3.3 Binding Strength of Enriched Library 89

4-4 Conclusions 91

Chapter 5: An Integrated SELEX Microchip 93

5-1 Introduction 93

5-2 Principles and Design 95

5-2.1 Design and Operation of the Microchip 95

5-2.2 Materials 98

5-2.3 Experimental Protocol 100

5-3 Initial Results and Ongoing Work 101

5-4 Conclusions 103

Chapter 6: Conclusions 104

6-1 Summary of Dissertation 104

6-1.1 A Microfluidic Cocaine Aptasensor 104

6-1.2 Integrated Microfluidic Bead-based PCR 105

6-1.3 Microfluidic Temperature-Specific Aptamer Isolation 106

6-1.4 Ongoing Work on Integrated Microfluidic SELEX 106

6-2 Future work 107

6-2.1 Bead-based Microfluidic Sensors 107

6-2.2 Integrated Sample-to-Answer Devices Using Bead-based Polymerase Chain Reaction 108

6-2.3 Efficiency Analysis of Integrated Microfluidic PCR 108

6-2.4 Temperature-Specific SELEX Against Novel Target Molecules 109

6-2.5 Multiplexed SELEX for Interrogation of Binding Schemes with Synthetic Nucleic Acids 110

6-3 Expected Developments and Final Words 110

Appendix 1: Supplementary Data for Bead-Based PCR 112

References 116

Acknowledgements

I gratefully acknowledge support from our funding agencies, the National Science Foundation, the National Institutes of Health, and the Alternatives Development Research Foundation. Without their support none of this research would have taken place. I would also like to thank my advisor, Dr. Qiao Lin, for supporting me throughout my Ph.D and encouraging me to pursue my research interests. The advice of my committee has been invaluable, and I am extremely grateful for their input. In particular, Dr. Milan Stojanovic, our collaborator, has been both extremely helpful and inspirational throughout the past 5 years. My various labmates and co-authors, from Morningside to Washington Heights and as far as the Chinese Academy of Sciences, have helped me gain the experience I have needed as an experimenter and as a writer. In particular, Dr. Huu Nguyen and Bin Wang have been invaluable labmates, teaching me the intricacies of microfabrication, on-chip thermal control, and fluorescent microscopy. Dr. Renjun Pei, Mihaela Barbu, and Dr. Marlin Halim have patiently taught me everything that I needed to know about SELEX, from designing primers for PCR to cloning and sequencing, and without them this dissertation would never have been completed. Finally I would like to thank all of the rest of my labmates and my department at Columbia for their help and support these past few years.

Dedication

I dedicate this dissertation to the people in my life who have helped me reach this point. Family, friends, teachers, co-workers – without all of you to guide me, I would certainly have lost my way.

List of Figures

Chapter 1

Figure 1-1. The SELEX protocol. A library of approximately 10^{14}-10^{15} nucleic acids with randomized sequences (a) is introduced to target molecules (b). During selection, unwanted non-binding and weakly bound nucleic acids are separated from strongly bound aptamer candidates (c) which are then chemically amplified (d). Single-stranded nucleic acids are then separated from the amplified double strands prior to repetition of the process (e).

Figure 1-2. The first attempt at microfluidic SELEX: the Hybarger prototype. This device used off-chip fluidics and temperature control, but showed that an integrated SELEX protocol was possible and could potentially revolutionize the field [1].

Figure 1-3. The CMACS (continuous flow magnetic actuated cell separation) system, used to separate weakly bound nucleic acids from aptamer candidates bound to target-conjugated magnetic beads in a microfluidic selection device [2].

Figure 1-4. Previously reported on-chip SELEX protocol. (i) DNA library is exposed to target-conjugated microbeads. (ii) Incubation of the library and beads results in aptamer candidates binding to beads. (iii) Weakly bound strands are washed away while strongly bound candidates remain adhered to magnetic beads held in place using a magnetic field. (iv) Aptamer candidates are amplified in situ in the microchamber, following introduction of amplification mixture. (v) Single-stranded aptamer candidates are eluted and used to restart the process. It is unclear how this last step of the process can be completed independent of manual user intervention (pipetting).

Chapter 2

Figure 2-1. (a) Schematic of the microfluidic cocaine sensor, and (b) fabrication process: (i) microfluidic features are defined in PDMS, (ii) heaters and temperature sensors are fabricated on a glass slide, (iii) the PDMS and glass slide are bonded together.

Figure 2-2. Signal-on aptamer-based cocaine detection. (a) A fluorophore-labeled aptamer is immobilized onto a solid surface. (b) A quencher-labeled short complimentary strand is introduced, decreasing fluorescence. (c) Unlabeled cocaine binds competitively to the aptamer, displacing the quencher and reducing fluorescence.

Figure 2-3. Measured electrical resistance of the temperature sensor as a function of temperature.

Figure 2-4. Effect of photobleaching on the relative fluorescence over time.

Figure 2-5. Transient response of the sensor to introduction of quencher solution.

Figure 2-6. Transient response of the sensor to introduction of cocaine (1 μM).

Figure 2-7. Response of the sensor to cocaine at varying concentrations.

Figure 2-8. Time-resolved relative fluorescence as cocaine is concentrated from a continuous flow (2 μL/min) of a highly dilute solution (10 pM).

Figure 2-9. Effect of temperature on relative fluorescence from a sensor incubated with 100 μM cocaine solution. Return of relative fluorescence to 1 indicates successful regeneration of the aptamer surface.

Figure 2-10. Reuse of the sensor after regeneration. In each cycle, the sensor was first thermally regenerated at 37°C (A), quenched (AQ), and finally exposed to cocaine (AQC).

Chapter 3

Figure 3-1. Device design. (a) The chip consists primarily of a PDMS chamber bonded to a glass slide which has been patterned with a micro heater and temperature sensor. Key dimensions of the PDMS microchamber have been included in projected top and side views (all dimensions in mm). (b) Also shown is the design of an integrated microfluidic device, in which weirs retain microbeads in the chamber while beads are exposed to streams of buffer or reagents.

Figure 3-2. Integration of microchip bead-based PCR. Primer-coated beads permit separation of DNA from impurities (a,b), and amplification produces a fluorescent signal on the bead surfaces (c) via microchip PCR. The beads then act as a mechanism for either storage or collection and analysis of ssDNA following thermally-induced dehybridization and release (d).

Figure 3-3. Temperature history of a typical PCR cycle.

Figure 3-4. Effect of temperature on fluorescence measurements, n = 3. The negligible change in fluorescence intensity indicates that temperature cycling does not degrade dual biotin functionalization and hence does not affect concentration of DNA at bead surfaces. Error bars indicate one standard deviation from the mean.

Figure 3-5. Gel electrophoresis analysis of PCR tests using the 181 bp *B. pertussis* DNA amplification chemistry. Gel (a) displays the results of a solution-based test, and gel (b) shows the results of a bead-based test. In both gels, lane (i) is a sample of PCR products mixed with loading buffer, and lane (ii) is a 100 bp ladder (dsDNA for length

reference). Arrow indicates direction of DNA movement, with smaller strands migrating faster.

Figure 3-6. Effect of annealing temperature on fluorescent intensity after bead-based PCR, n=3, with error bars representing one standard deviation from the mean.

Figure 3-7. Gel electropherogram showing effects of annealing temperature on amplified DNA following solution-based PCR.

Figure 3-8. Effect of bead concentration on fluorescent bead intensity following PCR, n = 3, with error bars representing one standard deviation from the mean. Results indicate there is a concentration of microbeads in the reaction mixture which optimizes signal intensity following the PCR reaction. The students' t-test confirms that the 200 beads/μL result is differentiable from the other results, $p < 0.11\%$.

Figure 3-9. Investigation of DNA detection limit. Fluorescent intensity of beads following the PCR reactions is plotted against concentration of templates in the reaction mixture. Error bars indicate one standard deviation from the mean of three experiments (n=3), and the reaction with zero templates (control) and a 1 pM template concentration (the detection limit) is differentiable with a probability of greater than 95%, according to the students' t-test.

Figure 3-10. Relationship between signal intensity and the number of PCR cycles used during amplification of a 1 pM sample. Mean values from multiple tests (n = 3) are shown, error bars indicate standard deviation.

Figure 3-11. Micrographs of the microchamber illustrate the process of integrated microfluidic bead-based PCR. In (a), a brightfield micrograph shows a microchamber in which beads have been inserted into the chamber and a DNA solution is being introduced

(fluid flowing from top to bottom). In (b), the DNA solution has been introduced, and template DNA is being captured from the solution onto bead surfaces by bead-bound reverse primers. Following PCR cycling, and washing with buffer, the fluorescent intensity of the microbeads was measured with minimal background fluorescence (c).

Chapter 4

Figure 4-1. Aptamer isolation via the SELEX process. A library of approximately 10^{14}-10^{15} nucleic acids with randomized sequences (a) is introduced to target molecules (b). During selection, unwanted non-binding and weakly bound nucleic acids are separated from strongly bound aptamer candidates (c) which are then chemically amplified (d). Single-stranded nucleic acids are then separated from the amplified double strands prior to repetition of the process (e).

Figure 4-2. Plan view of the integrated microchip, primarily consisting of microfluidic selection and amplification chambers with integrated resistive heaters and temperature sensors.

Figure 4-3. Characterization of the microchip. In (a), the linear relationship between temperature and resistor resistance for the (i) selection chamber and (ii) PCR chamber resistors allows determination of a temperature coefficient of resistance, in this case 1.554×10^{3} °C^{-1} and 1.613×10^{3} °C^{-1}, respectively. The passive mixer (b) fully mixes a stream of buffer and dye at 5 μL/min.

Figure 4-4. Gel electrophoresis of buffer samples containing weakly bound DNA washed away from target molecules during selection. The decreasing fluorescent

intensity with continuing washes indicates that the selection process is removing weakly bound DNA, leaving strongly bound DNA to eventually be captured and amplified.

Figure 4-5. Results from fluorescent analysis of bead-based PCR amplification of aptamer candidates.

Figure 4-6. Secondary structures of clones 12, 17, and 15.

Figure 4-7. Analysis of DNA-IgE binding. IgE-coated microbeads were exposed to fluorescently labeled DNA, and the fluorescence intensity of the beads, indicative of the surface concentration of DNA, was measured.

Figure 4-8. Temperature-dependence of DNA-IgE binding.

Appendix 1

Figure A1-1. DNA/Fluorescent Signal Generation. Primer-coated beads (a) hybridize to the DNA (b); an initial temperature cycle generates complementary ssDNA attached to the beads (c); during the following temperature cycle, fluorescently labeled primers are captured by the complementary ssDNA (d) and amplification generates fluorescently labeled dsDNA which remains attached to the beads (e).

Figure A1-2. Calibration data for an integrated resistive temperature sensor.

List of Tables

Table 1-1. Comparison of a conventional SELEX protocol (affinity column separation and conventional PCR) to newer microscale methods.

Table 3-1. Summary of PCR cycle parameters.

Table 4-1. Results of sequencing the enriched library

Table 5-1. Results of sequencing 10 clones from 5 pools of enriched library DNA.

Nomenclature

α	Temperature Coefficient of Resistance
[Aptamer]	Concentration of Aptamers
[Aptamer:Target]	Concentration of Aptamer-Target Complex
°C	Degrees Celsius
H	Channel Height
L	Channel Length
K_D	Dissociation Constant
μ	Micro-, $\times 10^{-6}$
μ M	Micromolar
μ TAS	Micro Total Analysis Systems
[NAf]	Concentration of free nucleic acids
[{NAf:T}]	Concentration of Nucleic Acid-Target Complex
Ω	Ohms
R_{ref}	Reference Resistance
[Target]	Concentration of Target
[Tf]	Concentration of free target molecules
T_{ref}	Reference Temperature

List of Abbreviations

bp	Base-pair
dsDNA	Double-stranded DNA
IgE	human Immunoglobulin E
MEMS	Microelectromechanical Systems
miRNA	MicroRNA
mM	Millimolar
NASBA	Nucleic Acid Sequence Based Amplification
nM	Nanomolar
nt	nucleotide
PCR	Polymerase Chain Reaction
PDMS	(poly)dimethylsiloxane
pM	Picomolar
RCA	Rolling Circle Amplification
RNA	Ribonucleic Acid
SELEX	Selective Evolution of Ligands by EXponential enrichment
SPR	Surface Plasmon Resonance
ssDNA	Single-stranded DNA
UV	UltraViolet radiation
UV/VIS	Ultraviolet-Visible Spectroscopy
VEGF	Vascular Endothelial Growth Factor

Chapter 1: Introduction

1-1 Biomedical Microelectromechanical Systems

The development of semiconducting materials and transistors in the latter half of the 20th century enabled the computing revolution, by miniaturizing the components necessary to perform mathematical functions. In the past 25 years, this technology has been adapted to miniaturize a wide variety of biomedical protocols and devices [3-7]. Also known as μTAS (Micro Total Analytical Systems) or Lab-on-a-Chip, these biomedical microelectromechanical systems (BioMEMS) devices are capable of performing common laboratory and clinical techniques more rapidly, cheaply, and efficiently than conventional technology. This is largely due to the much greater surface area to volume ratios typical of microfluidic devices, which can result in much higher efficiencies for surface-based chemical reactions. This inherent efficiency translates into reduced reagent consumption and minimized assay time for microfluidic protocols. In addition to their inherent efficiency, microdevices offer the opportunity to integrate and automate complex protocols, eliminating tedious pipetting steps which require large amounts of time and are significant sources of error. Applications of BioMEMS technology include biological separations, detection of analytes, and many other molecular biology protocols and medical applications [8, 9].

1-1.1 Affinity Binding in Microfluidics

A major challenge in microfluidics has been the ability to process “real” samples – that is, samples which have not been pretreated in some way to purify or extract the

intended analyte. Some of those most common technologies encountered in microfluidic devices are those that achieve separation of analytes from mixtures [10], to concentrate or purify a desired analyte prior to further analysis. Non-specific methods of separation, such as ion exchange and steric exclusion, are common but hindered by their inability to exclude impurities with properties similar to the desired molecules [10-13]. Affinity binding, however, captures target molecules with very high selectivity based on geometric and electrostatic target-ligand interactions [14]. Affinity interactions exploit a combination of weak intermolecular forces (ionic interactions, hydrogen bonds, hydrophobic interactions, and Van der Waals forces) to achieve a strong, specific bond [15]. In microfluidic devices, surfaces coated with affinity substances use these interactions to concentration and extract analytes from complex solutions prior to other functionalities, such as analysis. Common affinity binders used in these applications include antibodies (polyclonal and monoclonal), lectins, and enzymes. Arguably the most popular type of affinity binders are monoclonal antibodies, which are prized for their ability to individually target a wide variety of antigenic substances and their ability to be reproduced in large quantities relatively cheaply. Assays based on monoclonal antibodies are often capable of detecting minute quantities of target substances in complex mixtures.

1-2 Aptamers

Aptamers, discovered in 1990 by Andrew Ellington, Jack Szostak, Craig Tuerk, and Larry Gold, are relatively new, highly effective affinity binders [16, 17]. From Latin “aptus-“, “to fit,” aptamers are nucleic acids that join with target molecules via conformational binding, in which the structure of the nucleic acid changes to fit the

intended moiety. The ability of the aptamers to conform to fit their target molecule imparts high binding strength, as the molecules can conform to maximize the electrostatic and intermolecular interactions characteristic to affinity binding [18]. This is reflected by the dissociation constants (K_D) of aptamers and their targets, which range from micromolar to high picomolar values, where K_D is defined as $K_D = \frac{[\text{Aptamer}][\text{Target}]}{[\text{Aptamer:Target}]}$.

Aptamer structures include not only ssDNA and RNA, but synthetic nucleic acids such as locked nucleic acids (LNAs) [19], peptide nucleic acids (PNAs) [20, 21], and enantiomeric nucleic acids (referred to as spiegelmers) [22]. Different constituent components impart different characteristics to the binding sequence [23]. For example, ssDNA and RNA aptamers have no discernible difference in inherent binding strength [24]; but whereas ssDNA aptamers are more stable than RNA sequences, RNA sequences can potentially be expressed *in vivo* for therapeutic applications [25]. The aptamer selection process determines a nucleic acid sequence expressing binding affinity, which allows identical aptamers to be synthesized as needed with a wide variety of chemical modifications tailored to the intended application. This selection process, SELEX, which is evolutionary and repetitive in nature, allows for a wide variety of target molecules.

1-2.1 Comparison to other affinity binders

Their *in vitro* development gives aptamers a number of advantages over conventional affinity binders such as antibodies or enzymes [26]. Antibodies are produced by provoking an immune response in host tissue, after which the antibodies are collected and repurposed. The reliance upon a host organism for production imparts several disadvantages to antibodies [15]. These include batch-to-batch variation in

antibody production, due to the incomplete control over the *in vivo* process, and the need for target molecules to provoke an immune response in the host organism [27]. In addition, antibodies are generally not reusable – after binding to a target molecule, separation of the antibody-antigen complex requires permanent denaturation of the antibody. By comparison, aptamer-target complexes can be easily broken and the aptamers reused, allowing for the development of regenerable devices for sensing and other applications. Aptamer binding is completely reversible upon application of a variety of external stimuli, such as temperature or pH. In addition, nucleic acids can be safely stored and reused for several years after being synthesized, unlike antibodies or enzymes which are more easily denatured. Aptamer binding strength, as measured by the dissociation constant, is as strong or stronger than that of antibodies, however aptamer-target binding can be carefully tailored during the *in vitro* selection process and can therefore be far more effective. Aptamers have been developed which discriminate between small molecules whose structures differ by only a single methyl group [26], and can readily differentiate between a protein and the synthetic enantiomer (mirror-image) version [22]. Despite their drawbacks, however, antibodies have been used in a wide variety of conventional and microfluidic assays, and are only slowly being replaced by aptamers in their role as biorecognition elements.

1-2.2 Applications of Aptamers

Since their discovery, aptamers have been applied in fields such as biosensing [28], extraction and enrichment [29, 30], and therapeutics [31, 32]. Their wide applicability can be attributed to their well understood mechanism – affinity binding –

and their large range of potential targets. Aptamers have been developed that target proteins [26, 33], small molecules [34-36], whole cells [37, 38], and viruses [39-41]. Areas of applications for aptamers include detection of biological warfare agents [42], drug monitoring in human patients [43], and the treatment of cancer [44]. Aptamers have been recognized as a next-generation sensing element in the field of biosensing [45]. Aptamer-based therapeutics is a rapidly growing field, with many clinical trials currently underway for treatment of a range of illnesses and at least one aptamer-based drug currently available [46]. Pegaptanib, marketed by Pfizer and OSI Pharmaceuticals under the trade name Macugen, treats age-related macular degeneration by interfering with the pathological processes resulting in vision loss. Pegaptanib consists of an anti-VEGF (vascular endothelial growth factor) aptamer which has been pegylated to increase therapeutic dwell time [47]. Several more aptamer-based therapeutics are currently undergoing clinical trials for treatment of ailments such as cancer and heart disease [31, 48].

In the field of microfluidic affinity binding, aptamers have been applied to a multitude of assays for microfluidic detection [28], separation [49], and purification [50] of analytes. One of the advantages of aptamers is their readily modifiable chemistry, which has been used to immobilize aptamers using a variety of methods such as covalent attachments and streptavidin-biotin linkages. As a result, aptamer-coated surfaces are readily available to provide biorecognition functionality in microfluidic devices [51], taking advantage of their inherently large surface area-to-volume ratios. Similarly, the range of geometries readily functionalized with nucleic acids has proven useful in a number of applications. In DNA-based optical detection, for example, functionalization

of nanostructured surfaces has been used to lower detection limits by enhancing the signal-to-noise ratio [52].

Their easily modifiable structure also lends versatility to microfluidic applications of aptamers by augmenting the already large array of possible functions. In aptamer-based microfluidic sensing, for example, a number of approaches use changes in the aptamer structure itself to transduce binding of the target molecule. Upon binding to a target, aptamers undergo changes to their size, shape, charge, and other properties. These can be monitored using techniques such as cyclic voltammetry to electrochemically measure changes in surface-bound charge to report analyte detection [53]. Alternatively, the aptamer structure can be directly modified with molecules that report the target presence or conformational changes via optical, chemical, or other methods [45, 54-56]. As a result of these advantages, microfluidic devices using aptamer technology benefit from better signal-to-noise ratios, faster assay times, reduced reagent consumption, and reductions in necessary labor via integration and automation.

1-3 Isolating Aptamer Sequences with SELEX

As discussed in the previous section, the protocol for determining the sequence of a target-binding aptamer is an evolutionary process called SELEX, or Selective Evolution of Ligands by EXponential enrichment [16, 17]. SELEX, as shown in Figure 1-1, primarily consists of repeated selection and amplification procedures which gradually transform a library of nucleic acids with randomized sequences into a pool of target-binding oligomers with a conserved sequence motif expressing binding affinity to a target molecule. The randomized library (Figure 1a) is exposed to target molecules, during

which time aptamer candidates become bound to the target molecules (Figure 1b). These strongly bound aptamer candidates are then separated from non-binding and weakly bound strands (Figure 1c), and biochemically amplified (duplicated) using the polymerase chain reaction (PCR) (Figure 1d). Single-stranded aptamer candidates are then collected from the double-stranded amplified library (Figure 1e), and used to restart the protocol. A conventional SELEX protocol requires 10-15 "rounds" of selection and amplification in order to converge the library to a consensus sequence, or aptamer. The nucleic acid library itself consists of a 10-200 nucleotide (nt) randomized region, flanked by two 5 – 40 nt known sequences. The known sequences serve as priming regions for amplification via PCR, while the randomized region must be large enough to contain the sequences which define the secondary structures that form the basis of the conformational binding to the target molecules. Random regions are typically 30-60 nt long, as both shorter and longer sequences have been shown to reduce selection efficiency [57, 58]. Priming sequences are typically 10 – 20 nt long, to ensure maximum annealing efficiency during PCR and minimize non-specific amplification.

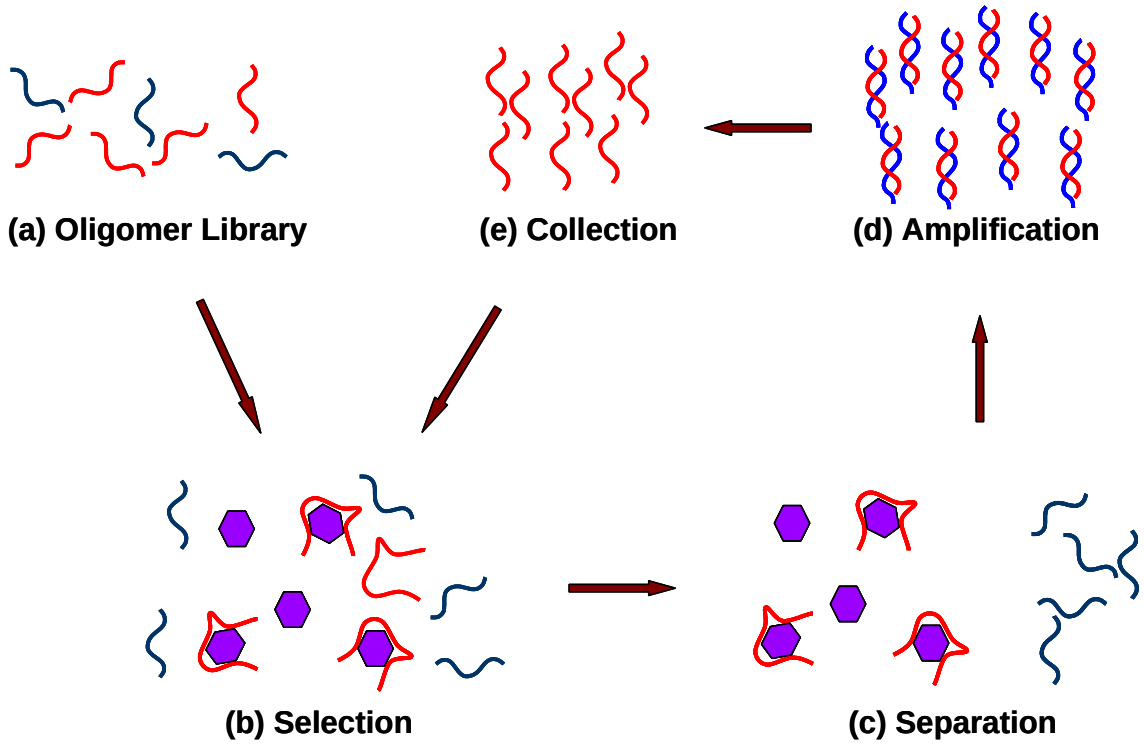

Figure 1-1. The SELEX protocol. A library of approximately 10^{14}-10^{15} nucleic acids with randomized sequences (a) is introduced to target molecules (b). During selection, unwanted non-binding and weakly bound nucleic acids are separated from strongly bound aptamer candidates (c) which are then chemically amplified (d). Single-stranded nucleic acids are then separated from the amplified double strands prior to repetition of the process (e).

A number of variations of this process have been demonstrated since its introduction in 1989 that are intended to produce varied outcomes of the process, such as controlled binding affinity to one or more molecules. For example, Toggle-SELEX [59, 60] and Counter-SELEX [61] generate binding affinity to multiple targets and eliminate affinity to undesired targets, respectively [62]. Non-SELEX requires no amplification, only selection, to generate aptamers [63], and Photo-SELEX uses photo-reactive groups

in the nucleic acid structure [64, 65]. In general, however, the aforementioned protocol acts as the template for a SELEX procedure intended to produce a ligand that binds to a target molecule.

1-3.1 Conventional SELEX Technology

The technology necessary to perform SELEX is not particular to this protocol; the two main aspects of SELEX, separation and amplification, are well-known biological protocols that have been extensively studied. SELEX almost exclusively relies upon PCR for amplification rather than rolling cycle amplification (RCA) or nucleic acid sequence based amplification (NASBA), due to the ability of PCR to rapidly generate duplicates of any DNA sequence based on a known priming region. A variety of different methods, however, are employed to separate the strongly-bound candidate aptamers from the random library during selection. Technology typically used for conventional selection includes substrates found in other implementations of affinity chromatography. Nitrocellulose filter paper, for example, retards the movement of positively charged particles (including proteins), while allowing negatively charged nucleic acids without bound targets to pass through [66]. Another very common technique is to couple the target molecule to an agarose or sepharose matrix in an affinity column [62]; such methods allow relatively simple control over selection stringency, by varying the intensity of the buffer washes used to wash away weakly bound nucleic acids. Other previously-reported techniques include solid-phase methods like SPR (surface plasmon resonance) [67], antibody-based methods [68], flow cytometry [69], and the use of magnetic beads [70]. Separation of non-binding strands from aptamer candidates bound

to targets immobilized onto magnetic beads is a highly effective separation method [71], and this approach has been adapted in microfluidic implementations. ”Solution-phase” separation procedures, such as electrophoresis, have also been applied to selection with the added advantage that they allow maximum binding between the target molecule and the library. Solution-phase methods include capillary and gel electrophoresis [72, 73], centrifugation [74], and electrophoretic mobility shift (EMSA) [75]. An advantage of the SELEX process is that it is flexible; it can be changed to meet the specific needs of the intended target molecule or application. As a result, there is a large variety of selection methods available, each with particular advantages and disadvantages [40].

While conventional SELEX technology is capable of generating high affinity aptamers (K_D of approximately 1 nM) for a wide range of targets (proteins, cells, etc.), it requires an immense amount of time and effort [76]. Conventional PCR reactions often require more than 45 minutes for thermal cycling alone, in addition to the necessary preparation time. Selection procedures are intensely laborious [40, 76], as they require many tedious pipetting steps that must be performed carefully by a trained technician. This time and effort is multiplied by the 15 to 20 rounds of SELEX required for a high affinity aptamer to be generated. The resource requirements of each step is multiplicative – the thousands of pipetting steps necessitate careful controls and additional procedures to ensure that, should an error occur, the process can be restarted without loss of data. As a result of these issues successful SELEX procedures require months of intense effort by highly trained personnel. This is the largest single drawback to more widespread use of aptamers.

In response to the large resource requirements of SELEX and the high demand for aptamers, great strides have been taken in recent years to improve the techniques for generation of aptamers. Initial efforts focused on automating SELEX using robotics, but this required large amounts of startup funding to purchase the required equipment [70, 77, 78]. More recently, microfluidic technology has been applied to this problem in an attempt to increase selection and protocol efficiency via automation and the high surface area to volume ratios inherent in BioMEMS devices.

1-3.2 Microfluidic SELEX Implementations

Microfluidics provides a clear answer to the issues associated with performing the SELEX protocol. The advantages that microfluidics imparts to biological protocols – greater efficiency, shorter assay times, and automated reactions – are of direct importance to SELEX. In the past decade, efforts have been made to miniaturize SELEX protocols onto microfluidic chips, attempting to realize the benefits that could be conveyed to the field of aptamer applications by miniaturizing the aptamer generation process [76]. These efforts have met with only mixed success. The first reported "microfluidic SELEX" device consisted of silica microlines connected to a complex system of dye-actuated valves (Figure 1-2) [1]. This device proved that the operations required for SELEX could be performed in an integrated device without the pipetting steps that make the conventional protocol so tedious, but failed to enrich a randomized library and was not truly "microfluidic" in that it used off-chip valves and capillaries and off-chip heaters for control of fluid flow and temperatures, respectively.

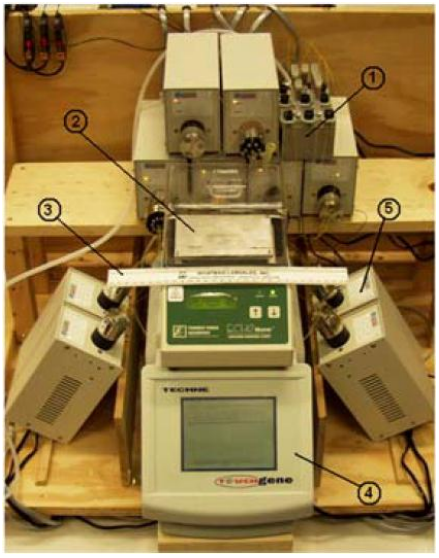

Figure 1-2. The first attempt at integrated microfluidic SELEX: the Hybarger prototype. This device used off-chip fluidics and temperature control, but showed that an integrated SELEX protocol was possible and could potentially revolutionize the field [1].

Following the publication of this work, efforts primarily focused on developing a more efficient microfluidic selection protocol. While microfluidic amplification had been explored extensively [79-81], microfluidic partitioning of non-binders from candidate aptamers was a novel approach and it was thought that the intrinsic efficiency of surface-based reactions in microfluidic devices would benefit solid-phase selection procedures. Similar to affinity chromatography using columns, target molecules were immobilized onto microbeads and exposed to randomized libraries [82]. Separation was achieved using a combination of hydrodynamic flow to remove the weakly bound nucleic acids and a magnetic field to physically isolate the magnetic beads (Figure 1-3). The initial attempt succeeded in generating an aptamer against Botulinum Neurotoxin with a K_D of approximately 33 nM after only a single round of selection, and subsequent efforts have

shown that the same technology can be used to achieve very high efficiency partitioning for separation of high-affinity ligands during SELEX [2, 82-85].

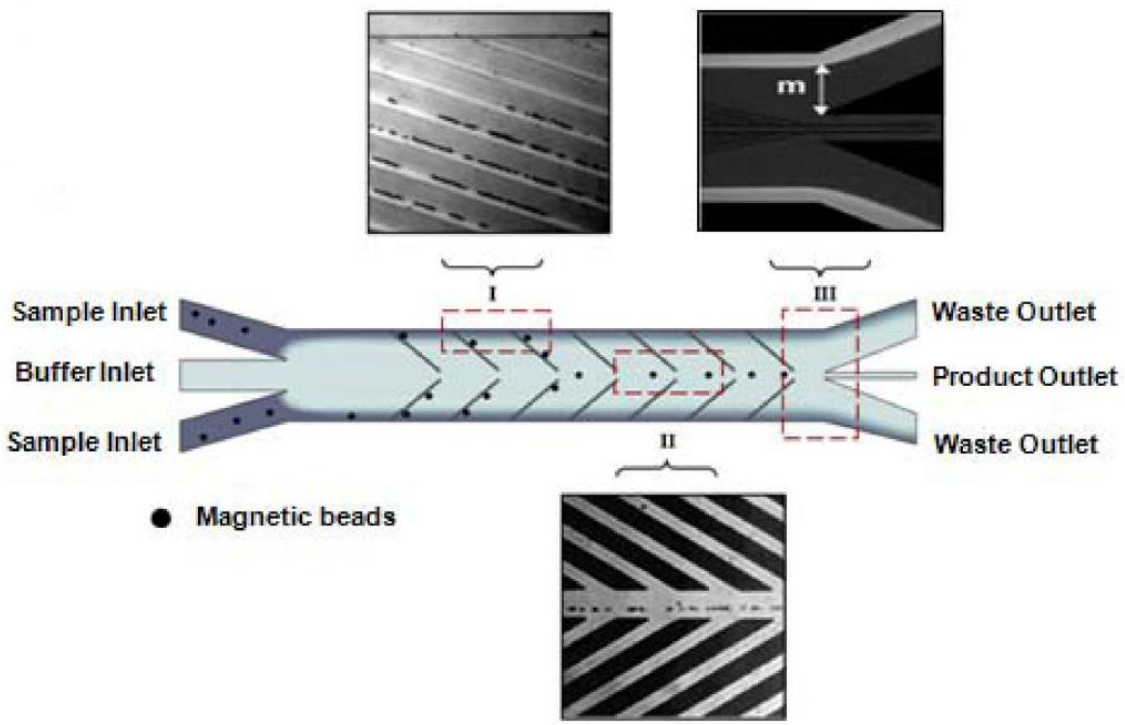

Figure 1-3. The CMACS (continuous flow magnetic actuated cell separation) system, used to separate weakly bound nucleic acids from aptamer candidates bound to target-conjugated magnetic beads in a microfluidic selection device [2].

The efficiency of microfluidic selection stems from the higher surface area-to-volume ratios of such devices and the nature of competitive binding during selection. As experimental and numerical studies have confirmed, the key to generating a stringent selection protocol is maintaining a high ratio of free nucleic acids to available target molecules [86]. Consider the definition of the dissociation constant expressed as

$$K_D = \frac{[NAf][Tf]}{[\{T:NA\}]} \qquad \textbf{Eq. 1.1}$$

where [NAf] represents the concentration of free nucleic acids, [Tf] that of the free target molecules, and [{T:NA}] is the concentration of bound target-nucleic acid complexes. While the total number of nucleic acids must remain high to ensure the possibility of finding the strongest binder, and the ratio [NAf]/[{T:NA}] is a constant for each round of SELEX, [Tf] may be kept very small during selection to exert downward pressure on K_D (the desired outcome). While this can be accomplished by using a very large volume for selection, this approach is unwieldy, time-consuming, and produces low dissociation rate constants that may be undesired [85]. Alternatively, target molecules immobilized onto a surface in a high surface area-to-volume ratio reaction chamber can maintain this ratio while minimizing the size of the reaction volume. The associated reduction in average path length (the distance a nucleic acid must travel to associate with a target molecule) means that the competition process requires less time, thereby reducing the time necessary for selection.

Finally, most recently there have been efforts made towards developing a fully-integrated microfluidic SELEX chip that performs both selection and amplification on-chip. The integration of those protocols would create the most efficient SELEX procedure, by minimizing the time and reagents necessary to perform both selection and amplification, and simultaneously performing a more effective selection with far less potential for human error. Some of the recent attempts achieving this goal show great promise, while still falling short of generating a fully capable SELEX device. The most relevant devices have used a similar magnetic-bead-based approach to microfluidic selection, and have

performed selection and amplification in a single microfluidic chamber [87, 88]. These devices have been shown to be capable of developing aptamers targeting proteins with nanomolar sensitivities, and achieve "sample-in aptamer-out" results similar to those achieved in integrated microfluidic detection devices [89-91]. However, the execution of the protocol itself leaves significant room for improvement, particularly with respect to selection and integration of amplification. In particular, the devices are incapable of selecting aptamers in buffer conditions besides those used for PCR, due to the single-chamber design (Figure 1-4). It is also unclear how collection of single-stranded library DNA is possible following amplification, and the resultant contamination of the aptamer pool with complementary DNA prior to further selection results in competition between these complementary strands and the target molecules for the aptamer candidates. This competition results in decreasing selection efficiency with each SELEX round, which may contribute to the apparent decrease in selection efficiency as compared to that reported in microfluidic selection devices using similar separation technology (6 rounds of SELEX as compared to 1 – 3).

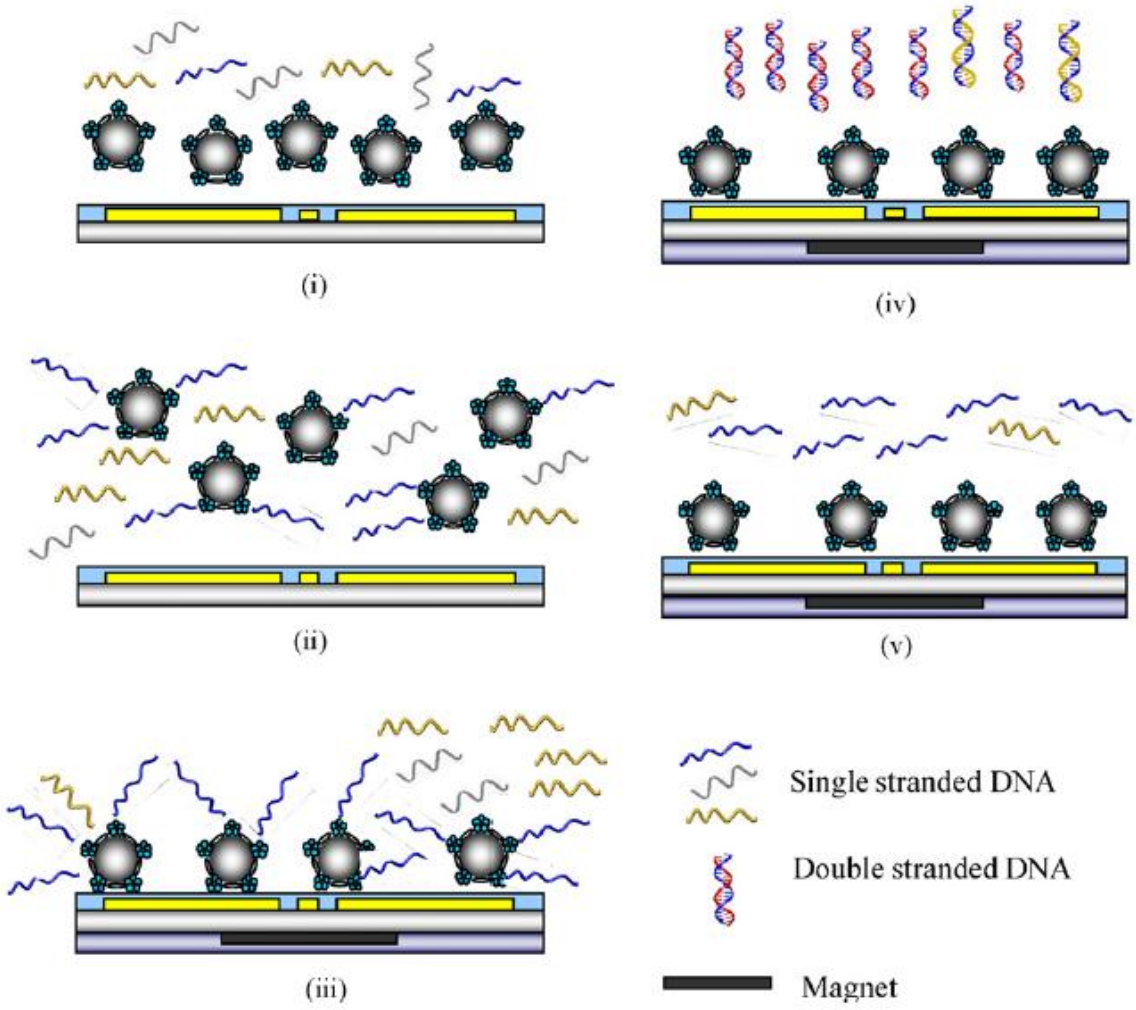

Figure 1-4. Previously reported on-chip SELEX protocol [87]. (i) DNA library is exposed to target-conjugated microbeads. (ii) Incubation of the library and beads results in aptamer candidates binding to beads. (iii) Weakly bound strands are washed away while strongly bound candidates remain adhered to magnetic beads held in place using a magnetic field. (iv) Aptamer candidates are amplified in situ in the microchamber, following introduction of amplification mixture. (v) Single-stranded aptamer candidates are eluted and used to restart the process. It is unclear how this last step of the process can be completed independent of manual user intervention (pipetting).

In summary, the present work in microfluidic aptamer generation demonstrates that microfluidics is capable of providing a highly efficient aptamer generation platform, but has yet to achieve its full potential. The capabilities of the most popular microscale SELEX protocols are compared to a conventional method in Table 1-1. Microfluidic selection has been proven highly effective as a standalone module, and integrated SELEX devices have demonstrated improvements in time and resource efficiency, but integrated SELEX devices have yet to achieve highly effective selection. Achieving this goal is the focus of this dissertation.

Table 1-1. Comparison of a conventional SELEX protocol (affinity column separation and conventional PCR) to newer microscale methods.

Selection Technique	# of Rounds Needed	Round Time	Overall Time Needed	Integrated/ Automated?
Affinity Column	10 - 20	Days	Months	No
Robotic [70]	15 - 20	4 hours	3 days	Yes
Sol-gel [92, 93]	7 - 9	3.5 hours	3 days	No
Capillary Electrophoresis [94]	1 - 3		2 days	No
Microbead μFluidic SELEX [88]	6	2 hours	1 day	Yes
M-SELEX [2, 82]	1 - 3	2 hours	1 day	No

1-4 Significance of This Work

Aptamers hold the promise of revolutionizing fields such as biosensing and therapeutics, but this potential has been hampered by the lack of available aptamers for potential targets. The detection of bioterror agents, identification of trace compounds, and cancer research are all fields of active aptamer-related research that are tremendously slowed by the requirements of SELEX. This problem - the immense effort necessary to

generate aptamers – is the problem which this dissertation addresses. Aptamer generation primarily consists of two procedures: a separation of nucleic acids, and biochemical amplification. These procedures, separately, have been the subject of a great deal of microfluidic research, but have not been effectively executed and combined to create an efficient microfluidic SELEX device. By integrating them to perform SELEX, dramatic advances in a number of fields would be enabled vis-à-vis the much greater availability of aptamers for potential targets. In particular, this dissertation addresses two key issues with the current state of the art in microfluidic SELEX devices: integration of highly efficient microfluidic selection and amplification to maximize efficiency, and temperature-specific microfluidic selection.

1-4.1 Integration of microfluidic selection and amplification for highly efficient SELEX

A key failing of previous microfluidic SELEX implementations has been that the most efficient selection protocols, those found in microfluidic devices, have not been integrated to perform microfluidic SELEX on-chip. These protocols, in which hydrodynamic flows separate unwanted nucleic acids from those bound to target-conjugated magnetic beads held in place with a magnetic field, are capable of developing high-affinity aptamers in 1 to 3 rounds of selection. However, users still perform conventional PCR and manually pipette solutions during the process, requiring more time and increasing the opportunity for user-introduced errors. In addition, the integrated devices developed thus far do not effectively couple the amplification and selection protocols, resulting in loss of efficiency due to contamination of the candidate pool with

unwanted nucleic acids. This dissertation will exploit a bead-based PCR scheme to successfully integrate highly effective microfluidic selection with microscale PCR in an integrated device to generate high-affinity aptamers in the shortest time possible.

1-4.2 Temperature-specific microfluidic selection

The ability to predetermine binding traits has been an active area of investigation in SELEX research. For example, approaches have been developed to allow selection of aptamers with particular dissociation constants (K_D) and thermodynamic binding characteristics [95, 96]. In addition, the temperature-sensitive nature of aptamer-target binding has been exploited to develop aptamers which bind to targets at predetermined temperatures [33, 69]. With conventional selection technology, this is particularly time-consuming, as the experimental setup is cumbersome. In this dissertation, local temperature control on microfluidic chips is exploited to enable highly accurate temperature-specific selection of target-binding aptamers. The significance of this improvement is twofold: firstly, all previous microfluidic SELEX devices implement isothermal selection. Incorporation of temperature specificity in the microfluidic selection protocol is therefore highly novel. Second, temperature control during selection is not a thoroughly explored aspect of aptamer selection, most likely due to the difficulties associated with implementing temperature-specific selection with conventional SELEX equipment. The use of temperature as a second domain across which to isolate target-binding sequences may have important implications in the larger field of SELEX. Therapeutics is rapidly becoming a very popular area of aptamer research, and aptamers intended for *in vivo* applications benefit from increased binding strength at physiological

temperatures. While temperature-specific binding has previously been demonstrated, it may be possible to select aptamers with a wider range of temperature stability. This trait would be highly advantageous to aptamers with applications in therapeutics or extreme environments.

1-4.3 Summary

This work represents the first time a microfluidic SELEX device with integrated temperature-specific selection has been reported. In addition to performing SELEX, the devices exploit another newly developed technology, microfluidic bead-based polymerase chain reaction, to allow successful on-chip integration of highly efficient selection with amplification. The dissertation also describes a novel microfluidic cocaine aptasensor, which uses the same bead-based microfluidic platform to perform highly specific detection of cocaine.

1-5 Organization of dissertation

This dissertation develops the technology necessary to fabricate and operate an integrated microfluidic SELEX device which generates high-affinity aptamers with temperature-specific binding properties. Following this introduction, Chapter 2 discusses the implementation of a microfluidic aptasensor for cocaine which uses microbeads as an affinity binding surface. This device develops the bead-based microfluidic architecture that will be applied in following chapters. Chapter 3 builds upon the bead-based microfluidic platform by demonstrating a microfluidic bead-based polymerase chain reaction device that is capable of integrated operations. This device is shown to be

capable of detecting DNA, but also functions as a DNA capture and purification component of an integrated microfluidic device. In Chapter 4, the bead-based PCR device is integrated with a microfluidic selection chamber, demonstrating that this strategy for an integrated SELEX device is feasible by performing a single round of SELEX. In Chapter 5 this design is further developed by "closing the loop," performing multiple rounds of SELEX in an integrated microfluidic device. Future work and conclusions will be presented in Chapter 6.

Chapter 2: A Microfluidic Affinity Sensor for the Detection of Cocaine

2-1 Introduction

The detection and quantification of trace amounts of illicit substances such as cocaine continues to be important for law enforcement and clinical medicine. Law enforcement officials must be able to detect trace amounts of cocaine in probationary offenders, and larger concentrations concealed by suspected users employing masking agents. In clinical medicine the detection of street drugs in patients of pain management practices requires frequent testing [97] that can be prohibitively expensive. Conventional methods available for cocaine detection include chromatography, presumptive testing, and immunoassays. Among these, gas chromatography-mass spectrometry (GC-MS) continues to be the gold standard in illicit material detection [98] given its sensitivity and reliability. Other chromatographic techniques, such as liquid chromatography (LC) and thin-layer chromatography (TLC) are also commonly used. In GC a sample of analyte is pushed through a column of adsorbent media, separating the constituents. LC systems are very similar, using a liquid as the carrier fluid instead of a gas, and TLC draws fluids across an adsorbent using capillary action. Unfortunately, GC-MS is inherently expensive, requiring a great deal of time, complicated equipment, and trained personnel. LC is typically even more expensive, and along with TLC gives poorer results due to its limited separation efficiency [99]. A more time-efficient alternative to chromatographic methods is presumptive testing using colorimetric reagents that rapidly react with a number of chemicals, but this approach is limited by a lack of specificity in that the reagents react

non-specifically with target analytes [100, 101]. To address the limitations of conventional techniques for detecting cocaine such as non-specificity and expense, the use of affinity sensing is highly attractive.

In affinity sensing, a target analyte is recognized by affinity binding with a receptor. That is, the analyte and receptor molecules join via specific hydrogen bonds, stacking of moieties, and analyte-induced receptor conformational changes which result in highly specific and reversible binding. Commonly used affinity receptors include antibodies, lectins, enzymes, and in particular, aptamers [102]. Aptamers are single stranded DNA and RNA oligonucleotides specifically selected for their binding affinity towards a specific target molecule [103]. Exposure to a target molecule induces conformational changes in aptamer structure facilitating binding that is both highly specific and reversible. Aptamers are easily chemically modified and are generated *in vitro*, resulting in no batch-to-batch variation in binding efficiency. As such, aptamers are attractive affinity receptors for cocaine detection. For instance, colorimetric sensing of cocaine was reported using aptamers conjugated to gold nanoparticles [104, 105]. Additionally, UV absorption spectroscopy combined with aptamer-based solid-phase extraction was used to detect cocaine at micromolar concentrations in complex media on a large-scale liquid chromatography platform [106]. Cocaine sensing using aptamers has also been demonstrated using Raman scattering methods, in which aptamers bound to a silver colloid surface and labeled with a Raman reporter allowed detection of micromolar quantities of cocaine [107]. Furthermore, cocaine binding with a surface-immobilized aptamer can be measured via reduction of an electroactive species tethered to the distal end of the aptamer. This has allowed cocaine detection at the micromolar level using

electrochemical methods [108], or with 1 nM detection limits using electrochemiluminescent methods [109]. Implemented on conventional platforms, these aptamer-based cocaine sensing approaches generally involve large reagent consumption, require bulky equipment, and are labor-intensive. These limitations hinder the realization of cocaine detection in portable, user-friendly systems.

Miniaturization technology holds potential for rapid, sensitive detection of cocaine with minute sample quantities. A microfluidic adaptation of a standard presumptive test for cocaine was fabricated, consisting of a microchannel into which was deposited a small amount of cobalt thiocyanate [110]. While still limited by conventional presumptive testing, the microfluidic device led to reduced sample consumption and allowed for device regeneration. In a different approach, a microfluidic sensor based on antibodies attached to a quartz crystal microbalance demonstrated rapid detection (<1 minute) of nanograms of cocaine [111]. However, the use of antibodies makes the sensor regeneration difficult, and may also lead to batch-to-batch variations in sensor performance. More recently, a microfluidic continuous-flow aptasensor was reported that uses an electrochemical method for detection of cocaine amongst other compounds in blood serum-based samples [43]. Micromolar detection limits were demonstrated.

This chapter presents a microfluidic aptamer-based biosensor for cocaine that uses a cocaine-specific DNA aptamer modified with a fluorophore. Based on a device architecture designed for highly specific solid-phase extraction [112, 113], this sensor is capable of low-cost quantitative cocaine detection in a highly specific, signal-on, and label-free manner. The device is demonstrated to be capable of specifically detecting cocaine at concentrations as low as 10 pM, with a linear response over four orders of

magnitude. Additionally, the device can be conveniently regenerated for reuse by a modest temperature change via on-chip temperature control. As such, the device can potentially be used for sensitive and rapid detection of cocaine in practical clinical and law enforcement applications.

2-2 Principle and Design

The device consists of a microfluidic chamber and channels fabricated from (poly)dimethylsiloxane (PDMS) and bonded to a glass substrate integrated with a resistive micro heater and temperature sensor (Figure 2-1a). The inlet and outlet microchannels are utilized for sample and buffer introduction and removal from the device, while an auxiliary microchannel is used for bead packing. Microweirs (15 μm high) separate the microchamber (130 μm high) from the inlet and outlet microchannels and serve to retain the beads in the microchamber. The on-chip microheater has a serpentine layout and directly covers the microchamber area to facilitate uniform heating of the microchamber area. A resistive temperature sensor is placed at the center of the microchamber to provide accurate temperature measurement for thermal control. The device was fabricated using soft lithography and lift-off techniques (Figure 2-1b). A mold was fabricated from the negative photoresist SU-8, and a 10:1 mixture of PDMS pre-polymer and curing agent was cast over the mold to fabricate microchannels in a PDMS slab. This was bonded to a glass slide with integrated heaters and sensors. Details of the fabrication process are described elsewhere [113].

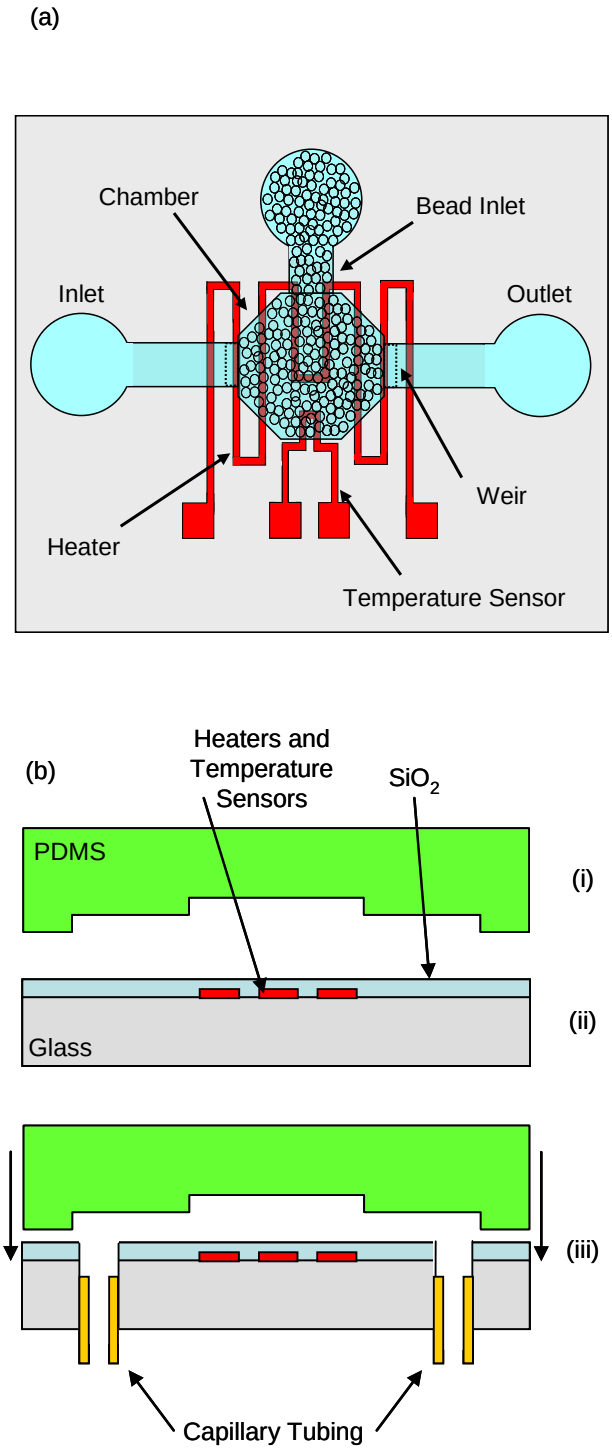

Figure 2-1. (a) Schematic of the microfluidic cocaine sensor, and (b) fabrication process: (i) microfluidic features are defined in PDMS, (ii) heaters and temperature sensors are fabricated on a glass slide, (iii) the PDMS and glass slide are bonded together.

A Förster resonance energy transfer (FRET) system is utilized to signal cocaine binding to the aptamer. FRET systems involve the coupling of a fluorescent molecule that emits visible light (fluorophore) to another fluorescent molecule that absorbs visible light and emits at invisible wavelengths (quencher). Carboxyfluorescein (FAM) is used in this work as a visible-range fluorophore, which, attached to a cocaine-specific aptamer (below), is characterized by a peak absorption wavelength of 494 nm and a peak emission wavelength of 518 nm [114]. Dabcyl is employed as a quencher molecule, which absorbs light over a wide range of wavelengths and dissipates the light as infrared energy. When placed in close proximity to FAM, Dabcyl causes a drastic reduction in visible emission during excitation at 494 nm. To exploit the FRET system within the microfluidic device for aptamer-based cocaine detection, a DNA aptamer is employed that is adapted from the sequences originally obtained for free solution aptamer-cocaine binding [34]. A FAM molecule is attached to the 5′ end of the aptamer, and a biotin molecule at its 3′ end. This allows the aptamer to be immobilized onto a streptavidin functionalized surface via biotin-streptavidin interaction with the FAM molecule at the free end (Figure 2-2a). In order to establish a baseline signal, a Dabcyl molecule, attached to the 3′ end of a short DNA strand complementary to the aptamer, is introduced. This strand hybridizes to the distal end of the aptamer (Figure 2-2b), bringing the FAM fluorophore and Dabcyl quencher into close proximity. Thus, the baseline consists of a drastically reduced level of fluorescence. Upon introduction of unlabeled cocaine (i.e. cocaine molecules not altered by any labeling group for transduction), the aptamer selectively and conformably binds to the cocaine, which disrupts the interaction of the relatively weaker binding

quencher strand, as shown in Figure 2-2c. The displacement of the Dabcyl molecule results in a recovery of fluorescence (i.e., a signal-on response) in proportion to the concentration of cocaine. In this manner, the device accomplishes signal-on, label-free detection of cocaine.

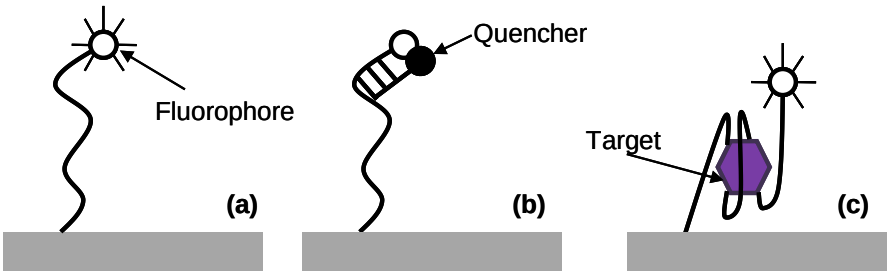

Figure 2-2. Signal-on aptamer-based cocaine detection. (a) A fluorophore-labeled aptamer is immobilized onto a solid surface. (b) A quencher-labeled short complimentary strand is introduced, decreasing fluorescence. (c) Unlabeled cocaine binds competitively to the aptamer, displacing the quencher and reducing fluorescence.

2-3 Experimental

2-3.1 Materials and Instrumentation

DNA was obtained from Integrated DNA Technologies (IDTDNA), Coralville, IA, in lyophilized form. The aptamer is of sequence 5′-FAM-A TCT CGG GAC GAC AGG ATT TTC CTC AAT GAA GTG GGT CGT CCC-Bio-3′, and the quencher-modified short complimentary strand is of sequence 5′-GTC GTC CCG AGA T-Dabcyl-3′. A stock concentration of each strand at 100 μM concentration was created using buffer solution consisting of pH 7.4 Tris-HCl, 150 mM NaCl, 5 mM KCl and 2 mM $MgCl_2$. Stock solutions were then diluted and aliquoted prior to testing. Ultralink Streptavidin-

coated microbeads (80 – 120 μm in diameter) consisting of a copolymer of bis-acrylamide and azlactone were obtained from Thermo Scientific Pierce Protein Research Products. Microfabrication materials such as SU-8 2050, 2100 (MicroChem) and S1818 (Microposit), Sylgard 184 PDMS (Dow Corning), glass microscope slides (Fisher Science), and glass capillary tubing (Polymicro Technologies) were purchased from Microchem, Robert McKeown, Fisher Science, and Polymicro Technologies respectively. Fluorescence measurements were conducted on a Nikon Diaphot 300 Inverted Fluorescence Microscope coupled to a CCD digital camera (Micrometrics 190CU) and a Nikon HB-10103AF light source. Thermal measurement and feedback were conducted using a LabView program incorporating a proportional-integrative-derivative (PID) controller, 5½ digit NI PCI-4060 PCI digital multimeter card, and Agilent E3631A Power Supply. A New Era Pump Systems syringe pump model NE-1000 was used for pneumatic flow actuation.

2-3.2 Experimental Protocol

The temperature dependence of resistivity of the temperature sensor was characterized using an environmental chamber, where the internal temperature was monitored with a platinum resistance temperature detector (RTD) probe (Hart Scientific 5628) and benchtop digital multimeter (Agilent 34420A). The temperature sensor resistance exhibited a linear response over the experimental temperature range. A temperature coefficient of resistance for the sensor can be calculated using equation 2.1.

$$R_{ref}\left[1+\alpha\left(T-T_{ref}\right)\right]=R \qquad \textbf{Eq. 2.1}$$

Following thermal characterization, the microbeads were introduced into the biosensor prior to experimentation. A buffer diluted sample of microbeads was pumped through the bead inlet until complete packing was achieved. This inlet was then sealed and the sensor placed in an enclosure on the microscope stage to block ambient light. A 10 μL sample of 2 μM aptamer solution was then introduced into the microchamber at 2 μL/min via the solution inlet. Following incubation and a wash with 10 μL of pure buffer, this step was repeated. This procedure was then repeated with 2 samples of 5 μM quencher solution. In every such procedure, two samples of solution (aptamers or quenchers) were used to ensure adequate and uniform coating of the microbeads. Images were taken after each wash with buffer solution to provide baseline fluorescence readings. When testing the response of the sensor to a concentration of cocaine, similar procedures were used for sample introduction with the exception that one sample of cocaine was used, followed by a wash in pure buffer. When testing the ability of the sensor to concentrate cocaine, the subsequent buffer wash was omitted.

After each introduction, incubation and washing procedure involving aptamers, quenchers, or cocaine, the sensor was briefly (<5 s) excited with blue light using the fluorescent light source. Image acquisition was accomplished by opening the microscope shutter to the fluorescent light source and exciting a darkfield image of the transparent sensor. Resulting fluorescent emissions were captured by the inverted microscope and recorded by the attached Micrometrics CCD camera and associated software. Digital photographs were then analyzed using ImageJ software, brightness intensity was measured, and these values were used to calculate values of relative fluorescence. The

sensor was otherwise kept in a dark environment to minimize the effect of photobleaching.

2-4 Results and Discussion

2-4.1 Device Calibration

Prior to testing with cocaine detection, the response of the on-chip temperature sensor and the effect of photobleaching on the system were characterized. Measurements show that the resistance of a typical temperature sensor varies linearly with temperature in the desired experimental range (Figure 2-3) with a temperature coefficient of resistance of approximately 2.2×10^{-3} °C^{-1}. The effect of photobleaching on the biosensor was then tested with an aptamer-functionalized bead packed microchamber (Figure 2-4). Over a time period representative of this work, the signal changes by approximately 4%, a negligible rate of decay. These results indicate that photobleaching can be eliminated as a potential source of signal drift during the cocaine sensing experiments.

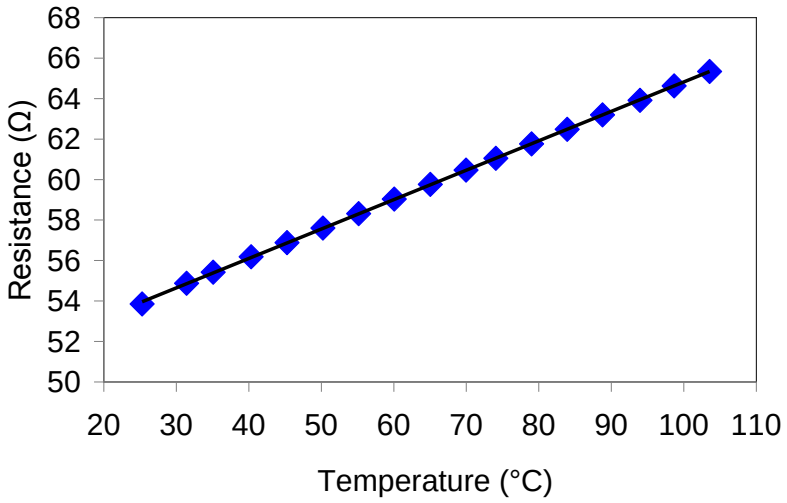

Figure 2-3. Measured electrical resistance of the temperature sensor as a function of temperature.

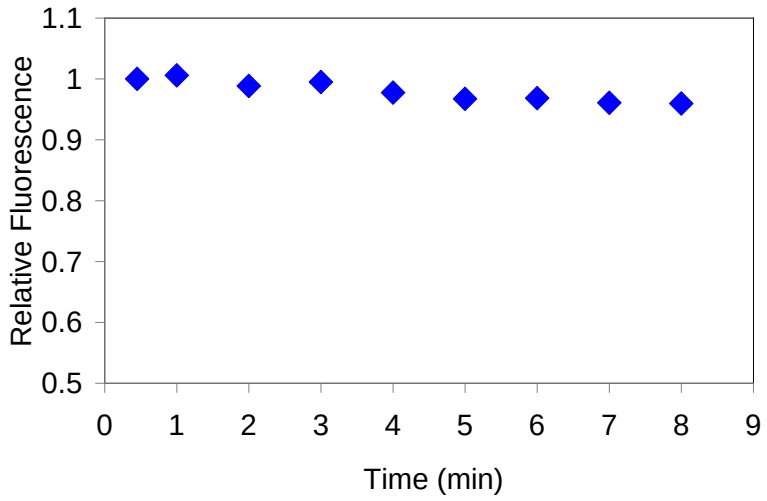

Figure 2-4. Effect of photobleaching on the relative fluorescence over time.

2-4.2 Transient Response

For accurate fluorescence measurements, the aptamer-binding system must have reached equilibrium prior to exciting the fluorophores and acquiring a signal. To ensure this was achieved during experimentation, the transient response of the biosensor following introduction of all sample types (aptamers, quenchers, and cocaine) was characterized. The transient fluorescent response to addition of aptamers was found to be near instantaneous (data not shown). To test the transient response of the quenchers, a standard 5 μM sample of quencher solution was introduced and fluorescence response was measured intermittently over a period of 8 minutes (Figure 2-5). The transient response of the biosensor to quencher introduction was slower than that of aptamer introduction, with full quenching occurring within 8 minutes. This time response is most likely a result of the difference in kinetics between biotin-streptavidin binding and the hybridization of the complimentary strand to the aptamer. As a result, all future quenching solutions were allowed to incubate for at least 10 minutes before cocaine introduction.

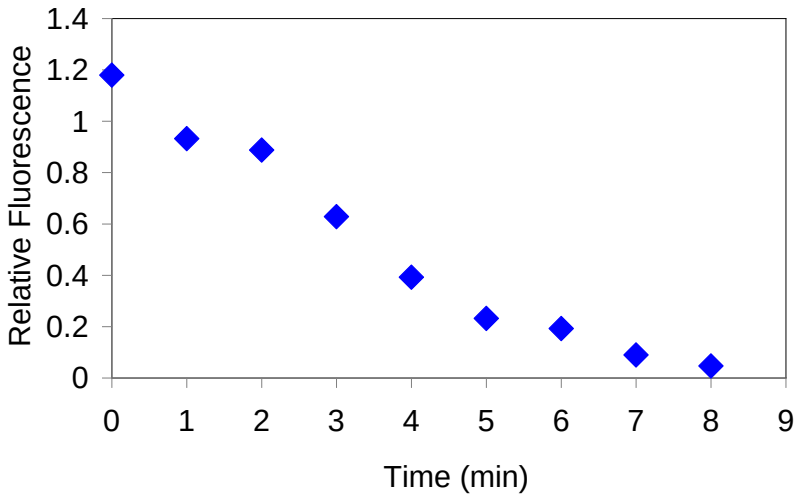

Figure 2-5. Transient response of the sensor to introduction of quencher solution.

Subsequently, the time-dependent fluorescence response of the sensor to introduction of cocaine was measured. Specifically, a 1 μM sample of cocaine was introduced to a prepared sensor and the fluorescence response was measured versus time for six minutes (Figure 2-6). Fluorescence intensity appeared to achieve steady state after a period of approximately three minutes, indicating that the sensor has a time constant of approximately 1.2 minutes, and a settling time of almost 5 minutes with respect to cocaine. This result was expected, as the aptamers express a higher affinity for the cocaine molecules than the quencher-labeled short complimentary strands but lower than that of a biotin-streptavidin interaction. As a result, equilibrium with the target analyte was achieved at a faster rate than with the quencher molecules, but slower than with introduction of aptamers alone. This test was repeated at several other cocaine concentrations with similar results (data not shown), indicating that the transient response was independent of the concentration of cocaine being tested. During subsequent

experiments, a cocaine sample would be incubated before washing for at least five minutes to ensure complete interaction of the cocaine and aptamer for maximum fluorescence response. This information was also used to estimate a flowrate necessary for experiments in which a device would be exposed to a continuous flow of cocaine.

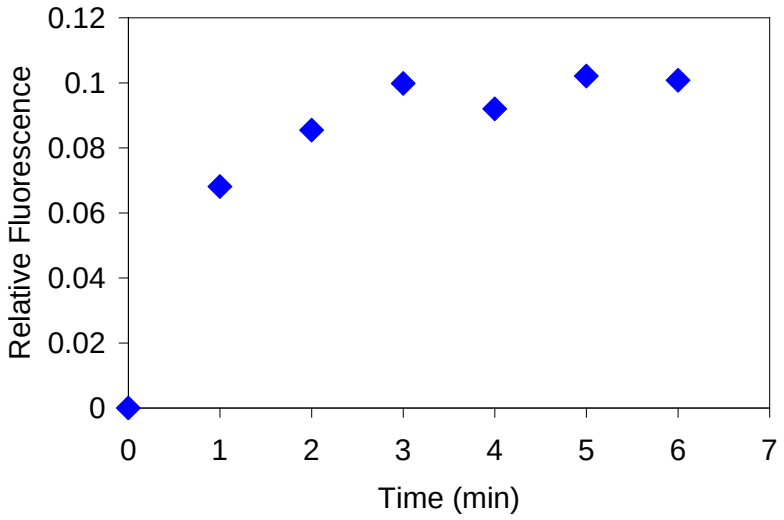

Figure 2-6. Transient response of the sensor to introduction of cocaine (1 μM).

2-4.3 Detection of Cocaine

The response of the sensor to various concentrations of cocaine was then tested. The sensor was tested using practically relevant concentrations of cocaine, from 1 nM to 100 μM, in a buffer solution designed to mimic the environmental conditions (pH, salt content) of human bodily fluid (Figure 2-7). Previously published data indicated that for a single dosage of cocaine, the maximum concentration of cocaine in the blood plasma of the user would be 1 μM [115]. As concentrations higher than 1 μM may be of interest in law enforcement forensics, a test at a concentration of 100 μM was included as well. The

sensor exhibits a considerably linear response over the range of concentrations tested, indicating a four orders of magnitude linear range. As an experimental control, introduction of a control molecule, Deoxycholic Acid (DCA) in the identical concentration range, was also performed using the biosensor. DCA was chosen given its structural similarity to cocaine and common presence in the body. No appreciable signal was observed above a relative fluorescence of 0.2 for even the largest tested concentration (1 mM), which is equivalent to that of approximately 10 nM cocaine. Although this would indicate detection ambiguity during experiments involving low concentrations of cocaine, this is not anticipated to occur in practice since physiological DCA concentration is relatively low compared to tested levels [116]. It is concluded from this data that the sensor is capable of detecting practically relevant concentrations of cocaine and compares well with previously reported aptamer-based cocaine sensors [105, 108]. A relatively large degree of variability from test to test can be observed from Figure 2-7, where error bars are computed based on three independent tests. Analysis suggests that this can be largely attributed to the limited resolution of the rudimentary fluorescence microscopy system used for this study. Therefore, it is anticipated that improved fluorescence imaging would considerably reduce this variability. Additional sources of error may include variations in bead packing density, the presence of bubbles in the sensing chamber, and loss of sample due to dead volumes. These issues will be investigated in future work.

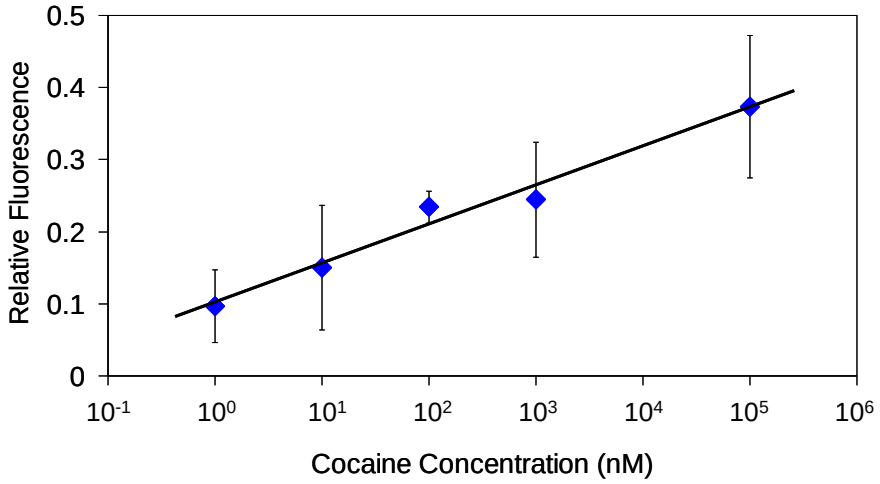

Figure 2-7. Response of the sensor to cocaine at varying concentrations.

2-4.4 Improving Detection Limits by Continuous-Flow Concentration

Previous work has demonstrated the ability of aptamers to concentrate and purify target analytes [113]. Due to the equilibrium-binding nature of the aptamer-analyte system, repeated exposure of the sensing surface to low concentrations of target analyte results in continued extraction of the analyte from the solution. Here, this phenomenon is exploited to concentrate dilute samples of cocaine for subsequently improved detection. The sensor was continuously infused with a sample of 10 pM cocaine solution at a rate of 2 μL/min. This flowrate was calculated based on the size of the sensing chamber (1 μL) and the transient response of the sensor to introduction of cocaine. As a result of the increasing concentration of cocaine at the sensing surface, the relative fluorescent signal increased to a value similar to a much higher concentration of cocaine (Figure 2-8). At time intervals of 5 to 30 minutes, fluorescence intensity was measured, which increased until a saturation value of approximately 0.18 relative units was achieved after 175 minutes. This fluorescence value corresponds to a single sample of 5 nM cocaine,

indicating that the sensor concentrated the cocaine by a factor of 500. This technique allows for detection of trace amounts of cocaine in concentrations otherwise undetectable by other aptamer-based cocaine sensors [108, 109].

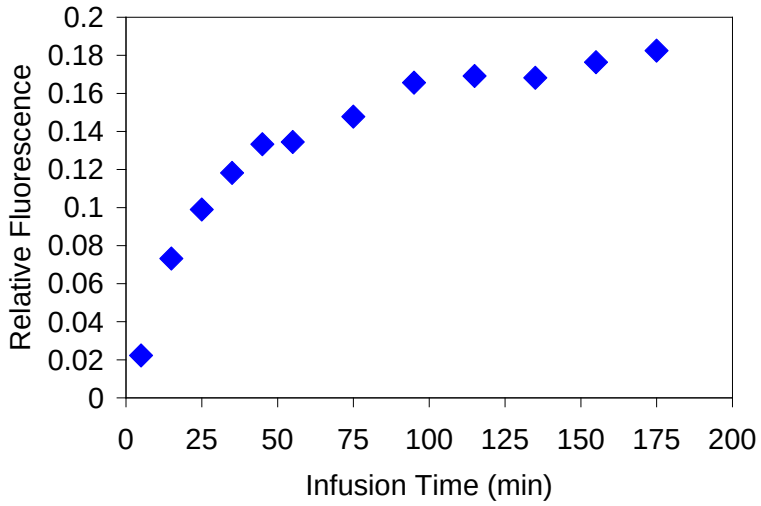

Figure 2-8. Time-resolved relative fluorescence as cocaine is concentrated from a continuous flow (2 μL/min) of a highly dilute solution (10 pM).

2-4.5 Thermally Based Device Regeneration

There are many device applications for which continued reuse of a single sensor would be advantageous. This device makes use of the temperature-sensitive nature of aptamer-analyte binding to render it fully reusable. In order to investigate the ability of the sensor to be regenerated, the effect of temperature on the sensing surface was tested (Figure 2-9). Following introduction of a 100 μM sample of cocaine, the on-chip heater and temperature sensor were used to raise the temperature of the chamber from room temperature to 37°C while flowing pure buffer solution at 10 μL/min. Upon starting the test, a small increase in relative fluorescence at low temperatures was witnessed. This is

likely attributed to hydrodynamic forces removing a small amount of quencher strands prior to the onset of temperature-induced conformational changes. As the chamber temperature was increased, a larger change in fluorescence intensity was seen at approximately 33°C. This indicates that at this temperature, changes in the secondary structure of the aptamer result in the release of the cocaine molecule and leftover quencher strands. Signal increase continued until it saturated at approximately 37°C at a value of 1, demonstrating successful regeneration of the aptamer surface. This indicates that the sensor can be heated to a relatively modest temperature to effectively release cocaine using a single homogeneous phase.

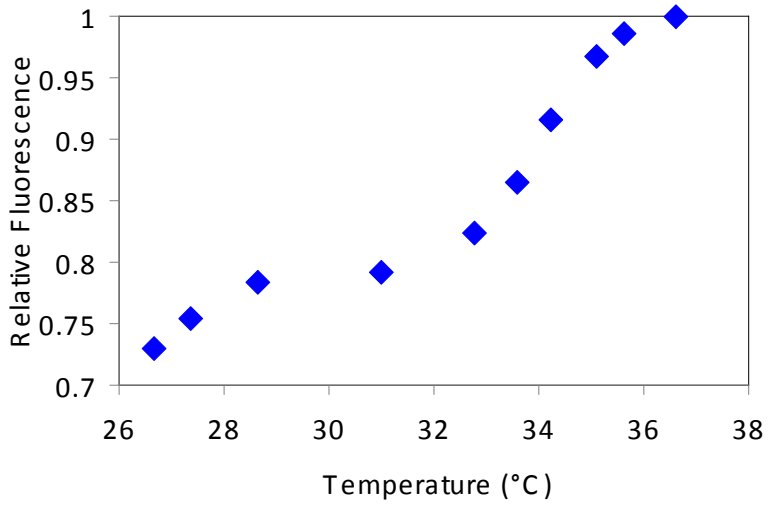

Figure 2-9. Effect of temperature on relative fluorescence from a sensor incubated with 100 μM cocaine solution. Return of relative fluorescence to 1 indicates successful regeneration of the aptamer surface.

In order to be fully regenerable, the device must retain functionality following thermal release of cocaine. The device was subjected to multiple sensing cycles using a changing concentration of cocaine for each cycle (Figure 2-10). In each cycle, the standard procedure for testing a concentration of cocaine was used, followed by thermal regeneration that was implemented by raising the temperature of the sensing chamber to 37°C while flowing pure buffer through the chamber at 10 μL/minute. The hatched bars indicate relative fluorescence following regeneration (surfaces coated with aptamers only). Gray bars indicate quenched sensors, and the black bars indicate sensor response to incubation of a sample of cocaine. The data indicates that the device behaves predictably without significant drift, with the response to cocaine concentration changing predictably with each consecutive test. The device was capable of detection of 1 nM cocaine concentration after regeneration (data not shown). Thus, modest heating and washing grants the device repeated use without loss of functionality, an improvement over previously reported cocaine sensors [108, 111].

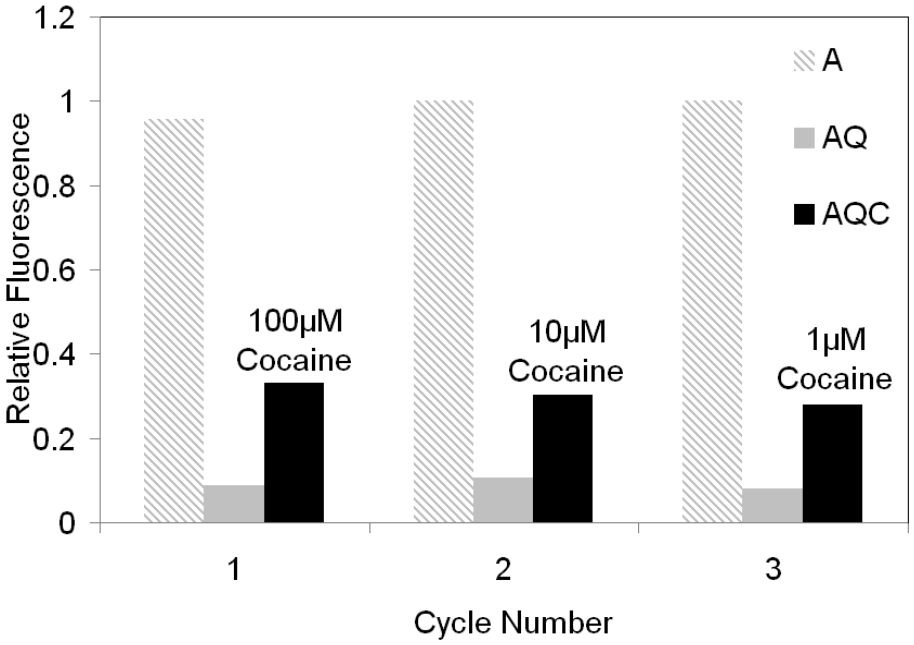

Figure 2-10. Reuse of the sensor after regeneration. In each cycle, the sensor was first thermally regenerated at 37°C (A), quenched (AQ), and finally exposed to cocaine (AQC).

2-5 Conclusions

Detection of trace amounts of illicit substances such as cocaine continues to be an important function in law enforcement and clinical medicine. Prevalent methods of detection in these fields such as GC-MS and presumptive testing allow for either accurate, specific detection involving expensive testing or rapid, economized detection that is unreliable due to its lack of specificity. This chapter describes a novel microfluidic fluorescence aptamer-based biosensor which can rapidly detect low concentrations of cocaine. The device is characterized by high selectivity and sensitivity (10 pM), as well as rapid response and reduced sample consumption. The transient response of the sensor (equilibration in less than 5 minutes) is comparable to the detection time of cocaine in a

GC-based system, but with the potential to bypass the need for cumbersome equipment and highly-trained technicians. When testing samples of cocaine, the sensor responded linearly to cocaine concentration from 1 nM to 100 μM using only 10 μL of cocaine sample with a 5 minute response time. Due to the nature of aptamer-target binding, which is sensitive to external stimuli, it was shown that an increase in temperature from ambient to 37°C results in the release of the bound cocaine. Full reusability of the device was then demonstrated by multiple tests involving sensing and regeneration following a wash with pure buffer and a mild increase in temperature. As the sensor is designed along standard microfabrication principles, mass production to reduce manufacturing costs should be possible. This represents an improvement over previous aptamer-based cocaine sensors as well as a viable alternative to conventional methods of cocaine detection. Further work will include possible improvements to the cocaine sensing system, including alternate choices of chamber geometries and fluorophore-quencher pairs.

Chapter 3: Bead-Based Polymerase Chain Reaction on a Microchip

3-1 Introduction

Chemical amplification of nucleic acids is most commonly realized with the polymerase chain reaction (PCR), in which a DNA molecule, referred to as a template, is exponentially duplicated via repeated thermal denaturation and enzymatic replication [117]. Bead-based PCR is a variant of the PCR procedure that uses primers (short DNA fragments complementary to a specific region of the template) attached to microbeads. This procedure results in bead-tethered template DNA duplicates; it is hence an attractive analytical tool that simultaneously accumulates signals from DNA-based transducers and allows manipulation of DNA itself via solid-phase extraction (SPE) techniques.

In recent years, bead-based PCR has been used in a variety of applications including DNA sequencing, protein screening, and pathogenic DNA detection. For example, whole genome sequencing has been demonstrated with reduced cost and assay time by using bead-based PCR to facilitate the organization and detection of amplified sections of a fragmented *E. coli* genome [118]. Compartmentalization of DNA in emulsions [119] combined with bead-based PCR [120, 121] also provides a method of rapidly screening an entire genome for DNA binding proteins [122] and for cell-free protein synthesis [123]. In addition, genomic DNA (gDNA) has been detected using bead-based PCR [124], or similarly via PCR on nanostructured surfaces [52]. While demonstrating the utility of bead-based PCR, these examples primarily rely on

conventional instrumentation for reaction control (temperature cycling), involve tedious and error-prone manipulation of primer-coupled beads, and require laborious sample pre-treatment (e.g., for the separation of gDNA from cell lysate) prior to the PCR reaction. These limitations are a major hindrance to the widespread use of bead-based PCR.

Microfluidics technology addresses the limitations of conventional PCR schemes, most notably by providing a more rapid and efficient reaction platform. Extensive applications of microfluidics to PCR [79-81] have taken advantage of the more efficient heat transfer properties to create rapid, miniaturized PCR devices [125] capable of detecting as little as a single molecule of DNA [126]. Microfluidics has also enabled integrated chip-based systems that perform tasks such as sample pre-treatment and post-amplification analysis [89-91, 127], further improving reaction speed and test accuracy by shifting more operations to the microscale domain. In particular, microfluidic PCR has been used to detect gDNA [89, 91, 128, 129], resulting in improvements in sensitivity, specificity and turnaround times over other pathogen detection methods, such as cell culturing and antibody-based assays. However, these works have almost exclusively involved solution-based PCR (i.e., PCR with primers residing in solution), and while microfluidics holds the same advantages for solid-phase amplification there are far fewer applications of microfluidics to solid-phase PCR implementations such as bead-based PCR. Much of the bead-based PCR literature relies upon bead-based PCR in emulsions, in which case the emulsions are typically amplified in a conventional thermal cycler [120, 121, 123, 130-132]. In one relevant investigation reported recently, primers were tethered to nanostructured surfaces of a biochip to allow optical detection of human gDNA indicative of hemolytic diseases such as autoimmune hemolytic anemia [52]. However,

the nanostructures were based on a flat surface, limiting the surface area-to-volume ratio and leading to a practically inadequate sensitivity.

This chapter investigates bead-based PCR on a microfluidic chip by applying it to DNA pre-conditioning and detection, as demonstrated by the capture, amplification, and detection of trace quantities of a synthetic DNA sequence identical to a repetitive segment of the genome of *Bordetella pertussis* (*B. pertussis*). Trace DNA is introduced into the device microchamber along with PCR reagents and microbeads, and thermally cycled using an integrated heater and temperature sensor. The microbeads provide a high surface area to volume ratio platform for accumulation of transducing labels, creating a rapid, simple method to detect trace amounts of DNA. The bead-based design allows for simple integration with other functionalities, including sample purification [133] and downstream analysis. Experimental results show that a synthetically generated segment of the *B. pertussis* genome 181 base pairs (bp) in length can be detected in 10 PCR cycles (within 15 minutes) at a clinically relevant concentration of 1 pM (approximately 6×10^5 copies/μL). This approach is then demonstrated to perform integrated DNA capture, amplification, detection, and purification in a single microchamber. Bead-based PCR is thus shown to be both an effective DNA detection method and a DNA pre-conditioning, detection, and analysis system that can be simply integrated into microfluidic devices.

3-2 Materials and Methods

3-2.1 Bead-Based PCR Principle

PCR is a biochemical amplification process which uses a thermostable enzyme to dehybridize and duplicate template DNA. During a PCR reaction, cyclic changes in

temperature cause denaturation of template dsDNA and then hybridization of primers to the separated single-stranded DNA (ssDNA) strands. A temperature cycle consists of three steps: dsDNA melting (denaturation) at 95°C, primer annealing (hybridization) at 50 – 62°C, and DNA extension at 72°C. PCR reactions also typically include an initial melting step at 95°C (pre-melting) and a final extension step at 72°C. Reagents include two sets of primers: reverse primers that hybridize to template ssDNA, and forward primers that hybridize to the complementary ssDNA. Extension of these template-primer pairs by the thermostable Taq polymerase produces dsDNA consisting of the template and its complementary strand. Repeated temperature cycles result in amplification, i.e., generation of exponentially increasing duplicate copies of the dsDNA.

Bead-based PCR is a solid-phase implementation of PCR, in which DNA is duplicated while tethered to the surfaces of microbeads in solution. In bead-based PCR, one of the two primer sets (typically the reverse primer) is tethered to a bead surface, while the untethered (forward) primer can be labeled with a detectable tag (e.g., a fluorophore). Bead-bound reverse primers are mixed with template ssDNA, labeled forward primers and other reactants (e.g., nucleotides and Taq) in solution, and hybridize to template ssDNA molecules. This results in the capture of template DNA by the microbeads and is hence effectively a SPE process. This completes the first temperature cycle, which produces unlabeled dsDNA. During the second temperature cycle, the dsDNA from the previous cycle is denatured, allowing template DNA and fluorescently labeled forward primers to hybridize to bead-bound ssDNA (complementary strands of the template). Extension then generates labeled duplicates of template DNA hybridized to the bead-bound complementary strands. This process is then repeated with further

temperature cycles to produce exponentially increasing copies of dsDNA consisting of labeled template and unlabeled, bead-tethered complementary strands.

3-2.2 Microchip Design and Fabrication

The bead-based PCR microchip consists of a microfluidic chamber, which is fabricated in the elastomer polydimethylsiloxane (PDMS) and bonded to a glass slide with an integrated resistive heater and temperature sensor (Figure 3-1a). The heater has a serpentine geometry covering the chamber area as well as a large surrounding area to generate a sufficiently uniform temperature field in the chamber, while the resistive temperature sensor is located at the center of the chamber area. The cylindrical chamber is open to atmosphere and consists of two vertically aligned connected compartments of different diameter. The lower compartment contains the aqueous PCR sample, and expands to the upper compartment of larger diameter that retains a layer of mineral oil over the PCR sample. The entire chamber surface is conformally coated with a layer of the polymer Parylene C. The mineral oil and Parylene coating eliminate water evaporation that would otherwise occur directly to open air or through the PDMS, while minimizing the potential formation of air bubbles. The Parylene also provides a PCR-compatible surface, which, along with the use of additives such as bovine serum albumin (BSA) and Tween, minimizes adsorption of reaction components such as DNA and Taq polymerase [134].

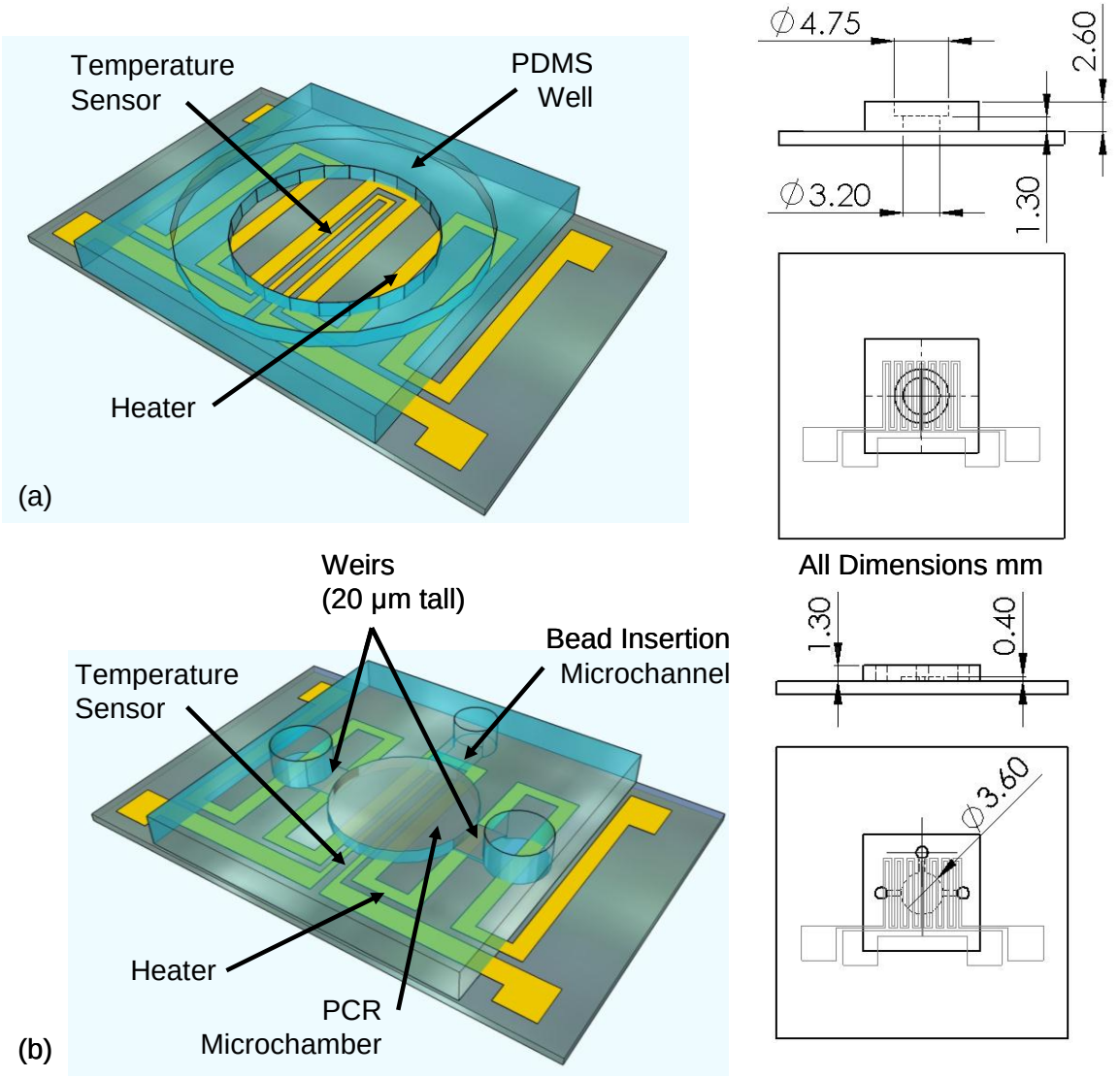

Figure 3-1. Device design. (a) The chip consists primarily of a PDMS chamber bonded to a glass slide which has been patterned with a micro heater and temperature sensor. Key dimensions of the PDMS microchamber have been included in projected top and side views (all dimensions in mm). (b) Also shown is the design of an integrated microfluidic device, in which weirs retain microbeads in the chamber while beads are exposed to streams of buffer or reagents.

Devices were fabricated using standard microfabrication techniques. Chrome and gold layers (thicknesses: 20 and 200 nm) were thermally deposited onto glass microscope slides and patterned using contact lithography and wet etching techniques. Patterning generated a 5.67 cm long by 200 μm wide heater having a resistance of approximately 20 ohms and covering an area of 0.242 cm^2, and a 1.04 cm long by 40 μm wide resistive temperature sensor having a resistance of approximately 30 ohms. The thermal elements were then passivated with SiO_2 (thickness: 1 μm) formed using plasma-enhanced chemical vapor deposition, with openings for electrical connections formed using a shadow mask. The SiO_2 not only passivates the electrical components, it provides an efficient bonding surface for PDMS. To generate PDMS for the microfluidic chambers, PDMS prepolymer was mixed 10:1 with a curing agent and poured onto a clean silicon wafer, baked for 30 minutes at 75°C, and then peeled from the wafer. Microfluidic chambers were defined by puncturing holes in the PDMS using a hole punch. The bottom PDMS piece was 1.3 mm thick with a 3.2 mm diameter hole, and the top piece was 1.3 mm thick with a 4.75 mm diameter hole. The glass substrate and PDMS sections were then treated using UV-generated ozone for 10 minutes, and bonded by baking at 75°C for 30 minutes. During bonding, the PDMS holes were aligned to the center of the integrated heater patterned onto the glass slide. The chip was then conformally coated with a layer of Parylene C approximately 1 μm in thickness via chemical vapor deposition, with scotch tape used to block electrical pads.

The chip design was also modified to demonstrate integrated microfluidic PCR, by incorporation of microfluidic channels enabling bead insertion and retention during wash steps (Figure 3-1b). Optical lithography was used to define an SU-8 mold for a 4

μL PCR chamber 400 μm in depth and 3.6 mm in diameter. The mold incorporated two inlets with flow restrictions limiting the local vertical channel clearance to 20 μm, serving as passive weirs to retain microbeads in the chamber, and a third inlet with no weir to be used for bead insertion. The microchamber and channels were again fabricated from PDMS, and bonded to a glass slide integrated with a resistive heater and temperature sensor.

In addition to designing and fabricating the microchip, the bead-based primers were designed to allow rapid and simple operation of the device. Biotin-streptavidin coupling was used in this study to attach the reverse primers to the beads, as this bond is both strong and formed spontaneously in the presence of both molecules. The reverse primers were synthesized with a dual-biotin label at the 5' end, followed by a spacer molecule adjacent to the nucleotide sequence. The dual-biotin moiety minimizes loss of signal due to thermal denaturation as investigated in Results and Discussion. Spacer molecules provide greater lateral separation between DNA on the beads, reducing hybridization issues due to steric hindrance. Synthetically generated template DNA was used to obtain controlled, consistent experimental results for characterization of DNA detection using bead-based PCR.

3-2.3 Application to Pathogenic DNA Detection

The bead-based PCR chip is applied to pathogenic DNA detection, demonstrated with a DNA sequence associated with *B. pertussis*. *Bordetella pertussis* is a gram-negative bacteria that infects approximately 48.5 million patients (with 300,000 fatalities) annually worldwide [135]. While early detection is key to the treatment of this disease,

current methods (e.g., cell culturing) for detecting the *B. pertussis* bacterium take days or even weeks of turnaround time [136, 137]. This limitation can be potentially addressed by the bead-based PCR microchip, which is designed to allow rapid, sensitive, and specific detection of *B. pertussis*.

Pathogenic DNA detection using bead-based PCR on a microchip can be accomplished as shown in Figure 3-2. Bead-tethered reverse primers on the chip can be exposed to a raw sample, such as cell lysate (Figure 3-2a). Pathogenic DNA in the sample is then captured and purified onto the beads via its specific hybridization to the reverse primers (Figure 3-2b), as demonstrated in previously published work [133]. Following capture and purification, template DNA can be mixed on-chip with PCR reactants and bead-based PCR of the template DNA can then be performed using fluorescently labeled forward primers (Figure 3-2c). This process rapidly generates exponentially amplified, fluorescently labeled template copies on microbeads, which can be detected by fluorescent microscopy. The use of beads in the detection volume generates an enhanced signal-to-noise ratio in comparison to amplification on flat solid surfaces [52, 118] due to a significant increase in the fluorophore-coated surface area. Finally, the labeled copies of the template can be freed from their bead-bound complements by denaturation and eluted into pure buffer for further analysis, while the bead-bound complementary strands (cDNA) can be retrieved from the chip and stored as cDNA libraries [138] (Figure 3-2d).

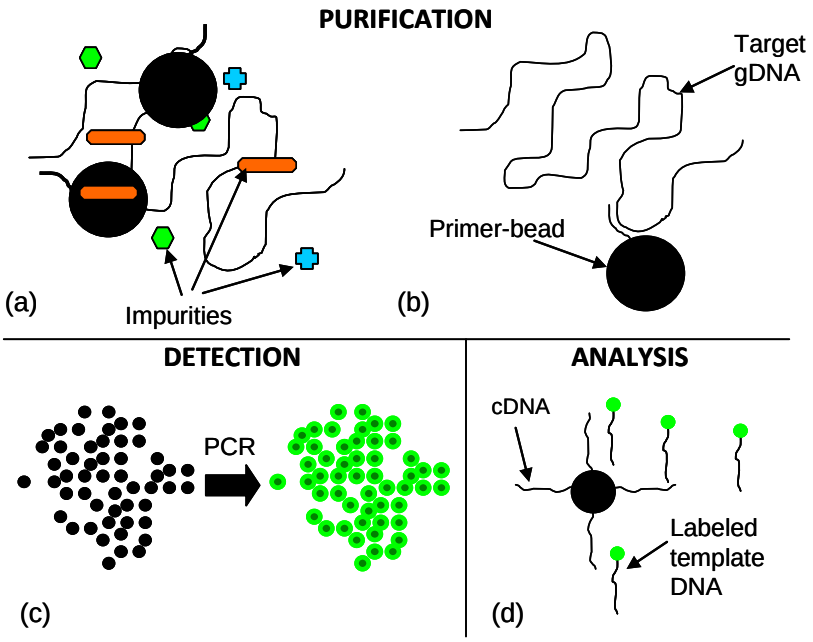

Figure 3-2. Integration of microchip bead-based PCR. Primer-coated beads permit separation of DNA from impurities (a,b), and amplification produces a fluorescent signal on the bead surfaces (c) via microchip PCR. The beads then act as a mechanism for either storage or collection and analysis of ssDNA following thermally-induced dehybridization and release (d).

3-2.4 Materials, Reagents, and Experimental Procedures

For detection of DNA associated with *B. pertussis*, the following materials and reagents were used. All DNA was obtained in lyophilized form from Integrated DNA Technologies, Coralville, IA. The primers are designed as a PCR assay for determination of *B. pertussis* infection [139, 140]. The DNA sequences used are as follows. Forward primer: 5'-FAM-Spacer-GAT TCA ATA GGT TGT ATG CAT GGT T-3', reverse primer: 5'-Double Biotin-Spacer-TTC AGG CAC ACA AAC TTG ATG GGC G-3', and template: 5'-GAT TCA ATA GGT TGT ATG CAT GGT TCA TCC GAA CCG GAT

TTG AGA AAC TGG AAA TCG CCA ACC CCC CAG TTC ACT CAA GGA GCC CGG CCG GAT GAA CAC CCA TAA GCA TGC CCG ATT GAC CTT CCT ACG TCG ACT CGA AAT GGT CCA GCA ATT GAT CGC CCA TCA AGT TTG TGT GCC TGA A-3'. The forward primer has been modified with the fluorescent label carboxyfluorescein at the 5' terminus, while the reverse primer incorporates a dual-biotin modification at the 5' end. Both molecules contain an inert spacer molecule between the 5' modifications and the nucleotide sequence. PCR was performed using Taq enzyme, deoxynucleotide triphosphates (dNTPs), and PCR reaction mixture containing appropriate buffers (Promega GoTaq Flexi PCR Mix). Reverse primers were immobilized onto streptavidin-coated polymer-based microbeads (Thermo Scientific Pierce Protein Research Products Ultralink Streptavidin Resin) averaging 80 μm in diameter. Concentration and purity measurements of DNA samples were conducted using UV/VIS (Thermo Scientific Nanodrop). Materials used in microfabrication included photoresist (Rohm & Haas Electronic Materials S1818, Microchem SU-8 2000), PDMS prepolymer (Dow Corning Sylgard 184), and Parylene C prepolymer (Kisko diX C).

PCR reaction mixture for *B. pertussis* DNA detection experiments was prepared as follows. Each lyophilized DNA sample was suspended in deionized H_2O and diluted to the desired concentration. The PCR mixture consisted of the following: 5× PCR Buffer (2 μL), 25 mM $MgCl_2$ (0.6 μL), 10 mM dNTPs (0.4 μL), 50 μg/mL BSA (0.4 μL), 5% (by volume) Tween 20 (0.1 μL), microbeads (0.5 μL), water (4.1 μL), 25 μM forward primer (0.4 μL), 25 μM reverse primer (0.4 μL), and enzyme (0.1 μL). The ingredients were mixed with template DNA (1 μL of synthetic template DNA with a concentration range of 1 aM to 100 pM) without the enzyme and the mixture was then degassed at -0.4 psi for

30 minutes in a darkened container (to prevent photobleaching of the fluorophore label). Testing in the PCR device also occurred under an enclosure to prevent excess light from reaching the DNA. Following degassing, enzyme was added to the mixture and the 10 μL PCR sample was pipetted into the chip, followed by 30 μL of mineral oil. During experiments with the integrated device, PCR reaction mixture was degassed without primer-coated beads. These were inserted into the device, followed by template DNA, after which the DNA and beads were allowed to incubate for 10 minutes. This solution was then removed (with the beads retained by the weirs), and the PCR reaction mixture was introduced. The temperature of the sample was then cycled using the Labview control program to implement the reaction.

During testing, the reaction temperature was controlled using a Labview program that utilized sensor feedback to maintain a constant temperature field inside the PDMS chamber. A desktop power supply (Agilent E3631A) and a digital multimeter card (NI PCI-4060) provided electrical power and resistance measurements. An inverted fluorescence microscope (Nikon Diaphot 300) was used for all fluorescence measurements, while an attached digital camera (Pixelink PL-B742U) was used to record images of the excited fluorescent field. The microscope contains a dichroic mirror which attenuates light above the peak absorption wavelength of the fluorophore (approximately 494 nm) during excitation and passes the higher emission wavelengths (which peak at approximately 512 nm) through the objective for observation and measurement.

Following PCR, the sample was pipetted to a darkened 0.5 mL microcentrifuge tube. Beads were washed 6 times with 1× SSC buffer to remove excess labeled primers. Bead washing was implemented by mixing the sample with buffer, allowing the beads to

settle via gravity, and removing the supernatant with a pipette. A five microliter aliquot of each test sample was pipetted into an individual 3.2 mm diameter PDMS well on a glass slide, and was observed using the fluorescent microscope. During integrated device testing, microbeads were washed by passing buffer through the chamber while being retained by the weirs (Section 3-2.2) prior to fluorescent measurement. The microscope was kept in an enclosure to prevent ambient light from interfering with the measurements or bleaching the fluorescent labels. The samples were briefly excited with light using the fluorescent light source and the resulting emission was recorded using the CCD camera microscope attachment. Camera exposure times were optimized based on fluorescent signal intensity during device characterization (Sections 3-3.1 and 3-3.2) to maximize the signal-to-noise ratio, defined here as the ratio of the measured fluorescence intensity to the intensity of background fluorescence. While this did not guarantee a single baseline signal intensity during the tests, the use of relative fluorescence intensity allowed consistent interpretation of the experimental results. Digital images were analyzed using ImageJ software.

3-3 Results and Discussion

We tested the ability of the fabricated device to detect pathogenic DNA via the bead-based polymerase chain reaction. The device was first calibrated to determine physical characteristics such as the temperature coefficient of resistance (TCR) of the on-chip temperature sensors, and the thermal response of the PCR chamber. Following physical characterization, the effects of experimental parameters on bead-based PCR results were investigated. By varying the time and temperature of individual PCR steps,

reactant concentrations, and bead concentration their impact on signal intensity was examined. Then, the ability of the device to detect pathogenic DNA was tested by determining the minimum detectable concentration of DNA and the minimum assay time. Finally, the bead-based PCR method was demonstrated in an integrated microfluidic device and shown to be able to capture, amplify, detect, and release single-stranded DNA.

3-3.1 Physical Characterization of the Device

The resistive heater and sensor were first characterized to enable accurate on-chip temperature control. The chip was placed in a temperature-controlled environmental chamber and its temperature varied. Chamber temperatures were measured using a platinum resistance temperature detector probe (Hart Scientific 5628) and on-chip resistances were measured with a digital multimeter (Agilent 34420A). Resistance measurements of temperature sensors indicated a linear relationship between resistance and temperature. This data was used to calculate a TCR for the sensor of 2×10^{-3} °C^{-1} (see Appendix 1). The heater was found to have a resistance of approximately 20 Ω.

The accuracy of on-chip temperature measurements and the heating rate of the chip were then tested. A 1.5 mm diameter insulated K-type thermocouple probe (Omega Engineering) was inserted into the sample chamber along with a pure water sample. The chamber temperature was then controlled (heated cyclically) as would occur during a typical PCR test, but without the amplification reagents. According to the time course of temperature obtained during this control test (Figure 3-3), the chip achieves target temperatures with minimal overshoot. The device exhibited an average time constant of heating (based on an exponential fit) of approximately 1.4 s. In addition, the

thermocouple readings agreed with the temperature setpoints to within plus or minus 0.5 °C (data not shown). This indicates that the chamber temperature can be controlled to produce rapid and efficient amplification reactions.

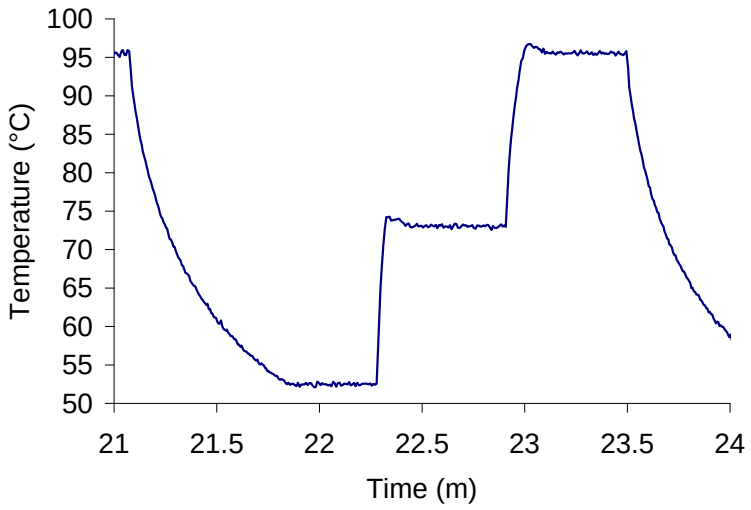

Figure 3-3. Temperature history of a typical PCR cycle.

The effects of test conditions, such as ambient light and temperature, on test results were also investigated. Biotin-streptavidin binding was chosen as a simple and effective alternative to covalent methods for DNA immobilization [120, 141], however streptavidin molecules may denature as a result of the elevated temperature necessary to dehybridize DNA [142]. Dual-biotin functionalization has been implemented in previous work to counteract this effect [120, 121], however no quantitative data was reported to support the effectiveness of this technique. To generate such data, temperature cycling equivalent to typical PCR testing was performed on linkages between streptavidin and dual-biotin labeled DNA. Beads coated with streptavidin were mixed with 1 μM dual-biotin labeled primers and an equal concentration of fluorophore-labeled complementary

strands. The solution was subjected to temperature cycling, returned to room temperature, and washed to remove any DNA in solution. In Figure 3-4, the fluorescent intensity is shown for untested beads (zero temperature cycles) and for beads subjected to 10, 20, 30, or 40 rounds of temperature cycling. Intensity, measured in arbitrary fluorescence units (afu), did not vary from baseline (zero temperature cycles) as a result of temperature cycling. This indicates that the concentration of DNA on the bead surfaces changes negligibly as a result of the PCR process, producing minimal error as a result. Another potential source of error is the effect of ambient light on the fluorescent labels. This effect, known as photobleaching, was found to be negligible for this experimental setup in previous work [143].

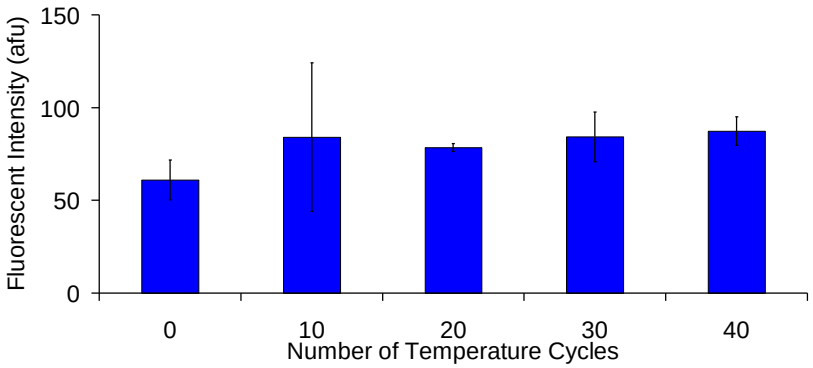

Figure 3-4. Effect of temperature on fluorescence measurements, n = 3. The negligible change in fluorescence intensity indicates that temperature cycling does not degrade dual biotin functionalization and hence does not affect concentration of DNA at bead surfaces. Error bars indicate one standard deviation from the mean.

3-3.2 Effects of Experimental Parameters on Bead-Based PCR

The effects of experimental parameters on bead-based PCR were studied to optimize the ability of the device to detect DNA. During a series of PCR reactions, parameters were varied individually and the results studied to determine the parameters that would generate maximum signal intensity, thus lowering the detection limit of the device.

Control for Effects of Bead-Based Amplification. First, solution-based PCR (i.e., excluding microbeads) was performed to confirm device calibration and sequences of both DNA primers (25 bases) and template (181 bases). Following amplification, gel electrophoresis was performed and results indicate that a strand of the expected length (181 bp) was produced (Figure 3-5a). This confirms that the device temperature control is accurate enough to perform PCR, and that the DNA has been properly designed and synthesized. This test was then repeated using bead-based PCR and produced identical results (Figure 3-5b) following DNA recovery from the beads via biotin-streptavidin denaturation in a 95°C formamide bath. Following ethanol precipitation of the DNA and resuspension in distilled H_2O, gel electrophoresis was performed. These results indicate that coupling the reverse primers to the beads does not cause improper DNA amplification (such as the generation of spurious products). In addition to the comparison with solution-based PCR, bead-based PCR tests were conducted with smaller reaction volumes (5 μL), and this was not found to influence the average fluorescent signal intensity following amplification.

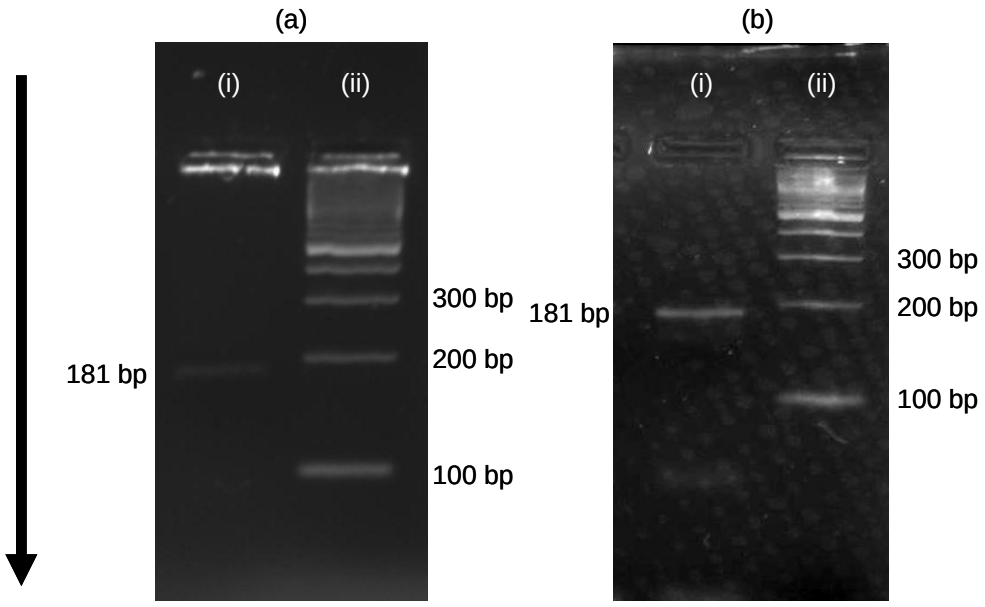

Figure 3-5. Gel electrophoresis analysis of PCR tests using the 181 bp *B. pertussis* DNA amplification chemistry. Gel (a) displays the results of a solution-based test, and gel (b) shows the results of a bead-based test. In both gels, lane (i) is a sample of PCR products mixed with loading buffer, and lane (ii) is a 100 bp ladder (dsDNA for length reference). Arrow indicates direction of DNA movement, with smaller strands migrating faster.

Determination of Optimum Magnesium Concentration and Dwell Time. Optimum magnesium concentration was determined to be 1.5 mM, consistent with typical $MgCl_2$ concentrations for PCR studies (see Appendix 1) [144, 145]. A series of tests also determined that a consistent 20 s dwell time, or time spent at each temperature setpoint during a PCR cycle, would produce DNA most efficiently (see Appendix 1).

Determination of Optimum Annealing Temperature. The effect of annealing temperature on the concentration and length of DNA generated during PCR was then studied. The annealing temperature affects the hybridization of the primers to the template DNA; a higher annealing temperature typically results in more specific

hybridization (less erroneous hybridization of a primer to an unspecified DNA sequence) but less total hybridization of DNA (and therefore less product DNA after PCR) [144, 145]. A series of bead-based PCR tests was conducted using the *B. pertussis* primer set in which the annealing temperature was varied. The results indicated that fluorescent intensity of the beads following PCR remained approximately consistent (Figure 3-6). Large variation in individual test results was observed for tests with an annealing temperature of 54°C; it is possible that non-specific annealing at this temperature causes wide variability in reaction efficiency.

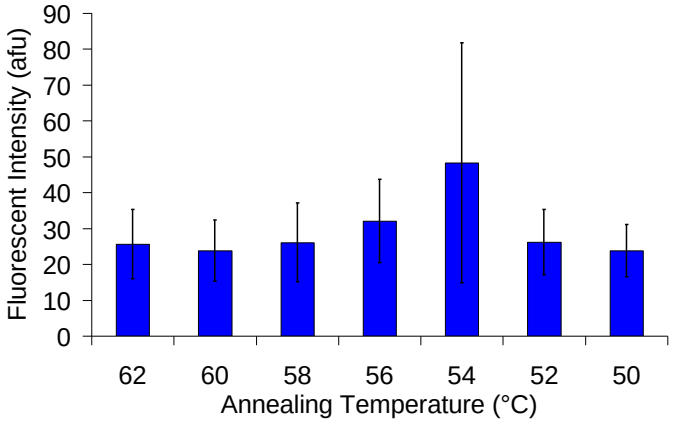

Figure 3-6. Effect of annealing temperature on fluorescent intensity after bead-based PCR, n=3, with error bars representing one standard deviation from the mean.

The annealing temperature test was then repeated with conventional solution-based PCR, and the results were analyzed using gel electrophoresis (Figure 3-7). Results indicated no amplification at 52°C, very close to the temperature at which a high degree of variability was observed in the bead-based tests. As it appears that this range of annealing temperatures produces sporadic results, a higher annealing temperature was

chosen for future testing. The results from the solution-based experiments suggested that an annealing temperature of 58°C minimized generation of primer-dimers, a type of non-specific amplification which occurs when two primers hybridize and are extended during PCR. Bead-based PCR results cannot discern the length of generated DNA, so non-specific amplification represents a source of false positive readings during DNA detection. This effect must be inhibited to maximize sensor specificity. The optimized PCR cycle parameters (cycle times and temperatures) have been summarized in Table 1.

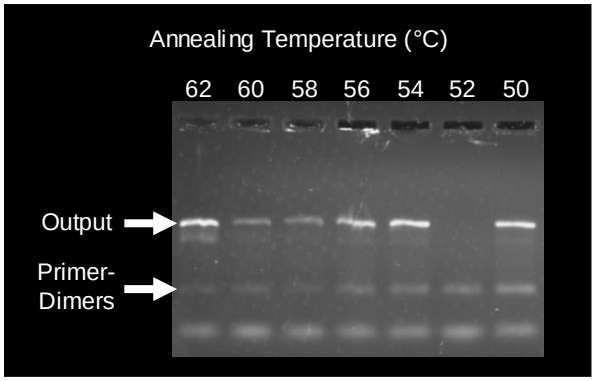

Figure 3-7. Gel electropherogram showing effects of annealing temperature on amplified DNA following solution-based PCR.

Table 3-1. Summary of PCR cycle parameters.

Stage	Temperature (°C)	Dwell Time (s)
Pre-melting	95	60
Thermal Cycling	95	20
	58	20
	72	20
Post-extension	72	180

Investigation of Effects Bead Concentration on Bead-Based PCR. Next, the bead-based PCR detection device was optimized with respect to the concentration of

beads in the reaction mixture. The presence of a solid surface in bead-based PCR introduces steric and geometric effects, affecting the reaction efficiency [141, 146]. Previous studies of solid-phase amplification [147-149] focused on maximizing the final concentration of DNA, however the primary concern of this study is detection of DNA. The concentration of microbeads in the reaction mixture was therefore investigated and optimized to produce the greatest fluorescent signal. To test the effects of bead concentration on fluorescent signal intensity, bead-based PCR reactions were performed using optimized conditions (58°C annealing temperature, 1.5 mM $MgCl_2$ concentration, 10 pM template concentration) and three different concentrations of beads (Figure 3-8). It can be seen that approximately 200 beads/µL generates the most intense fluorescent signal on the beads, with a significant decrease in signal intensity at either a lower or a higher concentration.

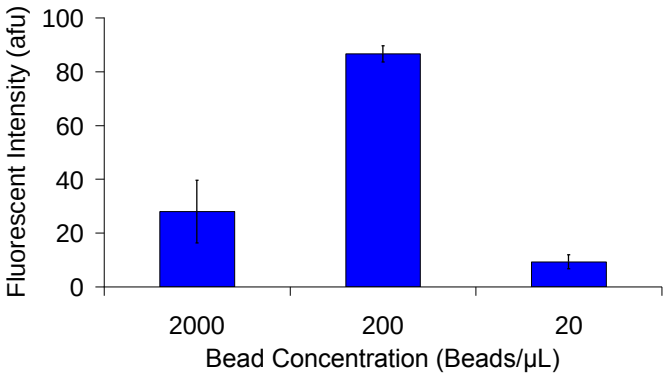

Figure 3-8. Effect of bead concentration on fluorescent bead intensity following PCR, n = 3, with error bars representing one standard deviation from the mean. Results indicate there is a concentration of microbeads in the reaction mixture which optimizes signal

intensity following the PCR reaction. The students' t-test confirms that the 200 beads/μL result is differentiable from the other results, $p < 0.11\%$.

The sharp peak in Figure 3-8 can be explained by the relationship between the concentration of microbeads in the reaction mixture and the total surface area of the surface-based PCR reaction. At higher concentrations of microbeads the fluorescently labeled product DNA is spread across a larger number of beads. The greater surface area results in a weaker fluorescent signal because the signal strength is proportional to the surface density of the fluorescent labels. On the other hand, a lower concentration of beads does not imply a higher surface concentration of DNA. At these bead concentrations, the greater density of reverse primers limits the reaction by steric hindrance between molecules at the bead surfaces. As noted in previous studies, increasing proximity of reverse primers to one another on solid surfaces can hinder the ability of DNA in solution to hybridize to the bead-bound primers [148, 149]. In addition to steric hindrance, the increasing density of the fluorophores on the bead surfaces may result in quenching to due to proximity of other fluorophores and nucleotides, which are known to inhibit fluorescence [150]. Alternatively, a lack of microbeads in the reaction will cause some reverse primers to remain in solution, as each bead can support a limited number of primers. The competition of these in-solution primers for the template DNA and the lower efficiency due to steric hindrance account for the drop in signal intensity at lower bead concentrations. Figure 3-8 shows that there is a ninefold decrease in signal intensity from 200 to 20 beads/μL, indicating that bead concentration strongly influences the ability of the sensor to detect DNA. Based on the results, in the future it may be

possible to predict the optimum concentration of beads for a DNA sensor using bead-based PCR.

3-3.3 Investigation of Detection Sensitivity

Finally, the device was tested to determine its ability to detect synthetic gDNA. Detection criteria included the limit of detection (the smallest concentration of DNA that could be detected) and the number of PCR cycles necessary for detection. The limit of detection of the device was investigated by performing a series of PCR reactions while changing the concentration of template DNA in the reactants. Concentrations ranging from zero templates to 1 pM (approximately 6×10^5 copies/μL) were tested. PCR reactions were run for 10 cycles (approximately 15 minutes) using the optimized test conditions discussed above (200 beads per microliter, 20 s dwell times, 58°C annealing temperature, and 1.5 mM $MgCl_2$). As can be seen in Figure 3-9, concentrations of 0.1 pM and less produced an increase in fluorescence above the zero template reaction. As indicated by the error bars, however, this increase is within one standard deviation of the average fluorescence for the zero template tests. Zero-template amplifications produce a fluorescent signal because non-specific amplification products such as primer-dimers are detected in addition to properly amplified DNA. This effect is investigated further in the following discussion of signal intensity versus cycle number. A template concentration of 1 pM, however, produced a signal distinguishable from the zero template control, as determined by the student's t-test with a 95% confidence level. These results are comparable to those obtained recently using a microfluidic quantitative PCR device [151]. In addition, this detection limit is orders of magnitude smaller than limits reported in

similar studies using PCR with electrochemical labels [124] or optical detection on a flat surface [52].

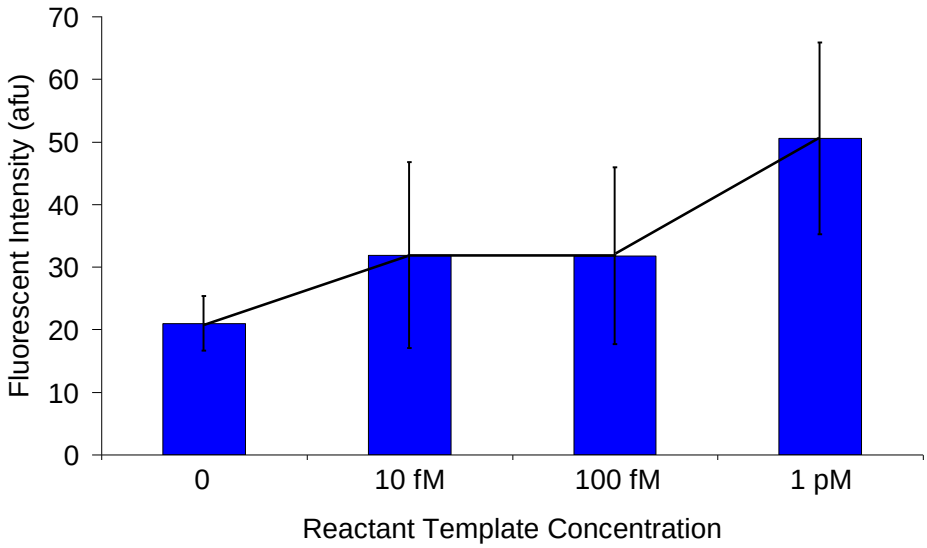

Figure 3-9. Investigation of DNA detection limit. Fluorescent intensity of beads following the PCR reactions is plotted against concentration of templates in the reaction mixture. Error bars indicate one standard deviation from the mean of three experiments (n=3), and the reaction with zero templates (control) and a 1 pM template concentration (the detection limit) is differentiable with a probability of greater than 95%, according to the students' t-test.

In addition to measuring the detection limit of the device, the relationship between signal intensity and the number of PCR cycles performed prior to detection was also investigated. It was possible that increasing the assay time (the number of PCR cycles) would improve the signal strength, thereby lowering the detection limit. For this investigation, bead-based PCR reactions were performed as discussed in the previous

section, but a 1 pM (approximately 6×10^5 copies/μL) concentration was consistently used and the number of PCR cycles was varied. As can be seen in Figure 3-10 signal intensity at 10 cycles is well above background levels and increases from 10 to 30 cycles. There is a slight decrease in signal from 10 to 20 cycles that can possibly be explained by several effects associated with solid-phase amplification. Previous studies have noted a number of detrimental effects, such as non-specific amplification between two surface-bound primers or creation of sterile (incomplete) molecules, both of which could then reverse themselves with further amplification [141, 148]. In addition to amplification of a 1 pM sample, a control sample with no template DNA was also amplified and the results are displayed in Figure 3-10. The control signal shows a linear increase in intensity, but consistently remains below that of the test sample.

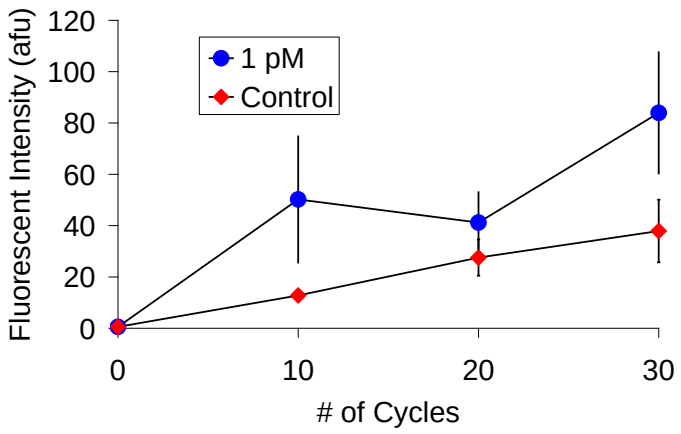

Figure 3-10. Relationship between signal intensity and the number of PCR cycles used during amplification of a 1 pM sample. Mean values from multiple tests (n = 3) are shown, error bars indicate standard deviation.

These results have two important indications for the design of a bead-based PCR DNA detection test. First, the zero template control signal remains below that of the 1 pM signal, indicating that non-specific amplification does not impair the specificity of the test. Second, that increasing the number of PCR cycles may not improve sensitivity. While the fluorescent signal intensity increases overall with increasing numbers of PCR cycles, the control signal increases as well. If this signal is considered to be background, the signal to background ratio as shown in this graph decreases with increasing numbers of PCR cycles, from 3.9 at 10 cycles to 2.2 at 30 cycles. This may be attributed to the continued generation of non-specific amplification products when amplifying with no template molecules [152]. As discussed in Section 3.2, the decrease in fluorescence may also be a result of quenching of fluorophores at the bead surfaces due to the proximity of other fluorophores and DNA. It appears that the signal does not mimic the exponential nature of PCR amplification; while data from the literature [121, 142, 153] and control tests (Figure 3-4) showed that this was not a result of loss of DNA from the beads at elevated temperatures, the exact nature of the relationship between fluorescent signal intensity and surface density of DNA needs to be further investigated.

3-3.4 Integrated Bead-Based PCR Operation

To demonstrate the utility of the bead-based PCR scheme in an integrated device, DNA capture, amplification, detection, and purification was performed in a single microfluidic chamber. A 5 μL volume of microbeads (concentration: approximately 200 beads/μL) was inserted into the microchamber (Figure 3-11a), and 10 pM template DNA (approximately 6×10^6 copies/μL) was then inserted and allowed to incubate for a period

of ten minutes (Figure 3-11b). This solution was then removed and PCR reaction mixture introduced, at which point the integrated heaters and sensors were used to cycle the chamber temperature to effect 10 cycles of PCR. Following amplification, the reaction mixture was removed by washing with pure buffer, leaving only beads coated with fluorescently-labeled DNA in the microchamber (Figure 3-11c). Analysis of the fluorescent micrograph indicated that the beads fluoresced with an intensity of 75.9 afu, well above the detection limit determined in previous experiments (Section 3-3.3). The chamber temperature was then raised to and maintained at 95°C for 5 minutes, denaturing the bead-bound ssDNA and eluting it into a pure buffer solution. UV/VIS spectroscopy confirmed that the eluent contained 163.6 ng/μL ssDNA. A fluorescent micrograph of the microbeads that remained in the microchamber (not shown) confirmed that product ssDNA had indeed been removed from the beads. These results illustrate that the use of bead-based PCR can enable the design of a highly integrated microchip for DNA purification and detection, with precise control of buffer conditions during on-chip procedures. In the future, devices using this approach could easily be automated to perform all of the above procedures independent of user intervention.

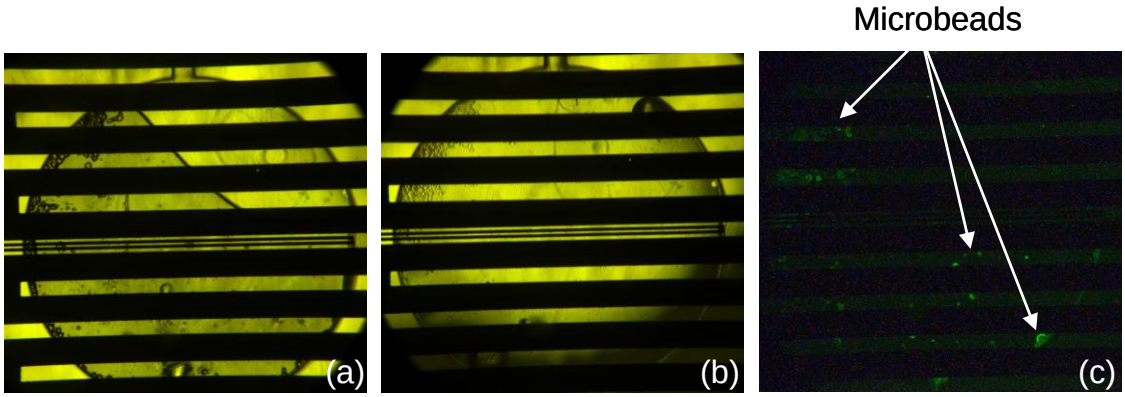

Figure 3-11. Micrographs of the microchamber illustrate the process of integrated microfluidic bead-based PCR. In (a), a brightfield micrograph shows a microchamber in which beads have been inserted into the chamber and a DNA solution is being introduced (fluid flowing from top to bottom). In (b), the DNA solution has been introduced, and template DNA is being captured from the solution onto bead surfaces by bead-bound reverse primers. Following PCR cycling, and washing with buffer, the fluorescent intensity of the microbeads was measured with minimal background fluorescence (c).

3-4 Conclusions

There is a strong need for innovative methods for DNA manipulation and detection to enable improved molecular biology analysis and diagnostics. Aiming to address this need, this chapter has demonstrated a microchip that is capable of amplifying and detecting trace amounts of DNA via bead-based PCR amplification and fluorescent labeling and detection. The device uses dual-biotin labels on the reverse primers and carboxyfluorescein labels on the forward primers to produce labeled dsDNA on the surface of streptavidin-coated microbeads. Positive detection of 1 pM of template DNA was achieved in only 10 PCR cycles within 15 minutes. This is similar to other PCR devices making use of fluorescent probes, in which similar starting template concentrations are typically detected in a comparable number of PCR cycles [151].

In contrast to the previous devices that have attempted integration of sample pre-treatment with amplification for isolation of gDNA from lysate [89, 91, 127], this approach exploits bead-based amplification and detection, and is hence potentially simpler and more efficient. Microfluidic PCR is capable of detecting as little as a single

DNA molecule, [126], and results have shown that the bead-based amplification process detects clinically relevant DNA concentrations and allows for single-chamber integration of amplification and detection to upstream and downstream processes that may have incompatible buffer requirements. While making use of polymer microbeads and streptavidin-biotin conjugation for simplicity, this design can easily be adapted to the use of other types of micro- or nanoscale beads (e.g., magnetic beads) as well as covalent attachment schemes that suit specific DNA amplification and analysis needs.

This approach could be extended in the future to include, for example, the improvement of the test specificity and signal to background ratio by generating primer sets that maintain specificity to a target genome while decreasing primer-dimer creation by minimizing affinity between the primers. This may minimize assay time by increasing the signal-to-noise ratio and reducing the number of PCR cycles necessary to attain detection. In addition, primer-coated beads could be used as a solid-phase extraction matrix for gDNA samples in lysate mixtures [133], demonstrating more complex protocols in relatively simple microfluidic devices. Thus, this approach can potentially lead to miniature clinical diagnostic systems with rapid sample-in, answer-out pathogen detection capabilities.

Chapter 4: Isolation of Thermally Sensitive Aptamers on a Microchip

4-1 Introduction

Aptamers are single-stranded oligonucleotide or peptide molecules that express binding affinity for a target molecule. With a wide range of possible applications from sensing [154] to therapeutics [46], the use of aptamers has been exploding in recent years. Aptamers are similar in function to antibodies, and as a result they are readily applicable in a wide range of fields [155]. Unlike antibodies, however, aptamers are synthetic, developed *in vitro*, and subject to less biodegradation [27]. Once an aptamer sequence is isolated, it can be consistently and rapidly reproduced with a wide variety of chemical modifications tailored to the desired application. The primary hindrance to the more widespread use of aptamers is the resource- and time-intensive nature of the *in vitro* protocol for discovering binding sequences.

That protocol, known as SELEX or Selective Evolution of Ligands by EXponential Enrichment, primarily consists of partitioning target-binding strands from unwanted nonbinding oligonucleotides, followed by their chemical amplification and repetition of this process several (10 – 15) times (Figure 4-1). SELEX typically requires weeks or months of dedicated work on the part of trained scientists, as well as a significant quantity of expensive reagents. Conventional partitioning methods, such as column- and nitrocellulose fiber-based separation have limited separation efficiency, contributing to the time necessary to complete the process. In addition, the repeated

amplification steps coupled with all of the necessary pipetting and analysis makes the SELEX process expensive and prohibitively time-consuming. A method for rapid isolation of aptamer sequences would greatly benefit fields such as aptamer-based therapeutics and sensing, by allowing scientists to more quickly and easily generate aptamers against potential targets [62].

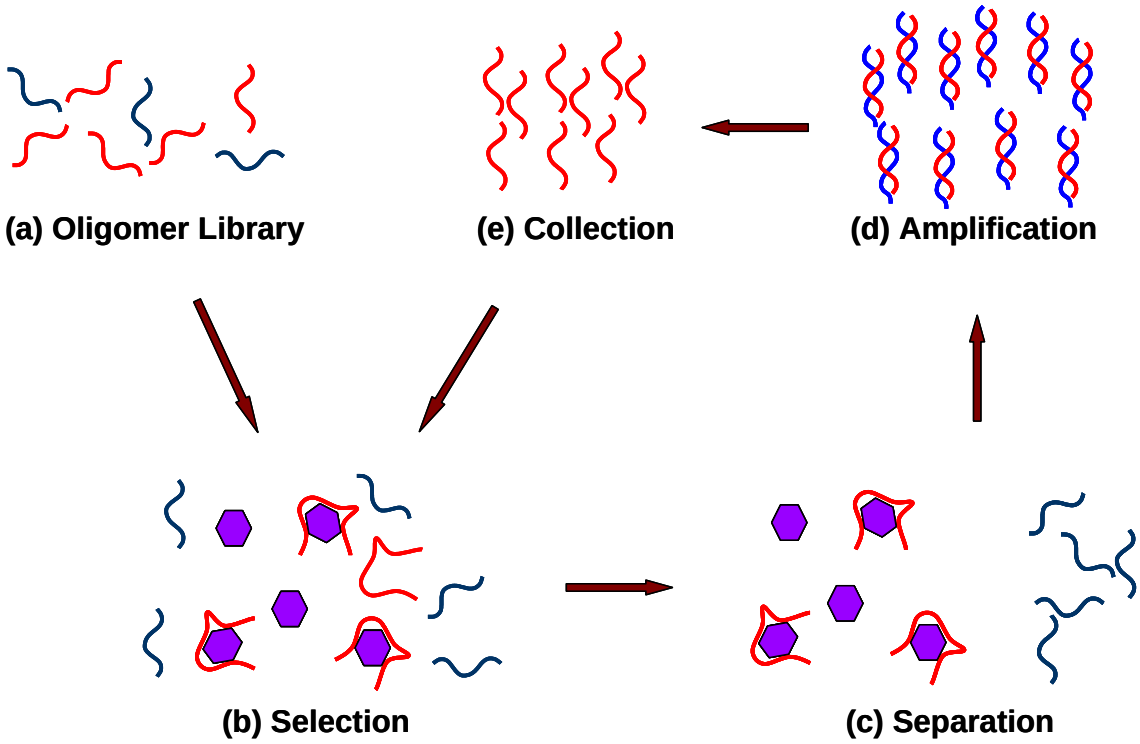

Figure 4-1. Aptamer isolation via the SELEX process. A library of approximately 10^{14}-10^{15} nucleic acids with randomized sequences (a) is introduced to target molecules (b). During selection, unwanted non-binding and weakly bound nucleic acids are separated from strongly bound aptamer candidates (c) which are then chemically amplified (d). Single-stranded nucleic acids are then separated from the amplified double strands prior to repetition of the process (e).

Recent work has demonstrated that aptamers can be rapidly isolated by using microfluidic technology to partition target-binding aptamers from randomized libraries. Microfluidic chips offer much greater surface area to volume ratios than conventional devices, which benefits surface-based reactions such as the selection of oligonucleotides binding to surface-bound target molecules. For example, using a continuous flow of target-conjugated magnetic microbeads in a microchannel, aptamers with nanomolar dissociation constants (K_D) have been developed with only a single round of selection and amplification [2]. This technology has not only sped up aptamer isolation, but allowed the development of aptamers with lower dissociation constants [83] and more customized binding traits [85]. Similarly, it has been demonstrated that capillary electrophoresis (CE) can be applied to separation of target-binding oligonucleotides to generate aptamers with specific values of K_D and other thermodynamic parameters [95, 96]. While these and other advances [92, 156] are promising, they focus only on the selection step of the SELEX process. Despite a significant field of literature that has demonstrated integration of amplification with a variety of other functions [157], efforts towards developing integrated SELEX microchips with both selection and amplification are still at an early stage. Current integrated SELEX prototypes are inadequate in areas such as miniaturization [1] and process control [87].

We have developed a fully integrated microchip for isolation of temperature-specific target-binding oligomers. The microchip makes use of a bead-based protocol for both selection and amplification that permits complete control over buffer and temperature conditions. Target-coated microbeads provide a means of surface-based selection in a microchamber, and primer-coated microbeads act as a surface for solid-

phase capture and amplification of candidate binding sequences. The device developed in this chapter is shown to be capable of integrated selection and amplification, enriching a randomized library to express temperature-dependent binding affinity to a target molecule, human immunoglobulin E (IgE). Analysis of cloned sequences from the enriched library showed an improvement to 25-66% agreement among the randomized sequence region. Operation of selection and amplification occurred on-chip with minimal external user intervention; this eliminated error-prone pipetting steps, reduced reagent use, and decreased the overall process time from several hours to just a single hour. The capability of the bead-based approach was thus demonstrated to allow a highly efficient isolation of target-binding oligomers in an integrated microfluidic chip.

4-2 Materials and Methods

4-2.1 Integrated Temperature-Specific Bead-Based Microfluidic Selection

The "selection" step of SELEX is the process by which randomized nucleic acids are exposed to the target molecule, and desired binding strands are partitioned from undesired nonbinders. Typically, selection procedures can be described as either "in-solution" or "solid phase," depending on the location of the target molecules during the process. In the design discussed in this chapter, target molecules are immobilized on a solid phase, via covalent attachment to polymer microbeads. These microbeads are inserted into the chip and held in place via flow restrictions (weirs). Selection is then performed by flowing solutions of library and buffer through the bead-packed chamber, while maintaining the chamber temperature via on-chip closed-loop control. Solutions of randomized oligomers (library) are exposed to the beads, allowed to incubate, and then

removed via washing. Nonbinding oligomers are then removed by washing with pure buffer, and the stringency of the selection can be controlled by varying wash conditions such as buffer volume and flowrate. This approach allows complete control over ambient selection conditions, including pH, buffer conditions, and temperature, giving the experimenter a high degree of control over final aptamer binding affinity. On a microfluidic chip, solid-phase selection protocols can lead to enhanced selection efficiency due to the high surface area to volume ratios associated with microscale designs. In addition, the immobilization of the target molecule simplifies intermediate steps in the protocol, such as changing buffers between selection and amplification. This promotes simplicity of chip design further enabling the integration of selection in an isolation microchip.

4-2.2 Integrated Bead-Based Polymerase Chain Reaction

During selection, aliquots of buffer wash over immobilized target molecules, removing either unwanted nucleic acids or candidate aptamers. These samples are then chemically amplified, to provide an indication of selection efficiency and/or to allow further processing, including cloning or further rounds of isolation. As with selection, proper temperature and buffer conditions are crucial for efficient amplification. In this design, polymer microbeads coated with reverse primers are used to generate a surface for specific DNA capture and amplification. As described in a previous publication [158], in bead-based PCR the immobilized reverse primers capture ssDNA via hybridization. Reagents necessary for amplification can then be introduced into the chamber and the temperature cycled to generate exponential copies of the captured template DNA. A

crucial aspect of this design is its insensitivity to the input and output buffer conditions; the microbeads can capture and release the DNA in a wide range of buffer conditions, simplifying integration of the amplification step in a SELEX microdevice.

Bead-based PCR has the additional advantage of acting as a platform for concentration of fluorescent signals that can be incorporated into the DNA structure during amplification. In this implementation, forward primers incorporate a carboxyfluorescein moiety at the 5' terminus. As PCR progresses and forwarded primers are incorporated into bead-bound dsDNA, more labels accumulate on the bead surfaces and can be detected by fluorescent optical microscopy. Given identical amplification reactions (number of temperature cycles, reagent concentration, etc.), the fluorescent signal intensity is then an indicator of initial template concentration. Generating PCR "profiles" by performing this procedure with agarose gel electrophoresis is an analysis used during conventional SELEX to investigate errors associated with DNA elution or selection efficiency. Alternatively, by calibrating fluorescent intensity to concentration of DNA following amplification and elution, the fluorescent intensity of the microbeads can indicate if the amplification reaction has produced enough DNA for downstream processing.

4-2.3 Design and Fabrication of Chip, Library, etc.

The aptamer isolation chip consists primarily of two PDMS microchambers for selection and amplification, respectively, on a glass substrate (Figure 4-2). Between these two chambers is a serpentine microchannel that acts as a passive mixer. On-chip flows are pressure driven, with no combination of flow path and average flowrate (between 1

and 10 μL/min) generating a pressure drop greater than 0.5 psi prior to bead introduction. Flowrates for the bead-packed chambers were calculated as in the relevant previous work [49] and also found to produce negligible pressure drop. The entire chip is coated with Parylene C to prevent microbubble formation and adsorption of DNA or PCR reactants.

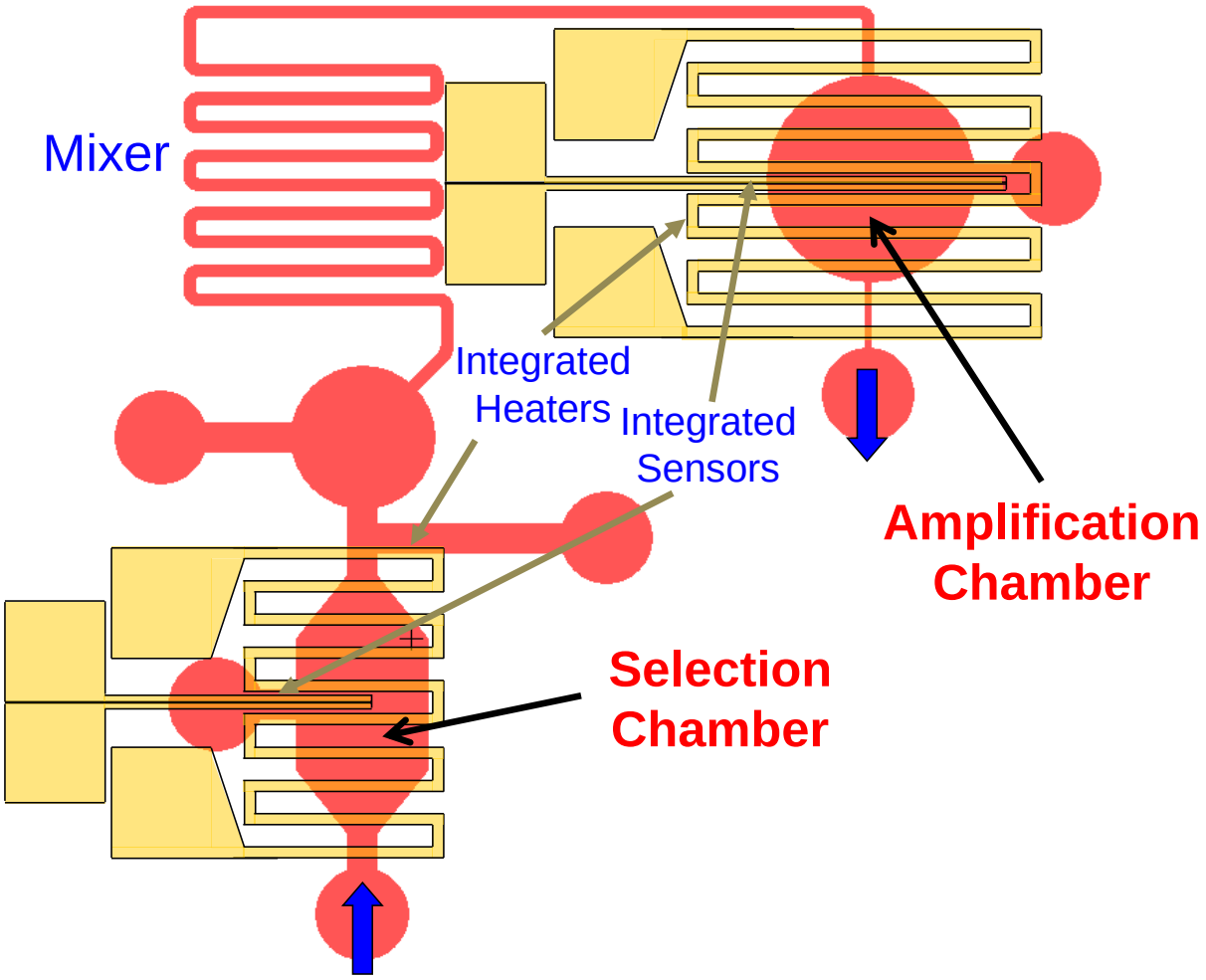

Figure 4-2. Plan view of the integrated microchip, primarily consisting of microfluidic selection and amplification chambers with integrated resistive heaters and temperature sensors.

The selection chamber is a 4 μL PDMS cuboid microchamber 400 μm tall with 2.3 mm sides. The chamber is placed over chrome/gold resistors which generate a sufficiently uniform temperature field and provide temperature measurements via a resistance-temperature relationship. The heater is 3.145 cm long by 300 μm wide, 200 nm thick with a nominal resistance of 20 ohms. The temperature sensor is 0.55 cm long by 40 μm wide, 200 nm thick with a nominal resistance of 100 ohms. The chamber has one inlet 400 μm tall for insertion and removal of target-coated microbeads. Two more inlets on opposite sides of the chamber are approximately 10 μm tall, allowing fluid flow while act as passive flow restrictions (weirs) to retain the microbeads which are approximately 100 μm in diameter.

The amplification chamber is a 4 μL cylinder, 400 μm tall with an 1800 μm radius. Two inlets are 400 μm tall, allowing insertion of microbeads, and one is a 10 μm passive weir. As with the selection chamber, chrome/gold resistors beneath the chamber act as an integrated heater and temperature sensor. The heater is 4.635 cm long by 300 μm wide, 200 nm thick with a nominal resistance of 60 ohms. The temperature sensor is 0.8 cm long by 40 μm wide, 200 nm thick with a nominal resistance of 120 ohms.

The microchip is fabricated using PDMS microchannels on a glass substrate using contact lithography. Positive lithography using S1800 series (Dow Chemical, Newark DE) photoresist and wet etching defines patterns for resistors and contact pads on a gold-coated glass substrate. These are then passivated with a 1 μm coating of SiO_2 generated using plasma-enhanced chemical vapor deposition (Oxford Instruments, Concord MA), with pieces of silicon used as shadow masks to define openings for electrical contacts. Negative lithography using SU-8 2000 (Microchem, Newton MA) photoresist on silicon

wafers defines molds for PDMS microchannels. PDMS prepolymer (Robert McKeown, Somerville NJ) is then mixed at a 10:1 ratio of base to curing agent, poured over the molds, and heater at 75°C for 25 minutes to generate PDMS microchannels and chambers. The PDMS microchannels are then bonded to the glass substrate following 10 minutes of exposure to UV-generated ozone (Uvocs, Lansdale PA) and heated to 75°C for 30 minutes to complete the bonding. Finally the entire chip is coated with Parylene C via chemical vapor deposition (Specialty Coating Systems, Indianapolis IN), with scotch tape used to define openings for electrical contacts.

Target molecules used for this aptamer isolation protocol were human immunoglobulin E (IgE), an antibody associated with allergic response. The randomized library is an 80-base DNA oligomer consisting of a 40 base central randomized region flanked by two 20 base priming regions. The buffer used for selection was phosphate buffered saline modified (PBSM) with 1 mM $MgCl_2$. The library/buffer system was designed based on previous work targeting IgE for development of a temperature-sensitive aptamer [33].

4-2.4 Materials

The following materials were used for the microchip aptamer isolation procedure. Human IgE was purchased from Athens Research, Athens, GA. All DNA was obtained in lyophilized form from Integrated DNA Technologies, Coralville, IA. The library is an 80mer ssDNA oligomer consisting of a 40 base randomized region flanked by two 20 base known priming regions. The purchased library sequence is as follows: 5’ – C TAC CTA CGA TCT GAC TAG CNN NNN NNN NNN NNN NNN NNN NNN NNN NNN

NNN NNN NNN NNG CTT ACT CTC ATG TAG TTC C– 3’. The forward primers used were 5’ – C TAC CTA CGA TCT GAC TAG C – 3’, with or without a 5’ carboxyfluorescein modification. The reverse primers used were 5’ – G GAA CTA CAT GAG AGT AAG C – 3’, with a 5’ dual biotin attachment. In each case an inert spacer molecule is incorporated between the sequence and the terminal modification. Microbeads used for aptamer selection were NHS-activated sepharose beads obtained from Bio-Rad laboratories. Microbeads used for bead-based PCR were Ultralink Streptavidin-coated beads obtained from Thermo Scientific Pierce Protein Research Products, Rockford, IL. Materials used in microfabrication included S1800 photoresist (Dow Chemical, Midland, MI), SU-8 2000 (Microchem, Newton MA), PDMS prepolymer (Dow Chemical), and Dix C Parylene prepolymer (Uniglobe Kisko, White Plains NY). PCR reagents included GoTaq Flexi PCR Mix (Promega, Madison WI), Taq enzyme (Promega), and deoxynucleotide triphosphates (dNTPs, Promega).

The reactants used for on-chip amplification of candidate aptamers consisted of the following: 5× PCR Buffer (2 μL), 25 mM $MgCl_2$ (0.6 μL), 10 mM dNTPs (0.4 μL), 50 μg/mL BSA (0.4 μL), microbeads (0.5 μL), water (5.6 μL), 25 μM forward primer (0.4 μL), and enzyme (0.1 μL). The reactants were degassed at -0.4 psi for 30 minutes in a darkened container prior to adding enzyme and proceeding with on-chip amplification. Reactants necessary for cloning and extraction of plasmid DNA are proprietary, and were purchased as part of the TOPO TA Cloning Kit and MiniPrep Extraction Kit from Invitrogen (Grand Island, NY).

4-2.5 Experimental Protocol

Prior to experimentation, the resistive temperature sensors were calibrated in an environmental chamber with a resistance temperature detector probe. Baseline temperature vs. resistance readings were also taken prior to every experiment. NHS-activated microbeads were coated with IgE by washing them with 1 μM IgE 3× in a filtration column followed by incubation for 5 hours. Unbound ester molecules were then passivated by incubating the beads for 1 hour in Tris buffer. Following another wash in pure PBS, the beads were suspended and stored in PBS. Streptavidin-coated microbeads were coated with reverse primers by incubation with 1 μM dual-biotin labeled primers for 30 minutes immediately prior to DNA capture.

The temperature of the selection chamber was set to 37°C using closed-loop feedback programming in LabView and maintained during library incubation and removal of nonbinding oligomers. Having introduced the target-coated beads to the selection chamber and washed them with PBSM, three 30 μL samples of 10 μM library DNA (in PBSM) were flowed through the chamber at 5 μL/min, and each aliquot was retained following washing. Ten 30 μL samples of pure PBSM were then flowed through the chamber at 5 μL/min, and each was retained afterward for analysis. At this point, the amplification chamber was filled with reverse-primer coated microbeads. The selection chamber temperature was then set to 57°C, and four 30 μL samples of PBSM were introduced at 1 μL/min. These were subsequently directed to wash through the amplification chamber, over the reverse-primer coated microbeads. Following each 30 μL wash, the aliquot was retrieved and stored, PCR reagents were introduced to the amplification chamber, and the chamber temperature cycled to perform PCR amplification of the candidate aptamers directly onto the microbeads. Microbeads were

subsequently washed with PBS buffer and visualized using fluorescent microscopy to visualize surface DNA. Target ssDNA was then eluted by raising the chamber temperature to 95°C and flushing with pure PBSM.

Fluorescent binding analysis was conducted using a selection chamber on a fresh microchip. Following device calibration, the chamber was filled with IgE-coated microbeads. Enriched library ssDNA was normalized to 1 μM concentration by measuring the concentration with UV/VIS spectroscopy and adding PBSM buffer. This sample was introduced to the chamber maintained at 37°C and fluorescence microscopy captured the fluorescent intensity of the microbeads. The experiment was repeated with random library also labeled with an identical fluorophore, purchased from IDT. Temperature-dependence of binding was measured in similar fashion, by incubating a 1 μM concentration of enriched library with the microbeads and then continuously flowing PBSM at 2 μL/min while varying the chamber temperature.

Cloning of enriched libraries was performed using the TOPO Cloning protocol, with plasmid DNA purified using the PureLink Quick protocol. Pools of enriched DNA were amplified using conventional PCR and unlabeled primer sequences for 25 cycles. Sequences were then cloned into the TOPO vector, and DNA sequences were harvested from E.coli and purified prior to sequencing. Sequencing was performed by the DNA Sequencing Lab at the Columbia University Protein Core Facility.

4-3 Results and Discussion

4-3.1 Physical Characterization of the Device

Having fabricated the aptamer isolation chip, integrated temperature sensors were calibrated and the mixer and amplification chamber tested for functionality. The chip was placed in an environmental chamber and its temperature varied while the resistance of the temperature sensor was measured. From the linear relationship between temperature and resistance (Figure 4-3a), the temperature coefficient of resistance was measured, enabling future resistance measurements to be correlated to on-chip temperature. The on-chip mixer was designed to fully mix reagents with library DNA. As shown in Figure 4-3b, the mixer fully mixes a clear stream of buffer with a stream of green-dyed PCR reagents. The amplification chamber was tested for its ability to properly amplify DNA by performing bead-based PCR of a sample of library DNA. Bead-based microfluidic PCR in an integrated device has been previously characterized [158]. Sample loss and bubble generation were minimized by coating the chip with Parylene C and degassing reagents prior to temperature cycling. A labview digital PID controller was programmed to achieve and maintain setpoint temperatures by measuring the resistance of the on-chip resistive temperature sensor and apply voltage to the resistive heater. Fluorescent and UV/VIS microscopy confirmed the generation of product DNA using on-chip amplification.

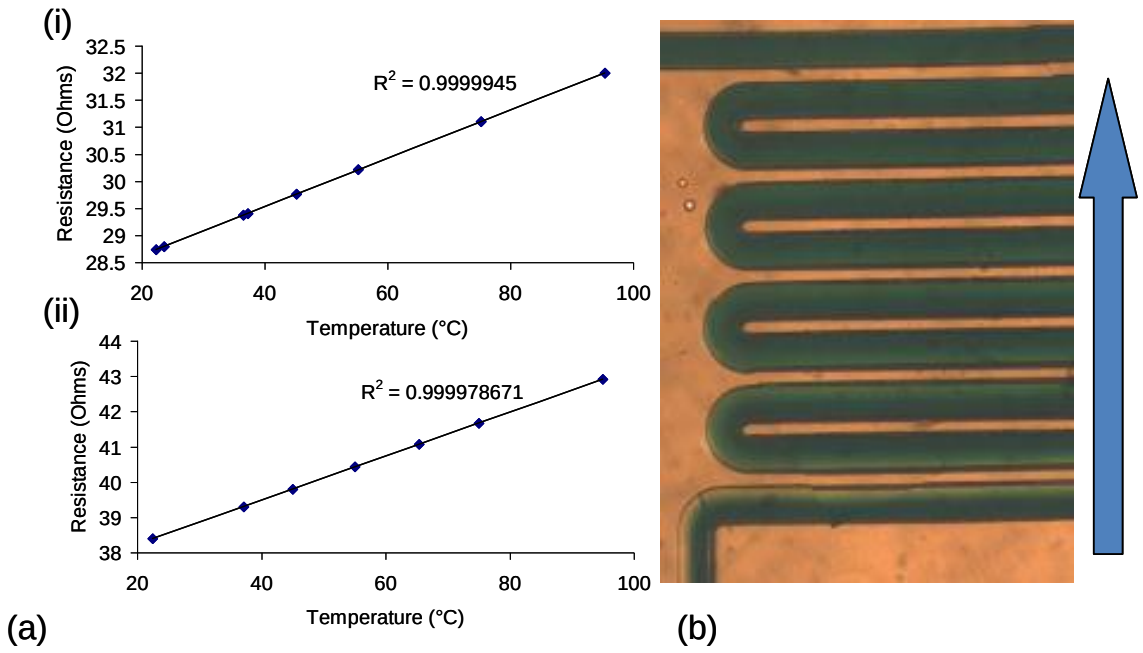

Figure 4-3: Characterization of the microchip. In (a), the linear relationship between temperature and resistor resistance for the (i) selection chamber and (ii) PCR chamber resistors allows determination of a temperature coefficient of resistance, in this case 1.554×10^{3} °C^{-1} and 1.613×10^{3} °C^{-1}, respectively. The passive mixer (b) fully mixes a stream of buffer and dye at 5 μL/min.

4-3.2 Microfluidic Aptamer Isolation

The operation of the microfluidic SELEX chip consists of two protocols: selection and amplification. The selection protocol serves to partition non-binding and weakly bound nucleic acids in the randomized library from the few oligomers which express temperature-dependent binding affinity to the target molecule. Initially, the entire library is incubated with the target-coated microbeads at the binding temperature, 37°C. Selection is then effected by maintaining the microchamber temperature and washing the microbeads with aliquots of pure buffer solution to elute undesired nucleic acids. As

samples of buffer were washed over the beads and recovered from the chip, each sample retained the unwanted nucleic acids. Samples of each buffer wash were amplified using PCR and visualized using slab-gel electrophoresis (Figure 4-4). As indicated by the intensity of the intercalating fluorescent dye, the concentration of DNA in each sample (identically amplified) decreases as the beads continue to be washed. This indicates that the wash steps removed more and more unbound DNA, presumably leaving only the more tightly bound strands.

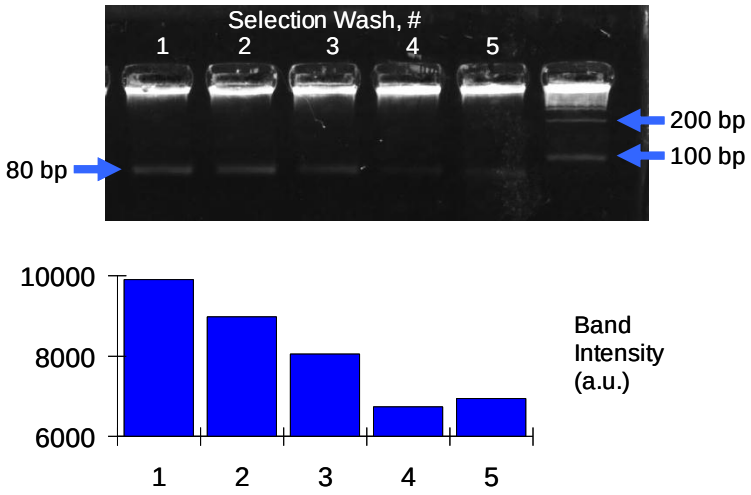

Figure 4-4. Gel electrophoresis of buffer samples containing weakly bound DNA washed away from target molecules during selection. The decreasing fluorescent intensity with continuing washes indicates that the selection process is removing weakly bound DNA, leaving strongly bound DNA to eventually be captured and amplified.

Following removal of unwanted nucleic acids during selection, desired strands were eluted by raising the microchamber temperature to 57°C and again washing with pure buffer. This aliquot of buffer, containing DNA expressing temperature-dependent

binding affinity to IgE, was driven to the amplification chamber and incubated with primer-coated microbeads. There, the primers captured the DNA onto the microbeads where it was amplified via PCR. Confirmation of the elution-capture-amplification process was obtained by incorporation of a fluorescent label on the forward (in-solution) primers used during PCR. Following amplification, fluorescent bead intensity was monitored via fluorescent microscopy to confirm the generation of labeled dsDNA on the bead surfaces. This elution-capture-amplification procedure was completed four times to ensure that all desired IgE-binding nucleic acids were captured from the selection chamber. As shown in Figure 4-5, an analysis of the fluorescent bead intensity following 25 cycles of amplification shows that DNA from the initial aliquot of buffer was successfully amplified onto the bead surfaces, but processing of further aliquots resulted in no detectable DNA. This indicates that not only did the process succeed in amplifying DNA, but that the elution-capture-amplification process efficiently captured the desired DNA in the first aliquot of buffer.

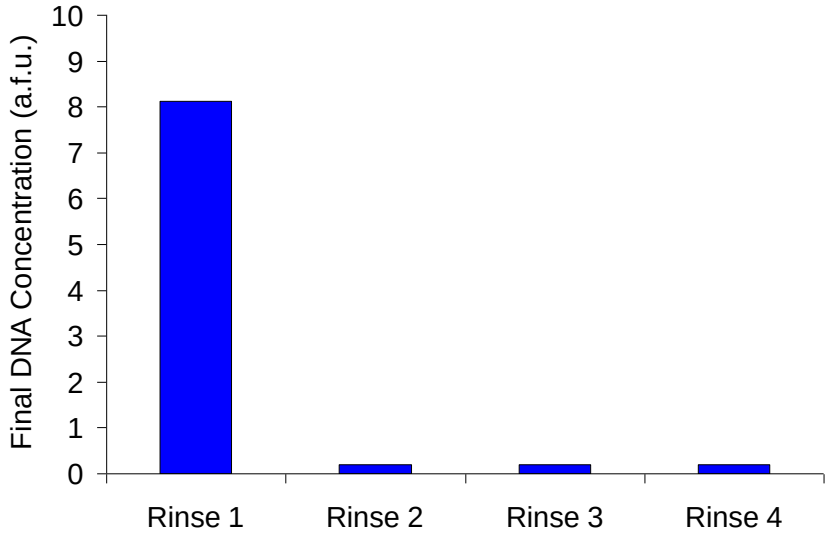

Figure 4-5. Results from fluorescent analysis of bead-based PCR amplification of aptamer candidates.

Following amplification, aptamer candidates were eluted as ssDNA into pure buffer solution and collected for further analysis. A 2 µL sample was amplified off-chip using unlabeled primers and cloned using the TOPO vector and E.coli. This process separated the many randomized strands into individual plasmids, each amplified by an individual bacterial colony. These colonies were harvested, cultured, and then subjected to DNA extraction. Twenty-four clones were chosen at random for sequencing, as shown in Table 3-1. A comparison of the sequences indicated that the library had not fully converged to a binding sequence. However, an alignment analysis indicated a 39 base region with 25-66% agreement among each base [159], a significant improvement from completely random data. Folding analysis of each clone showed the presence of secondary structures similar to those of a previous temperature-sensitive IgE-binding aptamer (Figure 4-6) [33].

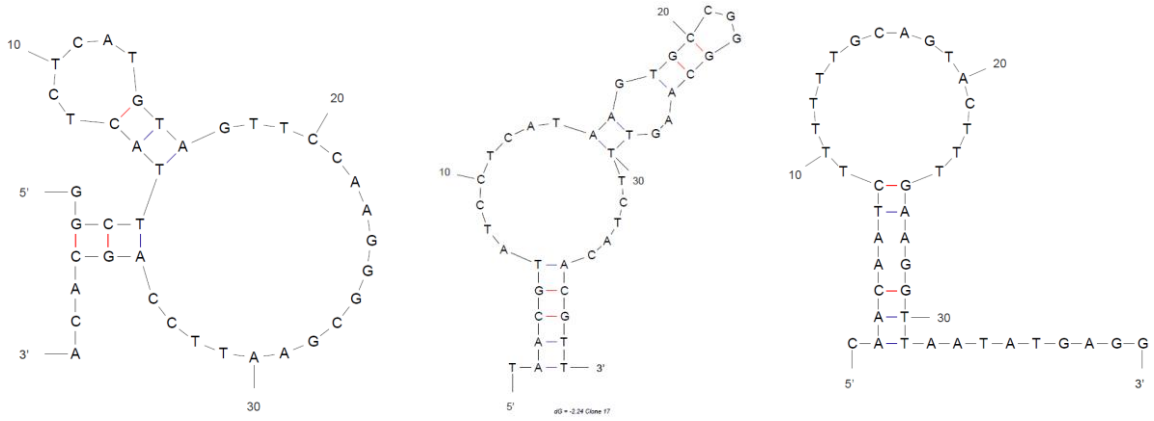

Figure 4-6. Secondary structures of clones 12, 17, and 15.

Table 4-1. Results of sequencing the enriched library

Clone ID		Randomized Region	
1	5' -	TGT CCC ACA GAT GAA TTG GTC GAT GGG GAG TAA TTT GGG C	- 3'
2	5' -	GGG TCG TCT GAT TGA AGC ATG TAC AGC TTG TGA GCA TCC T	- 3'
3	5' -	GGG GGT GCG GGC GCC CGG GCG GCG GGC GTG GGG GAG GGC G	- 3'
4	5' -	GAG GGC GGT ACA GCT GAG GGG GGA CAA TGT AGT GGG GGT G	- 3'
5	5' -	TAC GAA CCA CGA TTT ACT TAT GCA TCG TGA TCG CGT ACA T	- 3'
6	5' -	GAC TTA GAC GTA GTG TTC ACA CGT CAG TAG TGT ATA CTG G	- 3'
7	5' -	GTC AGC TGC ATG AAC GAC CAC AAT TTT ATG GGC TGG TCG T	- 3'
8	5' -	TAT GTT CAT GAT TTA GTA AGT TTG ATT CAT CCG GAN GGT C	- 3'
9	5' -	TGG AAG ATG TGC GGG GAG CAT GGC GGG GCT TTC TAG GGT G	- 3'
10	5' -	GGG GGT GCG GGC GCC CGG GCG GCG GGC GTG GGG GAG GGC G	- 3'
11	5' -	TGA GTG TTA GCG GTA CCT TTG GGC TGC GGG AGG CGC GTC G	- 3'
12	5' -	GGC TTA CTC TCA TGT AGT TCC AAG GGC GAA TTC CAG CAC A	- 3'
13	5' -	AAA TGG CAC TGA ATC GAA CCC GAG AGG AAT CTC CTG TGC G	- 3'
14	5' -	CGG GGT ATG GCG GTG TCC TTT ACT GGG GGC CAT GAT GCG G	- 3'
15	5' -	CAA CAA TCT TTT TTG CAG TAC TTT GAA GGT TAA TAT GAG G	- 3'
16	5' -	GAC GTG GCA GCA TTA GTC TCG GGG TCT CAT GGG TGT TGG G	- 3'
17	5' -	TAA CGT ATC CTC ATA AGT GCC GGG CAA GTT TCT ACA CGT T	- 3'
18	5' -	GTT AGG AGC GTA GTA CTT GTG TGG GTG GGA GTG GCN TTC G	- 3'
19	5' -	CCA AGT TAG GGG ACA GGT GGG CGG CTG CCG GGG GGA GGG G	- 3'
20	5' -	ATC TTG AGC CGA GTC TTT AAG GGG CTG TGT TTG GCT TTT A	- 3'
21	5' -	CCC TTA CTT CAA TAA GTG GTA TAA AAC TGT TCT GCG CTA G	- 3'
22	5' -	GTA AAC TGT CAG ATT TAG AAT CGG CTT GAT GCC CGT ATA G	- 3'
23	5' -	GGC TTA CTC TCA TGT AGT TCC AAG GGC GAA TTC CAG CAC A	- 3'
24	5' -	TAG GGG GGG CGT GGG GAA GAG GGG CGT CGC GGG GGG GGG G	- 3'

4-3.3 Binding Strength of Enriched Library

Following testing of the device, binding of candidate aptamers were analyzed using a fluorescent assay in which purified, fluorescently labeled ssDNA is introduced to a microchamber filled with target-coated microbeads and maintained at 37°C. The fluorescent intensity of the microbeads, indicative of the surface concentration of bound DNA, was then measured following incubation and washing with buffer. As shown in Figure 7, the enriched library generated a larger fluorescent signal compared to the randomized library, indicating that the SELEX process increased the pool's binding

affinity to IgE. Analysis of the fluorescent signals showed that the enriched library generated a 3.6× greater fluorescent signal.

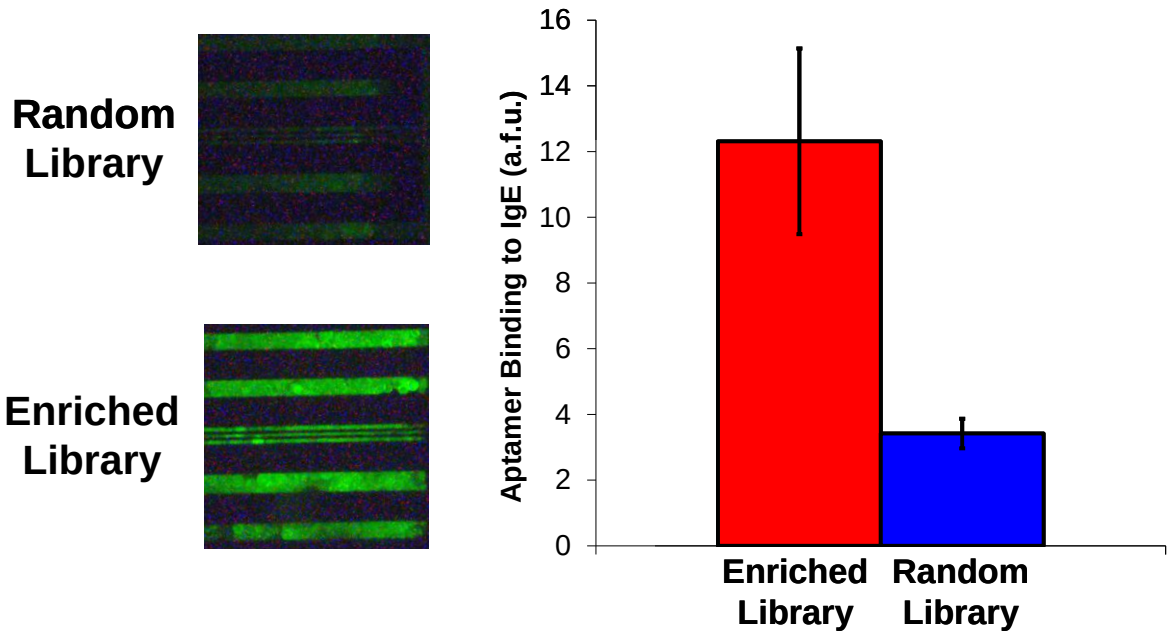

Figure 4-7. Analysis of DNA-IgE binding. IgE-coated microbeads were exposed to fluorescently labeled DNA, and the fluorescence intensity of the beads, indicative of the surface concentration of DNA, was measured.

Following the binding analysis at 37°C, the temperature-dependence of the DNA-IgE binding was analyzed using a similar approach. A microchamber filled with fresh IgE-coated microbeads was exposed to 1 µM enriched library DNA until the fluorescent signal saturated. Maintaining the chamber temperature at 37°C, fresh buffer was flowed through the chamber to ensure that binding equilibrium had been reached. The chamber temperature was then varied while flowing buffer solution, and the fluorescent intensity measured as a function of temperature. As shown in Figure 8, the concentration of

surface bound DNA varies strongly as a function of temperature, as intended by the temperature-specific selection.

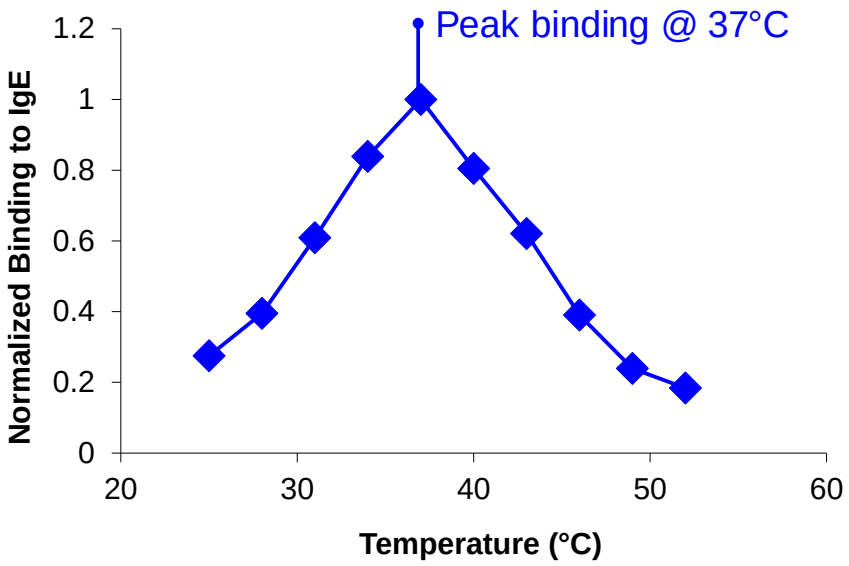

Figure 4-8. Temperature-dependence of DNA-IgE binding.

4-4 Conclusions

Aptamers have applications in a wide variety of fields, but their use has been hindered by the long development times and significant costs associated with generating binding sequences. In an attempt to address this problem, an integrated microchip process has been developed for the isolation of target-binding sequences. The bead-based selection and amplification protocol successfully separates weakly binding nucleic acids from desired strongly bound aptamer candidates, and allows on-chip amplification and collection of target ssDNA. The chip-based aptamer isolation protocol was shown to enrich a randomized library of DNA for temperature-sensitive binding to IgE. After one

round of enrichment, the DNA library showed enhanced binding and partial consensus, with individual sequences approaching a binding motif. The selection and amplification required only 3 hours and approximately 5 microliters of PCR reagents, significantly lower requirements for a standard round of aptamer isolation.

Previous attempts to improve aptamer isolation technology have included changes to selection protocols [2, 82], integration of selection and amplification [1, 87], and automation [70]. These efforts have in some cases reduced assay time or enhanced selection efficiency and effectiveness, but have generally failed to do both. A fully bead-based protocol on a microfluidic chip has the potential to accomplish this goal, by using a highly effective separation method and integrating the selection and amplification processes in one chip.

Chapter 5: An Integrated Microfluidic SELEX Chip

5-1 Introduction

Aptamers are single-stranded nucleic acids which express binding affinity to molecular targets. Their molecular recognition abilities are based on conformation of the nucleotide sequence to the structure of the target molecule, which enable a combination of weak forces (ionic interactions, hydrogen bonds, hydrophobic interaction, and van der Waals) to together create a very tight, highly specific bond. The process by which aptamer sequences are developed is called SELEX, or Selective Evolution of Ligands by EXponential Enrichment. SELEX is traditionally an iterative process in which alternating cycles of selection and amplification drive the evolution of a randomized library of nucleic acid sequences towards a binding motif.

As with most molecular biology protocols, SELEX is conventionally performed by pipetting samples between bench top instruments used for selection and amplification (typically via PCR, polymerase chain reaction). This approach to experimentation is necessarily slow and error-prone, due to the many individual steps required on the part of the experimenter. In addition, the underlying technologies employed for these steps have undergone significant improvements as SELEX has matured since its first use in 1989 [40, 62]. Initial targets for SELEX were primarily proteins, and this in part led to nitrocellulose filter paper being employed as a partitioning medium for the selection step, as the negative charge of the nitrocellulose helped to attract DNA bound proteins which are typically positively charged [66]. Since then, a variety of techniques have been applied including both macroscale technology (such as agarose filter columns with covalently attached target molecules) to microscale partitioning methods like capillary

electrophoresis [72] and M-SELEX [2, 82]. As these techniques are more efficient, fewer SELEX rounds are now required to evolve a binding sequence.

In addition to improvements in selection technology, automation of the SELEX process has improved process control. For example, robotic control of conventional SELEX resulted in a significant drop in the human resources required to perform the process [70]. This approach requires a large amount of startup capital, however. Alternatively, a SELEX device using microlines, pumps, and a connected PCR machine illustrated that integrated SELEX can potentially avoid manual pipetting steps by directly connecting equipment performing each necessary step of the process [1]. While the device was not fully successful, it illustrated that the "lab on a chip" approach to SELEX had great potential.

By miniaturizing protocols such as SELEX, time and resources can be conserved via more efficient surface-based chemical reactions, owing largely to the much greater surface area to volume ratios characteristic of such designs. Recently, microfluidics has been applied to selection and integrated SELEX to generate vastly improved devices capable of producing aptamers in days rather than weeks or months. For example, while many previous approaches to SELEX have made use of microbeads for selection [70, 71], doing so in a microfluidic selection device is a relatively recent advance [2, 82]. Such microfluidic microbead-based selection devices are capable of vast reductions in assay time, by requiring only 1-3 rounds of SELEX instead of 10-20. Microfluidics also offers enhanced amplification and automation [79, 80, 157], and as such, can render highly efficient aptamer generation devices. In addition to microfluidic selection, integrated microfluidic SELEX devices have recently been demonstrated that incorporate bead-

based selection with integrated amplification and collection of single-stranded DNA (ssDNA) [87, 88]. Such devices are capable of fully automated, rapid generation of aptamers. To date, however, an integrated microfluidic device with highly efficient selection (deriving aptamers in 1-3 rounds) has not been illustrated.

We present an integrated microfluidic device which utilizes a bead-based PCR approach to integrate selection, amplification, and collection of ssDNA, generating aptamers which bind to target molecules at predetermined temperatures. The process requires far less time and reagents than conventional SELEX protocols, and successfully integrates highly-efficient microfluidic selection with amplification and collection of ssDNA.

5-2 Principles and Design

5-2.1 Design and Operation of the Microchip

Much of the principle of operation of this device is described in Chapter 4. Briefly, the device draws on a previously reported partitioning technique, making use of bead-based selection to rapidly isolate target-binding nucleic acids from the randomized library. This approach has been augmented, however, with a bead-based PCR protocol which greatly simplifies the integration of SELEX on a microchip. Together they generate a rapid, efficient SELEX protocol capable of evolving aptamer sequences in 1 to 3 rounds of SELEX. The coupling of selection and amplification to generate a chip which rapidly isolates temperature-specific aptamers was discussed in Chapter 4. This chip essentially performed a single round of SELEX, accepting a randomized library and producing ssDNA enriched for temperature-specific binding affinity to human IgE. In this chapter,

this approach has been extended by designing a similar chip which can perform multiple rounds of SELEX and integrates a counter-selection step.

As shown in Figure 5-1, the integrated SELEX microchip consists of three primary chambers: selection, counter-selection, and amplification. As discussed in the previous chapter, microfluidic selection uses target-coated microbeads and integrated temperature control to partition strongly-bound aptamer candidates from unwanted weakly-bound ssDNA. In addition, a bead-based microfluidic PCR protocol is integrated to purify and amplify the desired aptamer candidates before elution into buffer (collection). In comparison to the previous chapter, this microchip is designed to perform multiple rounds of SELEX without intervention. Following amplification of the aptamer candidates in the integrated bead-based PCR microchamber, ssDNA can be eluted directly to the selection chamber for further rounds of SELEX. The design of the library, including primers modified for bead-based amplification and collection, is identical to that of the previous chapter. Changes to the design of the microchip include a more complex microfluidic channel network for directing flow to the microchambers, active valves for controlling the flow of fluid in the microchannels, and an integrated counter-selection chamber.

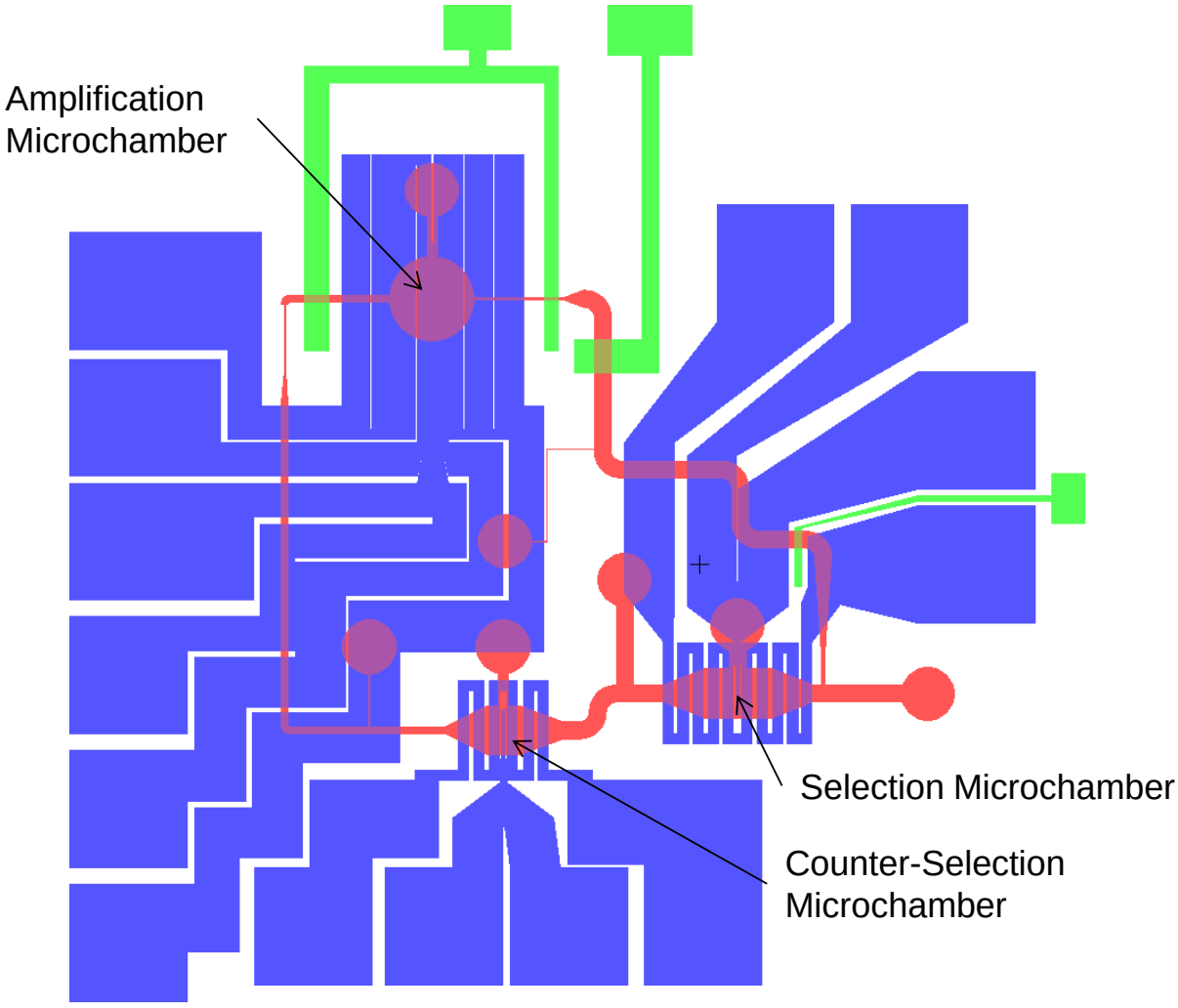

Figure 5-1. Layout of Integrated SELEX Microchip. Drawn in red and highlighted with arrows are the microfluidic chambers for selection, counter-selection, and amplification. Blue lines indicate resistive heaters and sensors, and green lines show the placement of pneumatic lines for integrated active valves.

Also shown in Figure 5-1 in green are pneumatic channels placed perpendicular to the fluidic channels. These channels are etched into the glass chip and separated from the fluidic channels by a thin elastomer membrane. Increasing the pressure in these channels via an off-chip source of compressed gas actuates the membrane, interrupting the flow of

sample and reagents in the fluidic microchannel. A sample cross-section of such a design is shown in Figure 5-2. Previous work has shown that this design produces highly effective microfluidic valves, with relatively simple fabrication and high diodicity [160].

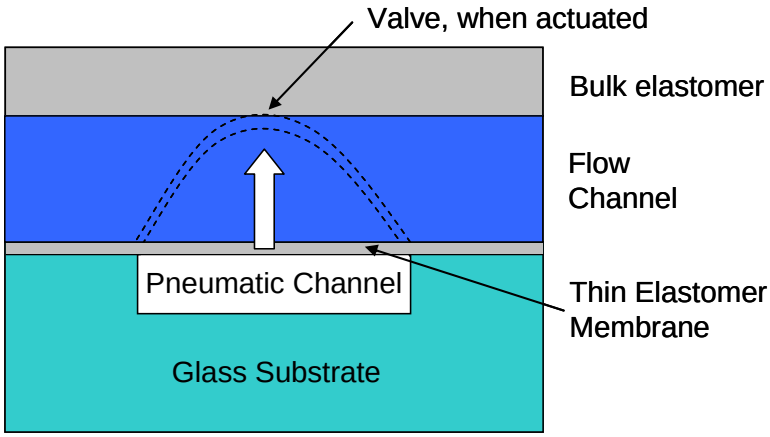

Figure 5-2. Pneumatic channel design.

Integrated counter-selection has been included in the chip design via a second selection chamber. The microbeads used for selection will be inserted into this chamber without target functionalization (the active NHS binding sites will be blocked with free primary amines using Tris buffer), and the chamber maintained at the binding temperature (still 37°C). To perform counter-selection against the beads, support molecules, and other unintended targets the DNA library will be incubated for 10 minutes in this chamber after 3 rounds of SELEX, prior to amplification. As a result, ssDNA that expresses binding affinity to these unintended target molecules will be eliminated from the pool.

5-2.2 Materials

The materials used for the design, fabrication, and operation of the microfluidic SELEX chip are identical to those of the aptamer isolation chip discussed in Chapter 4. Human IgE was purchased from Athens Research, Athens, GA. All DNA was obtained in lyophilized form from Integrated DNA Technologies, Coralville, IA. The library is an 80mer ssDNA oligomer consisting of a 40 base randomized region flanked by two 20 base known priming regions. The purchased library sequence is as follows: 5' – C TAC CTA CGA TCT GAC TAG CNN NNN NNN NNN NNN NNN NNN NNN NNN NNN NNN NNN NNN NNG CTT ACT CTC ATG TAG TTC C– 3'. The forward primers used were 5' – C TAC CTA CGA TCT GAC TAG C – 3', with or without a 5' carboxyfluorescein modification. The reverse primers used were 5' – G GAA CTA CAT GAG AGT AAG C – 3', with a 5' dual biotin attachment. In each case an inert spacer molecule is incorporated between the sequence and the terminal modification. Microbeads used for aptamer selection were NHS-activated sepharose beads obtained from Bio-Rad laboratories. Microbeads used for bead-based PCR were Ultralink Streptavidin-coated beads obtained from Thermo Scientific Pierce Protein Research Products, Rockford, IL. Materials used in microfabrication included S1800 photoresist (Dow Chemical, Midland, MI), SU-8 2000 (Microchem, Newton MA), PDMS prepolymer (Dow Chemical), and Dix C Parylene prepolymer (Uniglobe Kisko, White Plains NY). PCR reagents included GoTaq Flexi PCR Mix (Promega, Madison WI), Taq enzyme (Promega), and deoxynucleotide triphosphates (dNTPs, Promega).

The reactants used for on-chip amplification of candidate aptamers consisted of the following: 5× PCR Buffer (2 μL), 25 mM $MgCl_2$ (0.6 μL), 10 mM dNTPs (0.4 μL), 50 μg/mL BSA (0.4 μL), microbeads (0.5 μL), water (5.6 μL), 25 μM forward primer

(0.4 μL), and enzyme (0.1 μL). The reactants were degassed at -0.4 psi for 30 minutes in a darkened container prior to adding enzyme and proceeding with on-chip amplification. Reactants necessary for cloning and extraction of plasmid DNA are proprietary, and were purchased as part of the TOPO TA Cloning Kit and MiniPrep Extraction Kit from Invitrogen (Grand Island, NY).

5-2.3 Experimental Protocol

Device characterization was performed as in the previous chapter. Briefly, the resistive temperature sensor was calibrated in an environmental chamber. NHS beads were functionalized with IgE and then passivated with Tris buffer. Streptavidin-coated microbeads were incubated with primers for 30 minutes prior to bead-based PCR.

The primary selection protocol was performed identically to the previous chapter. Briefly, PBSM modified with 1 mM $MgCl_2$ was used as the buffer for incubation of library DNA and elution of candidate aptamers. The binding and release temperatures, 37°C and 57°C respectively, were maintained in the microchambers via closed-loop control using a LabView program. The counter-selection procedure was performed almost identically to the selection procedure: 1 mM PBSM containing the candidate aptamer pool was exposed to the microbeads at the binding temperature, which was maintained via closed-loop control. In this case, this temperature was maintained while the candidate pool was washed through the chamber at 1 μL/min. This solution was then passed to the amplification chamber to undergo bead-based PCR. The amplification protocol and reagents were consistent with those of the previous chapter. In this case elution of ssDNA was followed by further rounds of SELEX (not final analysis).

However, sample ports in the microfluidic chip were used to obtain samples of the ssDNA pool following each round of SELEX. These samples were analyzed by cloning and sequencing to determine the evolution of the pool at each step of the SELEX process. Cloning and sequencing of the pools, as well as the fluorescent analysis of the individual sequences, were consistent with the approach used in the previous chapter.

5-3 Initial Results and Ongoing Work

Multi-round microfluidic SELEX testing is currently underway. Currently, three pools of DNA are undergoing multiple rounds of SELEX to produce a temperature-specific high-affinity aptamer specific to IgE. Thus far, results consist of DNA sequences from 5 different cloning and sequencing protocols. SELEX pools 1 and 2 have undergone 2 rounds of SELEX each, and these sequences are prefixed 1-1, 1-2, 2-1, and 2-2, respectively. A third pool has undergone one round of SELEX, and the results are prefixed 3-1. The sequences are listed in Table 5-1 below.

Table 5-1. Results of sequencing 10 clones from 5 pools of enriched library DNA.

1-1-1	GGAAGGAATCGGTTAACCCTTCTCAAAGGTTCGCCGGAGG
1-1-2	AGGNTTTTTATGAGAGTTCTTTTCTAGATTGTCCCATCCG
1-1-3	GGGGCCGGGCTCAGAAGTCAGACTTTAGGTTGCGTTGGTA
1-1-4	GCGTATNCTGCNAAACAGATCGGTGTGGCNTATGTTTGANG
1-1-5	NCTNNNGTCCGTTACTTTGNTNGTANATTAATNCNNNTCG
1-1-6	CGCCCGAATTAAGATCTAGTTAGCCGCGGTATTGGTCTTG
1-1-7	TCATGCGGGACACAAGTATCTTTGTCTAAATTCGTATCC
1-1-8	CGCCTGAATAGGTCCGCGATCCGCGATGCCAATTGCTTCG
1-1-9	CAGTGATCCTTTGAGACAAGTGACCTATGCATTTGATGG
1-1-10	ATAAAAGCAACTACCATACTCCAATTAACTGAGGCGGACA
1-2-1	TACTCTGACGGGTAGTATATCCCGGGCTAGGTGGCGGGAA
1-2-2	CCTGTTTAACTCATGTGTGTCAACTGATATTGATGTCTGG
1-2-3	ACTAACTGAAAGTGGTGGAGTAGCCTACTGACACTAGGG
1-2-4	ATATTAATGTTTAAGCGGTATAGTAGTATGATCTATGCCG

1-2-5	TATCTATGAGAAAATCCGCTAACAATTCATATATACCTCA
1-2-6	TTGGTCAAGTAATGATCCTCATATGTGTCCTTGGAGGTAG
1-2-7	GTACGTGGTGCAGTATAATTCCTCTATGCCTTGTACTGCA
1-2-8	ACGTACNTTCATTGNNAAANAGGTGTTACTTGTGCNTGAA
1-2-9	GGAGGCGGCAGAGGCTAGTGGGGGCGGGGGTCGCGGGGGG
1-2-10	CGTGGCAGCAACCGNGGTGAATTATTTAGATCGTCTGAATTA

2-1-1	CATTGTGATATGTTTTCTATCCATGCTGAGCGGTAATAT
2-1-2	GAGTCTGTAGGACATGGTGCCAAAGGGCTTTGAGCATCTG
2-1-3	AGAGCTTCAAAGGGCTAACGGGCGCTAATGGGTCAAGTTT
2-1-4	CACCCTTTGCACGGAAGTAGCATAAATTAACACCTAGAGT
2-1-5	GTCCACAATTTTCATCGATCCAAAGGCAGTAGGATTAACG
2-1-6	TAAAAGCGGGGCGGGACAGGGCGGCGGCGGGGCGGGGCCA
2-1-7	GTTACGGTACAGCTGGCTCTGTTGATGGGACTGAGGCGGG
2-1-8	GTCCAGTTCGGTTGGTAGTGCTGAGTTAAATAAAGCCAAT
2-1-9	TTTATGGTTGTGGGCAATATTCAGTTGGGCAACATTACAG
2-1-10	ACTACCTTTCCGACGTTATAGGGTAAATGAAAGGTATCGG

2-2-1	TCAATACGTTCTGTCATGTATTTGGCAAGTTGTTATTTTA
2-2-2	TACGTTATAGAGTATTTACAAATAACATAAACGTAGTACT
2-2-3	CGCATTTTGAGGGATTGACTAGGGGGATTTGGTAGGTGAG
2-2-4	ATGACCTTTCTAATATGACACGTCATCTCTAATTGCTGCG
2-2-5	TTTTGCAGCCGAGTCCATTGGTGTGGCGGGCGAGGTGGGG
2-2-6	CCATGCTTAAGCTCAGCCTCAGTTCCTGTAGTGAGTGTGG
2-2-7	GGGCTGGTAGCCTATGGGGATGGCGTGGTGGGAGGGGTTC
2-2-8	GGTATGATTGGGTGTCAAGTACTTCATACCAGCGTTTGGG
2-2-9	TGCATATCCCTAGGAAATTAATCGGGTTTATTGACAATCG
2-2-10	AGCATAAGGGCCTTATGATAGTCATATTGCTTGGAATCTG

3-1-1	CAATTATTATCTTCGGCCTCTGATTGTTCCGTACTTGGGG
3-1-2	ACGTATAACGCGTGGGTGCACGCTGTTTATAAGTATTCCG
3-1-3	GGTCGCCATTGACTGAGCCTATTCAGCGGGTGGATCGTGG
3-1-4	CACACTTGTCATTCGTTTAAATTTACCACTGTCAAGTGCT
3-1-5	ATAATTTTTAGGTACGTCTTATGGTGGCATCGGTCGCCGG
3-1-6	CATAAATAGCGTCAGTCTGACATAAGTCGCGGTTCATTG
3-1-7	TTCTTGTCGATTTCATATTATGCACATAGTTATTAGTTAT
3-1-8	TAATTACTTCTCTTTAGACGTAAAGGTCATGTGGGCATTG
3-1-9	CCTTATCGTAATAGTTCTTTGCTTCAATTTTTGGGAAGGG
3-1-10	GCATCATGAGTGTGTATGTGTGTGGTGTTTGTGTGGCGTC

Ongoing work includes the analysis of the sequenced clones, as well as further rounds of SELEX. It is anticipated that at least 3-4 rounds of SELEX will be needed to demonstrate full library evolution, and more than one selection approach is being

undertaken to both ensure evolution and to provide a basis for comparison of effects of flowrate and temperature on selection. Future data will include further sequencing results, as well as analysis of the binding strength of individual clones via a fluorescence binding assay.

5-4 Conclusions

This work will be concluded following the publication of this dissertation.

Chapter 6: Conclusions

6-1 Dissertation Summary

Aptamers hold the potential to revolutionize a number of fields, including clinical diagnostics, therapeutics, and biological detection and separation. Molecules performing similar functions, such as monoclonal antibodies, are highly desired within these fields but are not as capable as their nucleic acid counterparts (see Introduction 1-2.1). The technology necessary to isolate target-binding aptamer sequences is available, but inadequate for the current demand (Introduction 1-3.1).

Recently, the application of microfluidics to SELEX has resulted in vast reductions in the amount of time necessary to generate binding sequences. Building on previous work, the goal of this dissertation was to generate microfluidic devices capable of generating high-affinity aptamer sequences in hours or days, rather than weeks or months as with conventional technology. In addition to building upon reported effective selection technology, this work implemented a new approach to integration of SELEX using a bead-based PCR technique, and took advantage of MEMS-based thermal control to generate aptamers with temperature-specific binding affinity. Specific results of this work include:

6-1.1 A microfluidic cocaine aptasensor

The fabrication and testing of a microfluidic cocaine aptasensor. Cocaine-specific DNA aptamers were immobilized onto microbeads and trapped in a PDMS microfluidic chamber with weir structures above an integrated temperature sensor and heater. The

aptamers transduced cocaine binding via changes in fluorescent intensity, and results using fluorescent microscopy showed a linear response over 4 orders of magnitude of cocaine concentration, including physiologically relevant (nanomolar) concentrations. In addition, the ability of aptamer-functionalized surfaces to enrich target molecules allowed the device detection limit to be lowered to 10 pM following enrichment using continuous flow of a rarefied concentration of cocaine. Finally, using on-chip temperature control, the device was made fully reusable via thermal regeneration of the aptamer-coated surfaces.

6-1.2 Integrated Microfluidic Bead-based PCR

A novel approach to integrated on-chip amplification was developed using bead-based PCR. A method was developed whereby target DNA was captured by primer-coated microbeads and amplified with fluorescently-labeled forward primers. In this way, the beads acted as a highly specific SPE surface, purifying the DNA from undesired ionic contamination and releasing the amplified DNA into a desired buffer solution. The incorporation of fluorescent labels transformed the amplification process into a detection scheme, by simultaneously concentrating the fluorescent labels on microbead surfaces enabling detection via fluorescent microscopy. It was demonstrated that the method was capable of detecting 1 pM DNA in only 10 cycles of amplification, and discerning this from a zero-template control (as determined by analysis of the data with the students' t-test). Furthermore, this process was integrated into a single temperature-controlled microchamber. It was demonstrated that a single microchamber with primer-coated

microbeads could capture, purify, amplify, detect, and release target DNA, potentially vastly simplifying an array of on-chip functions.

6-1.3 Microfluidic Temperature-Specific Aptamer Isolation

A single round of selection/amplification was performed in an integrated microdevice and a randomized library was enriched for temperature-specific binding to human IgE. This device exploited on-chip temperature control to perform selection at pre-specified temperatures, directing the evolution of the library towards a binding motif with predetermined temperature-dependent binding properties. The bead-based amplification scheme was also incorporated to specifically capture, purify, amplify, and collect the target ssDNA. The device was designed to perform a single round of SELEX, demonstrating the capability of the designed selection/amplification schemes to work in concert to perform a highly efficient SELEX procedure. Fluorescence binding assays indicated that the enriched library expressed increased binding to IgE and that the binding strength exhibited the intended correlation with temperature.

6-1.4 Ongoing Work on Integrated Microfluidic SELEX

In ongoing work, a fully integrated microfluidic device is being used to perform multiple rounds of temperature-specific SELEX. This device is capable of fully integrated, automated SELEX without the need for off-chip analysis or pipetting prior to collection of the fully enriched library. To demonstrate the effectiveness of the device, 3-4 rounds of temperature-specific SELEX are being performed against IgE, and the

sequence pools are being cloned after each round to capture and analyze the evolution of the library towards a temperature-specific binding motif.

6-2 Future Work

The devices demonstrated in this work represent proofs-of-concept, with several opportunities for subsequent applications and basic research.

6-2.1 Bead-based microfluidic sensors

The microfluidic cocaine aptasensor described in Chapter 2 represents not only a cocaine sensor, but a platform for detection of a large number of analytes. As described in detail in this dissertation, the primary hindrance to the development of aptamer-based systems is the lack of aptamer sequences. There are already a significant number of aptamers targeting proteins and small molecules, however, and the bead-based sensing platform described herein is general to all such targets. While this work has focused on cocaine, substitution of any aptamer whose target falls into a similar molecular weight range should in principle be compatible. Of course sensor operation will necessarily vary based on the different binding characteristics of other aptamer-target systems (equilibrium dissociation constant, dissociation rate constants, etc.), but in principle similar results should be achievable. It should be noted that the cocaine-aptamer system used in this work possesses relatively weak binding, having an equilibrium dissociation constant of 1 μM and being based almost solely on hydrophobic interactions. As a result, the tighter binding associated with other aptamer-target systems may result in even lower detection limits when acting as a sensing system.

6-2.2 Integrated sample-to-answer devices using bead-based polymerase chain reaction

As with the sensing platform described in Chapter 2, the bead-based PCR system has the potential to be used in a wide variety of applications. The primary utility of bead-based PCR is that it can bridge incompatibilities between amplification and pre-amplification steps such as differences in ionic, pH, or other buffer conditions. As such, protocols deriving nucleic acids from complex mixtures such as cell lysate for amplification and analysis have the potential to benefit from this protocol. Previous work has demonstrated that DNA-coated microbeads can be an effective SPE platform [133], and this dissertation has shown the power of integrating bead-based PCR with applications such as DNA detection and SELEX. Future applications for this technology include portable clinical diagnostic systems and integrated single-cell analysis of gene expression.

6-2.3 Efficiency analysis of integrated microfluidic PCR

The integrated multi-round SELEX device discussed in Chapter 5 must still be fully characterized. The ability of the device to converge a randomized library to a consensus binding sequence will be observed using both isothermal conditions and the temperature-specific selection protocol. The content of the randomized pools over several rounds of SELEX using both protocols may illustrate the effectiveness of the temperature-specific selection. Typical selection protocols maintain background conditions throughout selection to ensure that the generated binding sequence has high

affinity. In the temperature-specific approach, however, the background (i.e. temperature) conditions are varied, and this represents a second domain across which aptamers may be selected. The rate at which the library converges during selection to a binding motif may well vary between isothermal and temperature-specific methods, and this is of interest for further development of aptamer-generation devices.

6-2.4 Temperature-specific SELEX against novel target molecules

The use of human IgE as a target molecule served to validate the developed aptamer isolation process, as there are already IgE-specific binding sequences available, including a temperature-specific aptamer which binds to IgE at 37°C and releases at 57°C [33]. Tailoring temperature-specificity in aptamer selection has not been well explored, and has great potential for aptamers developed for therapeutic applications. For example, some target proteins are expressed more strongly at higher temperatures, such as heat shock proteins. The ability to generate aptamers whose structure either folds in a temperature-dependent manner or whose binding is temperature-insensitive across a range of interest would be of great interest for therapeutic applications involving such proteins. When culturing cells, temperature control is paramount to ensure that cells remain viable and maintain consistent surface protein expression during selection. Cell-SELEX, which is being widely explored for therapeutic purposes [161], would benefit greatly from a SELEX device which is capable of maintaining proper temperature control throughout the selection process.

6-2.5 Multiplexed SELEX for interrogation of binding schemes of synthetic nucleic acids

Along with precise control over device features, microscale fabrication architecture affords the ability to scale up production and design to minimize costs or maximize yield. Following minor design changes, the microfluidic SELEX chips described in this dissertation could be adapted to work in tandem in a number of ways. An example application of such a multiplexed nucleic acid screening device would be to investigate the relationship between short DNA and RNA strands and enantiomeric microRNA (miRNA) sequences. MicroRNAs are short RNA sequences found in eukaryotic cells that act as post-transcriptional regulators [162]. For example, miRNA-122 is a 74 nt miRNA found in liver cells, and is necessary for accumulation of hepatitis C virus (HCV) [163]. Inhibition of this miRNA with a locked nucleic acid complement was shown to suppress HCV in chimpanzees [164]. If the structural interactions between enantiomeric RNAs and their naturally structured DNA and RNA counterparts were well understood, enantiomeric RNA inhibitors for known miRNAs could be designed a priori without the need for screening binders using a SELEX-like process.

6-3 Expected Developments and Final Words

Aptamer-generation devices and services are already coming online for commercial use; companies such as RiNA GmbH, AptSci, Custom Array, NeoVentures Biotechnology, LC Sciences, BasePair Biotechnology, and Aptagen offer or have offered customized aptamer generation for protein targets. These services are still very expensive, and they come without a guarantee of both high-affinity aptamers and a reasonable

development time. In the near future it is expected that these services will expand and their costs will be driven downward by both competition and advances in technology. The microfluidic "lab-on-a-chip" approach is ideally suited to minimizing aptamer generation time, by making the process more efficient through high surface area-to-volume ratio surface-based selection and integrated, automated control of reaction conditions.

For the great expectations of aptamer-based devices to come to fruition, a better, cheaper way of finding aptamer sequences must be found. The traditional model – of dedicated researchers using months of time and liters of expensive reagents to find a single binding sequence – is unsustainable if aptamers are to be seen as a true alternative to other molecular recognition species. While sequences found as a result of publicly funded research are available for use by all, aptamer development costs must be reduced if the profit-driven private sector is to be persuaded to develop aptamers for more useful targets. This work represents a proof-of-concept approach to aptamer sequence isolation that can be readily duplicated to provide aptamer sequences to both publicly- and privately-funded enterprises.

Appendix 1: Supplementary Data for Bead-Based PCR

A1-1 Bead-Based PCR Scheme

Bead-based PCR is a solid-phase implementation of PCR, in which DNA is duplicated while tethered to the surfaces of microbeads in solution. In bead-based PCR, one of the two primer sets (typically the reverse primer) is tethered to a bead surface, while the untethered (forward) primer can be labeled with a detectable tag (e.g., a fluorophore). Bead-bound reverse primers are mixed with template ssDNA (Figure S1a), labeled forward primers and other reactants (e.g., nucleotides and Taq) in solution,and hybridize to template ssDNA molecules (Figure S1b). This results in the capture of template DNA by the microbeads and is hence effectively a SPE process. This completes the first temperature cycle, which produces unlabeled dsDNA (Figure S1c). During the second temperature cycle, the dsDNA from the previous cycle is denatured, allowing template DNA and fluorescently labeled forward primers to hybridize to bead-bound ssDNA (complementary strands of the template) (Figure S1d). Extension then generates labeled duplicates of template DNA hybridized to the bead-bound complementary strands (Figure S1e). This process is then repeated with further temperature cycles to produce exponentially increasing copies of dsDNA consisting of labeled template and unlabeled, bead-tethered complementary strands.

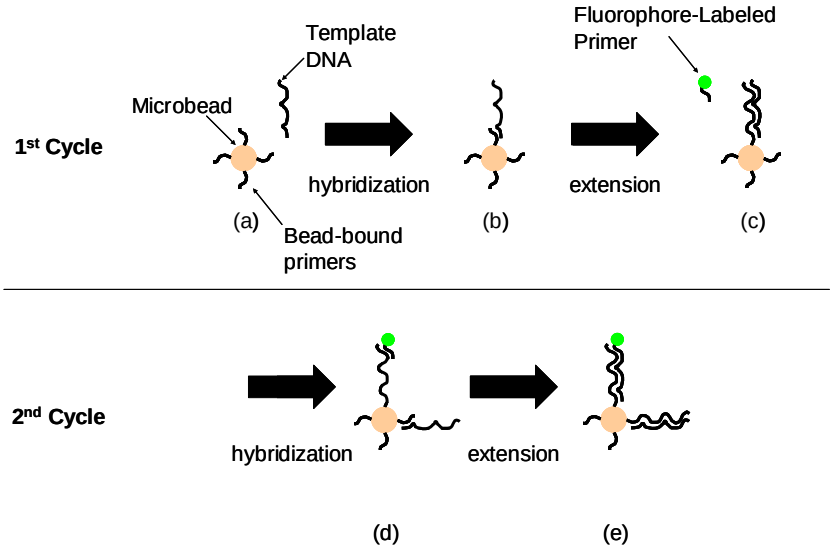

Figure A1-1. DNA/Fluorescent Signal Generation. Primer-coated beads (a) hybridize to the DNA (b); an initial temperature cycle generates complementary ssDNA attached to the beads (c); during the following temperature cycle, fluorescently labeled primers are captured by the complementary ssDNA (d) and amplification generates fluorescently labeled dsDNA which remains attached to the beads (e).

A1-2 Sensor Calibration

Resistance measurements of a typical temperature sensor are shown in Figure S2, illustrating the linear relationship between resistance and temperature. This data was used to calculate a TCR for the sensor of 2×10^{-3} °C^{-1}.

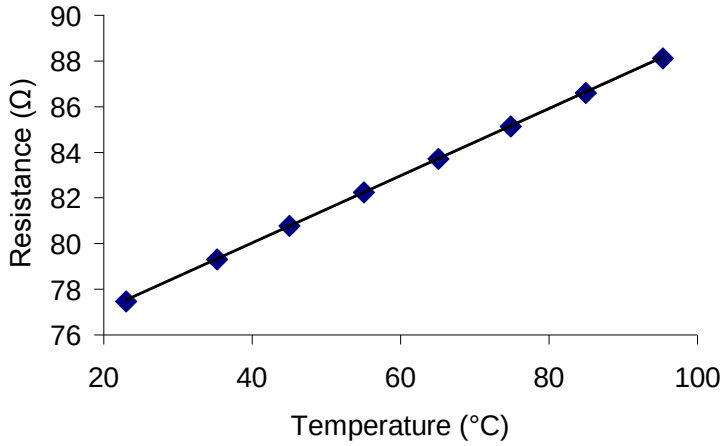

Figure A1-2. Calibration data for an integrated resistive temperature sensor.

A1-3 Optimization of Magnesium Concentration.

Optimum magnesium concentration was determined via a series of tests using different concentrations of $MgCl_2$ in the reaction mixture. *B. pertussis* DNA templates were introduced to PCR reactions at a final concentration of 10 pM using the PCR mixture recipe described and PCR was performed for 20 cycles with an annealing temperature of 52°C in a commercial thermal cycler. Gel electrophoresis of the amplified samples indicated that a concentration of 1.5 mM $MgCl_2$ produced the greatest amount of output DNA (data not shown), which is consistent with typical $MgCl_2$ concentrations for PCR studies. This result is expected to be sequence-dependent, and thus particular to this example and not general to bead-based PCR.

A1-4 Study of Optimum Dwell Time

Dwell times, the length of time the PCR sample is incubated at each temperature during each PCR cycle, were optimized to produce the maximum amount of DNA within the

shortest reaction time possible. An optimum dwell time exists for solution-based PCR such that a larger time results in a minimal increase, or possibly a decrease, in reaction efficiency. To investigate the effect of dwell time on the bead-based PCR device, PCR reactions were performed for 20 cycles using different dwell times (data not shown). The results of the testing indicate that a 20 s dwell time most efficiently produces output DNA. This is consistent with typical dwell time values for microscale PCR devices, which typically enable shorter dwell times than conventional PCR cyclers due to more rapid and uniform sample heating.

References

1 G. Hybarger, J. Bynum, R. Williams *et al.*, A microfluidic SELEX prototype, Analytical and Bioanalytical Chemistry, 384 1 (2006), 191-198.

2 X. Lou, J. Qian, Y. Xiao *et al.*, Micromagnetic selection of aptamers in microfluidic channels, Proceedings of the National Academy of Sciences, 106 9 (2009), 2989-2994.

3 P. A. Auroux, D. Iossifidis, D. R. Reyes *et al.*, Micro total analysis systems. 2. Analytical standard operations and applications, Analytical Chemistry-Washington DC-, 74 12 (2002), 2637-2652.

4 S. Lee, and S. Lee, Micro total analysis system (μ-TAS) in biotechnology, Applied Microbiology and biotechnology, 64 3 (2004), 289-299.

5 D. R. Reyes, D. Iossifidis, P. A. Auroux *et al.*, Micro total analysis systems. 1. Introduction, theory, and technology, Analytical Chemistry-Washington DC-, 74 12 (2002), 2623-2636.

6 A. van den Berg, and T. Lammerink, Micro total analysis systems: microfluidic aspects, integration concept and applications, Microsystem technology in chemistry and life science (1998), 21-49.

7 J. West, M. Becker, S. Tombrink *et al.*, Micro total analysis systems: latest achievements, Anal. Chem, 80 12 (2008), 4403-4419.

8 R. Bashir, BioMEMS: state-of-the-art in detection, opportunities and prospects, Advanced drug delivery reviews, 56 11 (2004), 1565-1586.

9 A. C. R. Grayson, R. S. Shawgo, A. M. Johnson *et al.*, A BioMEMS review: MEMS technology for physiologically integrated devices, Proceedings of the IEEE, 92 1 (2004), 6-21.

10 J. Lichtenberg, N. F. de Rooij, and E. Verpoorte, Sample pretreatment on microfabricated devices, Talanta, 56 2 (2002), 233-266.

11 B. S. Broyles, S. C. Jacobson, and J. M. Ramsey, Sample filtration, concentration, and separation integrated on microfluidic devices, Analytical Chemistry, 75 11 (2003), 2761-2767.

12 A. G. Crevillen, M. Hervas, M. A. Lopez *et al.*, Real sample analysis on microfluidic devices, Talanta, 74 3 (2007), 342-357.

13 A. J. de Mello, and N. Beard, Dealing with 'real' samples: sample pre-treatment in microfluidic systems, Lab on a Chip, 3 1 (2003), 11N-19N.

14 M. C. Peoples, and H. T. Karnes, Microfluidic immunoaffinity separations for bioanalysis, Journal of Chromatography B-Analytical Technologies in the Biomedical and Life Sciences, 866 1-2 (2008), 14-25.

15 D. S. Hage, *Handbook of affinity chromatography*: CRC, 2006.

16 A. D. Ellington, and J. W. Szostak, In Vitro Selection of RNA Molecules that Bind Specific Ligands, Nature, 346 6287 (1990), 818-822.

17 C. Tuerk, and L. Gold, Systematic Evolution of Ligands by Exponential Enrichment - RNA Ligands to Bacteriophage-T4 DNA Polymerase, Science, 249 4968 (1990), 505-510.

18 R. C. Conrad, L. Giver, Y. Tian *et al.*, In vitro selection of nucleic acid aptamers that bind proteins, Combinatorial Chemistry, 267 (1996), 336-367.

19 F. Darfeuille, J. B. Hansen, H. Orum *et al.*, LNA/DNA chimeric oligomers mimic RNA aptamers targeted to the TAR RNA element of HIV‐1, Nucleic Acids Research, 32 10 (2004), 3101-3107.
20 F. Le Floch, H. A. Ho, and M. Leclerc, Label-Free Electrochemical Detection of Protein Based on a Ferrocene-Bearing Cationic Polythiophene and Aptamer, Analytical Chemistry, 78 13 (2006), 4727-4731.
21 P. E. Nielsen, "Peptide nucleic acids: A new dimension to peptide libraries and aptamers," *Methods in Enzymology*, N. A. John, ed., pp. 426-433: Academic Press, 1996.
22 D. Eulberg, F. Jarosch, S. Vonhoff *et al.*, Spiegelmers for Therapeutic Applications–Use of Chiral Principles in Evolutionary Selection Techniques, The Aptamer Handbook (2006), 417-442.
23 A. D. Keefe, and S. T. Cload, SELEX with modified nucleotides, Current Opinion in Chemical Biology, 12 4 (2008), 448-456.
24 R. R. Breaker, DNA aptamers and DNA enzymes, Current Opinion in Chemical Biology, 1 1 (1997), 26-31.
25 A. Kulbachinskiy, Methods for selection of aptamers to protein targets, Biochemistry (Moscow), 72 13 (2007), 1505-1518.
26 M. Famulok, G. Mayer, and M. Blind, Nucleic acid aptamers - From selection in vitro to applications in vivo, Accounts of Chemical Research, 33 9 (2000), 591-599.
27 K.-M. Song, S. Lee, and C. Ban, Aptamers and Their Biological Applications, Sensors, 12 1 (2012), 612-631.
28 J. P. Hilton, T. H. Nguyen, R. Pei *et al.*, A microfluidic affinity sensor for the detection of cocaine, Sensors and Actuators A: Physical, 166 2 (2011), 241-246.
29 A. Geiger, P. Burgstaller, H. vonderEltz *et al.*, RNA aptamers that bind L-arginine with sub-micromolar dissociation constants and high enantioselectivity, Nucleic Acids Research, 24 6 (1996), 1029-1036.
30 T. S. Romig, C. Bell, and D. W. Drolet, Aptamer affinity chromatography: combinatorial chemistry applied to protein purification, Journal of Chromatography B-Analytical Technologies in the Biomedical and Life Sciences, 731 2 (1999), 275-284.
31 S. M. Nimjee, C. P. Rusconi, and B. A. Sullenger, Aptamers: An Emerging Class of Therapeutics, Annual Review of Medicine, 56 1 (2005), 555-583.
32 S. M. Nimjee, C. P. Rusconi, R. A. Harrington *et al.*, The potential of aptamers as anticoagulants, Trends Cardiovasc Med, 15 1 (2005), 41-5.
33 T. W. Wiegand, P. B. Williams, S. C. Dreskin *et al.*, High-affinity oligonucleotide ligands to human IgE inhibit binding to Fc epsilon receptor I, Journal of Immunology, 157 1 (1996), 221-230.
34 M. N. Stojanovic, P. de Prada, and D. W. Landry, Aptamer-based folding fluorescent sensor for cocaine, Journal of the American Chemical Society, 123 21 (2001), 4928-4931.
35 C. Mannironi, A. DiNardo, P. Fruscoloni *et al.*, In vitro selection of dopamine RNA ligands, Biochemistry, 36 32 (1997), 9726-9734.
36 M. Famulok, Oligonucleotide aptamers that recognize small molecules, Current opinion in structural biology, 9 3 (1999), 324-329.

37 J. Wang, and G. Li, Aptamers Against Cell Surface Receptors: Selection, Modification and Application, Current Medicinal Chemistry, 18 27 (2011), 4107-4116.

38 J. K. Herr, J. E. Smith, C. D. Medley *et al.*, Aptamer-conjugated nanoparticles for selective collection and detection of cancer cells, Analytical Chemistry, 78 9 (2006), 2918-2924.

39 Z. Balogh, G. Lautner, V. Bardóczy *et al.*, Selection and versatile application of virus-specific aptamers, The FASEB Journal, 24 11 (2010), 4187-4195.

40 S. C. B. Gopinath, Methods developed for SELEX, Analytical and Bioanalytical Chemistry, 387 1 (2007), 171-182.

41 W. James, Aptamers in the virologists' toolkit, J. Gen. Virol., 88 8 (2007), 351-364.

42 D. V. Lim, J. M. Simpson, E. A. Kearns *et al.*, Current and Developing Technologies for Monitoring Agents of Bioterrorism and Biowarfare, Clinical Microbiology Reviews, 18 4 (2005), 583-607.

43 J. S. Swensen, Y. Xiao, B. S. Ferguson *et al.*, Continuous, Real-Time Monitoring of Cocaine in Undiluted Blood Serum via a Microfluidic, Electrochemical Aptamer-Based Sensor, Journal of the American Chemical Society, 131 12 (2009), 4262-4266.

44 J. R. Kanwar, K. Roy, and R. K. Kanwar, Chimeric aptamers in cancer cell-targeted drug delivery, Critical reviews in biochemistry and molecular biology 00 (2011), 1-19.

45 C. K. O'Sullivan, Aptasensors - the future of biosensing, Analytical and Bioanalytical Chemistry, 372 1 (2002), 44-48.

46 D. H. J. Bunka, O. Platonova, and P. G. Stockley, Development of aptamer therapeutics, Current Opinion in Pharmacology, 10 5 (2010), 557-562.

47 E. W. M. Ng, D. T. Shima, P. Calias *et al.*, Pegaptanib, a targeted anti-VEGF aptamer for ocular vascular disease, Nat Rev Drug Discov, 5 2 (2006), 123-132.

48 P. Wang, Y. Yang, H. Hong *et al.*, Aptamers as Therapeutics in Cardiovascular Diseases, Current Medicinal Chemistry, 18 27 (2011), 4169-4174.

49 T. Nguyen, R. Pei, M. Stojanovic *et al.*, An aptamer-based microfluidic device for thermally controlled affinity extraction, Microfluidics and Nanofluidics, 6 4 (2009), 479-487.

50 T. H. Nguyen, R. Pei, M. Stojanovic *et al.*, Demonstration and characterization of biomolecular enrichment on microfluidic aptamer-functionalized surfaces, Sensors and Actuators B: Chemical, 155 1 (2011), 58-66.

51 T. Nguyen, R. Pei, D. W. Landry *et al.*, Microfluidic aptameric affinity sensing of vasopressin for clinical diagnostic and therapeutic applications, Sensors and Actuators B: Chemical, 154 1 (2011), 59-66.

52 H. M. Hiep, K. Kerman, T. Endo *et al.*, Nanostructured biochip for label-free and real-time optical detection of polymerase chain reaction, Analytica Chimica Acta, 661 1 (2010), 111-116.

53 L. Shen, Z. Chen, Y. Li *et al.*, A chronocoulometric aptamer sensor for adenosine monophosphate, Chemical Communications 21 (2007), 2169-2171.

54 Y. C. Lim, A. Z. Kouzani, and W. Duan, Aptasensors: A Review, Journal of Biomedical Nanotechnology, 6 2 (2010), 93-105.

55 T. Nguyen, J. Hilton, and Q. Lin, Emerging applications of aptamers to micro- and nanoscale biosensing, Microfluidics and Nanofluidics, 6 3 (2009), 347-362.
56 A. Sassolas, L. J. Blum, and B. D. Leca-Bouvier, Optical detection systems using immobilized aptamers, Biosensors & Bioelectronics, 26 9 (2011), 3725-3736.
57 R. C. Conrad, L. Giver, Y. Tian *et al.*, "In vitro selection of nucleic acid aptamers that bind proteins," *Methods in Enzymology*, N. A. John, ed., pp. 336-367: Academic Press, 1996.
58 M. Legiewicz, C. Lozupone, R. Knight *et al.*, Size, constant sequences, and optimal selection, RNA, 11 11 (2005), 1701-1709.
59 M. Bianchini, M. n. Radrizzani, M. G. Brocardo *et al.*, Specific oligobodies against ERK-2 that recognize both the native and the denatured state of the protein, Journal of Immunological Methods, 252 1–2 (2001), 191-197.
60 R. White, C. Rusconi, E. Scardino *et al.*, Generation of Species Cross-reactive Aptamers Using [ldquo]Toggle[rdquo] SELEX, Mol Ther, 4 6 (2001), 567-573.
61 A. Geiger, P. Burgstaller, H. von der Eltz *et al.*, RNA aptamers that bind L-arginine with sub-micromolar dissociation constants and high enantioselectivity, Nucleic Acids Research, 24 6 (1996), 1029-1036.
62 R. Stoltenburg, C. Reinemann, and B. Strehlitz, SELEX—A (r)evolutionary method to generate high-affinity nucleic acid ligands, Biomolecular Engineering, 24 4 (2007), 381-403.
63 M. Berezovski, M. Musheev, A. Drabovich *et al.*, Non-SELEX selection of aptamers, Journal of the American Chemical Society, 128 5 (2006), 1410-1411.
64 M. C. Golden, B. D. Collins, M. C. Willis *et al.*, Diagnostic potential of PhotoSELEX-evolved ssDNA aptamers, Journal of biotechnology, 81 2 (2000), 167-178.
65 K. B. Jensen, B. L. Atkinson, M. C. Willis *et al.*, Using in vitro selection to direct the covalent attachment of human immunodeficiency virus type 1 Rev protein to high-affinity RNA ligands, Proceedings of the National Academy of Sciences, 92 26 (1995), 12220.
66 S. Oehler, R. Alex, and A. Barker, Is Nitrocellulose Filter Binding Really a Universal Assay for Protein–DNA Interactions?, Analytical Biochemistry, 268 2 (1999), 330-336.
67 T. S. Misono, and P. K. R. Kumar, Selection of RNA aptamers against human influenza virus hemagglutinin using surface plasmon resonance, Analytical Biochemistry, 342 2 (2005), 312-317.
68 R. Pollock, and R. Treisman, A sensitive method for the determination of protein-DNA binding specificities, Nucleic Acids Research, 18 21 (1990), 6197-6204.
69 M. Blank, T. Weinschenk, M. Priemer *et al.*, Systematic Evolution of a DNA Aptamer Binding to Rat Brain Tumor Microvessels, Journal of Biological Chemistry, 276 19 (2001), 16464-16468.
70 J. C. Cox, and A. D. Ellington, Automated selection of anti-protein aptamers, Bioorganic & Medicinal Chemistry, 9 10 (2001), 2525-2531.
71 R. Stoltenburg, C. Reinemann, and B. Strehlitz, FluMag-SELEX as an advantageous method for DNA aptamer selection, Analytical and Bioanalytical Chemistry, 383 1 (2005), 83-91.

72 S. D. Mendonsa, and M. T. Bowser, In vitro evolution of functional DNA using capillary electrophoresis, Journal of the American Chemical Society, 126 1 (2004), 20-21.
73 W. Yao, K. Adelman, and J. A. Bruenn, In vitro selection of packaging sites in a double-stranded RNA virus, Journal of Virology, 71 3 (1997), 2157-62.
74 F. Zhang, and D. Anderson, In Vitro Selection of Bacteriophage ϕ 29 Prohead RNA Aptamers for Prohead Binding, Journal of Biological Chemistry, 273 5 (1998), 2947-2953.
75 R. Y. L. Tsai, and R. R. Reed, Identification of DNA Recognition Sequences and Protein Interaction Domains of the Multiple-Zn-Finger Protein Roaz, Molecular and Cellular Biology, 18 11 (1998), 6447-6456.
76 R. K. Mosing, and M. T. Bowser, Microfluidic selection and applications of aptamers, Journal of separation science, 30 10 (2007), 1420-1426.
77 J. C. Cox, A. Hayhurst, J. Hesselberth *et al.*, Automated selection of aptamers against protein targets translated in vitro: from gene to aptamer, Nucleic Acids Research, 30 20 (2002), e108-e108.
78 J. C. Cox, M. Rajendran, T. Riedel *et al.*, Automated acquisition of aptamer sequences, Combinatorial Chemistry and High Throughput Screening, 5 4 (2002), 289-300.
79 J. Y. Lee, J. J. Kim, and T. H. Park, Miniaturization of polymerase chain reaction, Biotechnology and Bioprocess Engineering, 8 4 (2003), 213-220.
80 M. G. Roper, C. J. Easley, and J. P. Landers, Advances in polymerase chain reaction on microfluidic chips, Analytical Chemistry, 77 12 (2005), 3887-3893.
81 C. S. Zhang, J. L. Xu, W. L. Ma *et al.*, PCR microfluidic devices for DNA amplification, Biotechnology Advances, 24 3 (2006), 243-284.
82 X. Lou, L. Viel, J. Qian *et al.*, "Microfluidic Screening of Aptamer Libraries," in μ TAS 2007, Paris, France, 2007.
83 K. M. Ahmad, S. S. Oh, S. Kim *et al.*, Probing the Limits of Aptamer Affinity with a Microfluidic SELEX Platform, Plos One, 6 11 (2011).
84 M. Cho, Y. Xiao, J. Nie *et al.*, Quantitative selection of DNA aptamers through microfluidic selection and high-throughput sequencing, Proceedings of the National Academy of Sciences, 107 35 (2010), 15373-15378.
85 S. S. Oh, K. M. Ahmad, M. Cho *et al.*, Improving Aptamer Selection Efficiency through Volume Dilution, Magnetic Concentration, and Continuous Washing in Microfluidic Channels, Analytical Chemistry, 83 17 (2011), 6883-6889.
86 H. A. Levine, and M. Nilsen-Hamilton, A mathematical analysis of SELEX, Computational Biology and Chemistry, 31 1 (2007), 11-35.
87 C.-J. Huang, H.-I. Lin, S.-C. Shiesh *et al.*, Integrated microfluidic system for rapid screening of CRP aptamers utilizing systematic evolution of ligands by exponential enrichment (SELEX), Biosensors and Bioelectronics, 25 7 (2010), 1761-1766.
88 C.-J. Huang, H.-I. Lin, S.-C. Shiesh *et al.*, An integrated microfluidic system for rapid screening of alpha-fetoprotein-specific aptamers, Biosensors and Bioelectronics, 35 1 (2012), 50-55.
89 C. J. Easley, J. M. Karlinsey, J. M. Bienvenue *et al.*, A fully integrated microfluidic genetic analysis system with sample-in-answer-out capability,

Proceedings of the National Academy of Sciences of the United States of America, 103 51 (2006), 19272-19277.
90 B. S. Ferguson, S. F. Buchsbaum, J. S. Swensen *et al.*, Integrated Microfluidic Electrochemical DNA Sensor, Analytical Chemistry, 81 15 (2009), 6503-6508.
91 R. H. Liu, J. N. Yang, R. Lenigk *et al.*, Self-contained, fully integrated biochip for sample preparation, polymerase chain reaction amplification, and DNA microarray detection, Analytical Chemistry, 76 7 (2004), 1824-1831.
92 J. Y. Ahn, M. Jo, P. Dua *et al.*, A Sol-Gel-Based Microfluidics System Enhances the Efficiency of RNA Aptamer Selection, Oligonucleotides, 21 2 (2011), 93-100.
93 S.-m. Park, J.-Y. Ahn, M. Jo *et al.*, Selection and elution of aptamers using nanoporous sol-gel arrays with integrated microheaters, Lab on a Chip, 9 9 (2009), 1206-1212.
94 S. D. Mendonsa, and M. T. Bowser, In vitro selection of high-affinity DNA ligands for human IgE using capillary electrophoresis, Analytical Chemistry, 76 18 (2004), 5387-5392.
95 A. Drabovich, M. Berezovski, and S. N. Krylov, Selection of smart aptamers by equilibrium capillary electrophoresis of equilibrium mixtures (ECEEM), Journal of the American Chemical Society, 127 32 (2005), 11224-11225.
96 A. P. Drabovich, M. Berezovski, V. Okhonin *et al.*, Selection of smart aptamers by methods of kinetic capillary electrophoresis, Analytical Chemistry, 78 9 (2006), 3171-3178.
97 E. Michna, R. Jamison, L.-D. Pham *et al.*, Urine Toxicology Screening Among Chronic Pain Patients on Opioid Therapy: Frequency and Predictability of Abnormal Findings, Clinical Journal of Pain, 23 2 (2007), 173-179.
98 K. Wolff, and M. Farrell, A review of biological indicators of illicit drug use, practical considerations and clinical, Addiction, 94 (1999), 1279.
99 B. Levine ed., Principles of Forensic Toxicology, 2nd ed.: AACC Press, 2003.
100 Y. Tsumura, T. Mitome, and S. Kimoto, False positives and false negatives with a cocaine-specific field test and modification of test protocol to reduce false decision, Forensic Science International, 155 2-3 (2005), 158-164.
101 J. Swiatko, P. R. D. Forest, and M. S. Zedeck, Further Studies on Spot Tests and Microcrystal Tests for Identification of Cocaine, Journal of Forensic Sciences, 48 3 (2003).
102 J. P. Chambers, B. P. Arulanandam, L. L. Matta *et al.*, Biosensor recognition elements, Current Issues in Molecular Biology, 10 (2008), 1-12.
103 C. Tuerk, and L. Gold, Systematic evolution of ligands by exponential enrichment: RNA ligands to bacteriophage T4 DNA polymerase, Science, 249 (1990), 505-510.
104 M. N. Stojanovic, and D. W. Landry, Aptamer-based colorimetric probe for cocaine, Journal of the American Chemical Society, 124 33 (2002), 9678-9679.
105 J. Liu, and Y. Lu, Fast Colorimetric Sensing of Adenosine and Cocaine Based on a General Sensor Design Involving Aptamers and Nanoparticles, Angewandte Chemie International Edition, 45 1 (2006), 90-94.
106 B. Madru, F. Chapuis-Hugon, E. Peyrin *et al.*, Determination of Cocaine in Human Plasma by Selective Solid-Phase Extraction Using an Aptamer-Based Sorbent, Analytical Chemistry, 81 16 (2009), 7081-7086.

107 J. Chen, J. Jiang, X. Gao *et al.*, A New Aptameric Biosensor for Cocaine Based on Surface-Enhanced Raman Scattering Spectroscopy, Chemistry - A European Journal, 14 27 (2008), 8374-8382.

108 B. R. Baker, R. Y. Lai, M. S. Wood *et al.*, An electronic, aptamer-based small-molecule sensor for the rapid, label-free detection of cocaine in adulterated samples and biological fluids, Journal of the American Chemical Society, 128 10 (2006), 3138-3139.

109 Y. Li, H. L. Qi, Y. Peng *et al.*, Electrogenerated chemiluminescence aptamer-based biosensor for the determination of cocaine, Electrochemistry Communications, 9 10 (2007), 2571-2575.

110 S. C. Bell, and R. D. Hanes, A microfluidic device for presumptive testing of controlled substances, Journal of Forensic Sciences, 52 4 (2007), 884-888.

111 T. Frisk, D. Ronnholm, W. van der Wijngaart *et al.*, A micromachined interface for airborne sample-to-liquid transfer and its application in a biosensor system, Lab on a Chip, 6 12 (2006), 1504-1509.

112 J. P. Hilton, T. Nguyen, R. Pei *et al.*, "A Microfluidic Affinity Cocaine Sensor," *Micro Electro Mechanical Systems, 2009. MEMS 2009. IEEE 22nd International Conference on Micro Electro Mechanical Systems.* pp. 344-347.

113 T. Nguyen, R. Pei, M. Stojanovic *et al.*, An aptamer-based microfluidic device for thermally controlled affinity extraction, Microfluidics and Nanofluidics 6 (2009), 479-487.

114 M. A. Behlke, L. Huang, L. Bogh *et al.*, Fluorescence and Fluorescence Applications, Integrated DNA Technologies (2005).

115 J. I. Javaid, M. W. Fischman, C. R. Schuster *et al.*, Cocaine Plasma Concentration - Relation To Physiological and Subjective Effects in Humans, Science, 202 4364 (1978), 227-228.

116 V. Costarelli, and T. A. B. Sanders, Plasma Deoxycholic Acid Concentration Is Elevated in Postmenopausal Women With Newly Diagnosed Breast Cancer, European Journal of Clinical Nutrition, 56 9 (2002), 925-927.

117 K. B. Mullis, and F. A. Faloona, "Specific synthesis of DNA in vitro via a polymerase-catalyzed chain reaction," *Methods in Enzymology*, W. Ray, ed., pp. 335-350: Academic Press, 1987.

118 J. Shendure, G. J. Porreca, N. B. Reppas *et al.*, Accurate multiplex polony sequencing of an evolved bacterial genome, Science, 309 5741 (2005), 1728-1732.

119 D. S. Tawfik, and A. D. Griffiths, Man-made cell-like compartments for molecular evolution, Nature Biotechnology, 16 7 (1998), 652-656.

120 F. Diehl, M. Li, Y. P. He *et al.*, BEAMing: single-molecule PCR on microparticles in water-in-oil emulsions, Nature Methods, 3 7 (2006), 551-559.

121 D. Dressman, H. Yan, G. Traverso *et al.*, Transforming single DNA molecules into fluorescent magnetic particles for detection and enumeration of genetic variations, Proceedings of the National Academy of Sciences of the United States of America, 100 15 (2003), 8817-8822.

122 T. Kojima, Y. Takei, M. Ohtsuka *et al.*, PCR amplification from single DNA molecules on magnetic beads in emulsion: application for high-throughput screening of transcription factor targets, Nucleic Acids Research, 33 17 (2005).

123 R. Gan, Y. Yamanaka, T. Kojima *et al.*, Microbeads display of proteins using emulsion PCR and cell-free protein synthesis, Biotechnology Progress, 24 5 (2008), 1107-1114.
124 A. Lermo, S. Campoy, J. Barbe *et al.*, In situ DNA amplification with magnetic primers for the electrochemical detection of food pathogens, Biosensors & Bioelectronics, 22 9-10 (2007), 2010-2017.
125 M. A. Northrup, B. Benett, D. Hadley *et al.*, A miniature analytical instrument for nucleic acids based on micromachined silicon reaction chambers, Analytical Chemistry, 70 5 (1998), 918-922.
126 C. Zhang, and D. Xing, Single-Molecule DNA Amplification and Analysis Using Microfluidics, Chemical Reviews, 110 8 (2010), 4910-4947.
127 N. Beyor, L. N. Yi, T. S. Seo *et al.*, Integrated Capture, Concentration, Polymerase Chain Reaction, and Capillary Electrophoretic Analysis of Pathogens on a Chip, Analytical Chemistry, 81 9 (2009), 3523-3528.
128 Y. Li, C. Zhang, and D. Xing, Fast identification of foodborne pathogenic viruses using continuous-flow reverse transcription-PCR with fluorescence detection, Microfluidics and Nanofluidics, 10 2 (2011), 367-380.
129 K. Y. Lien, S. H. Lee, T. J. Tsai *et al.*, A microfluidic-based system using reverse transcription polymerase chain reactions for rapid detection of aquaculture diseases, Microfluidics and Nanofluidics, 7 6 (2009), 795-806.
130 F. Diehl, M. Li, D. Dressman *et al.*, Detection and quantification of mutations in the plasma of patients with colorectal tumors, Proceedings of the National Academy of Sciences of the United States of America, 102 45 (2005), 16368-16373.
131 F. Diehl, K. Schmidt, K. H. Durkee *et al.*, Analysis of mutations in DNA isolated from plasma and stool of colorectal cancer patients, Gastroenterology, 135 2 (2008), 489-498.
132 P. Kumaresan, C. J. Yang, S. A. Cronier *et al.*, High-throughput single copy DNA amplification and cell analysis in engineered nanoliter droplets, Analytical Chemistry, 80 10 (2008), 3522-3529.
133 S. W. Yeung, and I. M. Hsing, Manipulation and extraction of genomic DNA from cell lysate by functionalized magnetic particles for lab on a chip applications, Biosensors & Bioelectronics, 21 7 (2006), 989-997.
134 Y. S. Shin, K. Cho, S. H. Lim *et al.*, PDMS-based micro PCR chip with parylene coating, Journal of Micromechanics and Microengineering, 13 5 (2003), 768-774.
135 S. Bettiol, M. J. Thompson, N. W. Roberts *et al.*, Symptomatic treatment of the cough in whooping cough, Cochrane Database of Systematic Reviews 1 (2010).
136 W. S. Probert, J. Ely, K. Schrader *et al.*, Identification and Evaluation of New Target Sequences for Specific Detection of Bordetella pertussis by Real-Time PCR, Journal of Clinical Microbiology, 46 10 (2008), 3228-3231.
137 A. M. Wendelboe, and A. Van Rie, Diagnosis of pertussis: a historical review and recent developments, Expert Review of Molecular Diagnostics, 6 6 (2006), 857-864.
138 A. Lonneborg, P. Sharma, and P. Stougaard, Construction of subtractive cDNA library using magnetic beads and PCR, Pcr-Methods and Applications, 4 4 (1995), S168-S176.

139 E. M. Glare, J. C. Paton, R. R. Premier *et al.*, Analysis of a repetitive DNA-sequence from Bordetella-Pertussis and its application to the diagnosis of pertussis using the polymerase chain reaction, Journal of Clinical Microbiology, 28 9 (1990), 1982-1987.
140 Q. S. He, J. Mertsola, H. Soini *et al.*, Comparison of polymerase chain-reaction with culture and enzyme-immunoassay for diagnosis of pertussis, Journal of Clinical Microbiology, 31 3 (1993), 642-645.
141 C. Adessi, G. Matton, G. Ayala *et al.*, Solid phase DNA amplification: characterisation of primer attachment and amplification mechanisms, Nucleic Acids Research, 28 20 (2000), e87.
142 M. González, C. E. Argaraña, and G. D. Fidelio, Extremely high thermal stability of streptavidin and avidin upon biotin binding, Biomolecular Engineering, 16 1-4 (1999), 67-72.
143 J. P. Hilton, T. H. Nguyen, R. J. Pei *et al.*, A microfluidic affinity sensor for the detection of cocaine, Sensors and Actuators a-Physical, 166 2 (2011), 241-246.
144 S. Harris, and D. B. Jones, Optimisation of the polymerase chain reaction, British Journal of Biomedical Science, 54 3 (1997), 166-173.
145 K. H. Roux, Optimization and troubleshooting in PCR, Genome Research, 4 5 (1995), S185-S194.
146 D. Erickson, D. Li, and U. J. Krull, Modeling of DNA hybridization kinetics for spatially resolved biochips, Analytical Biochemistry, 317 2 (2003), 186-200.
147 M. J. Krawczyk, and K. Kulakowski, Off-lattice simulation of the solid phase DNA amplification, Computer Physics Communications, 170 2 (2005), 131-136.
148 J. F. Mercier, G. W. Slater, and P. Mayer, Solid phase DNA amplification: a simple Monte Carlo lattice model, Biophysical Journal, 85 4 (2003), 2075-2086.
149 J.-F. Mercier, and G. W. Slater, Solid Phase DNA Amplification: A Brownian Dynamics Study of Crowding Effects, Biophysical Journal, 89 1 (2005), 32-42.
150 I. Nazarenko, R. Pires, B. Lowe *et al.*, Effect of primary and secondary structure of oligodeoxyribonucleotides on the fluorescent properties of conjugated dyes, Nucleic Acids Research, 30 9 (2002), 2089-2095.
151 J. H. Wang, L. J. Chien, T. M. Hsieh *et al.*, A miniaturized quantitative polymerase chain reaction system for DNA amplification and detection, Sensors and Actuators B-Chemical, 141 1 (2009), 329-337.
152 J. Brownie, S. Shawcross, J. Theaker *et al.*, The elimination of primer-dimer accumulation in PCR, Nucleic Acids Research, 25 16 (1997), 3235-3241.
153 A. Holmberg, A. Blomstergren, O. Nord *et al.*, The biotin-streptavidin interaction can be reversibly broken using water at elevated temperatures, Electrophoresis, 26 3 (2005), 501-510.
154 E. J. Cho, J. W. Lee, and A. D. Ellington, "Applications of Aptamers as Sensors," *Annual Review of Analytical Chemistry*, Annual Review of Analytical Chemistry, pp. 241-264, Palo Alto: Annual Reviews, 2009.
155 S. Kyung-Mi, L. Seonghwan, and B. Changill, Aptamers and Their Biological Applications, Sensors (14248220), 12 1 (2012), 612-631.
156 T. K. Kim, S. W. Lee, J. Y. Ahn *et al.*, Fabrication of Microfluidic Platform with Optimized Fluidic Network toward On-Chip Parallel Systematic Evolution of

Ligands by Exponential Enrichment Process, Japanese Journal of Applied Physics, 50 6 (2011).

157 C. S. Zhang, and D. Xing, Miniaturized PCR chips for nucleic acid amplification and analysis: latest advances and future trends, Nucleic Acids Research, 35 13 (2007), 4223-4237.

158 J. Hilton, T. Nguyen, M. Barbu *et al.*, Bead-based polymerase chain reaction on a microchip, Microfluidics and Nanofluidics (2012), 1-12.

159 H. Mcwilliam, F. Valentin, M. Goujon *et al.*, Web services at the European Bioinformatics Institute-2009, Nucleic Acids Research (2009).

160 M. A. Unger, H. P. Chou, T. Thorsen *et al.*, Monolithic microfabricated valves and pumps by multilayer soft lithography, Science, 288 5463 (2000), 113-116.

161 K. T. Guo, G. Ziemer, A. Paul *et al.*, CELL-SELEX: Novel perspectives of aptamer-based therapeutics, International journal of molecular sciences, 9 4 (2008), 668-678.

162 D. P. Bartel, MicroRNAs: Target Recognition and Regulatory Functions, Cell, 136 2 (2009), 215-233.

163 M. M. Fabani, and M. J. Gait, miR-122 targeting with LNA/2′ -O-methyl oligonucleotide mixmers, peptide nucleic acids (PNA), and PNA–peptide conjugates, RNA, 14 2 (2008), 336-346.

164 R. E. Lanford, E. S. Hildebrandt-Eriksen, A. Petri *et al.*, Therapeutic Silencing of MicroRNA-122 in Primates with Chronic Hepatitis C Virus Infection, Science, 327 5962 (2010), 198-201.